

**EPA-460/3-77-006**

**February 1977**

**EMISSION FORMATION  
IN HETEROGENEOUS  
COMBUSTION**



**U.S. ENVIRONMENTAL PROTECTION AGENCY  
Office of Air and Waste Management  
Office of Mobile Source Air Pollution Control  
Emission Control Technology Division  
Ann Arbor, Michigan 48105**

**EPA-460/3-77-006**

# **EMISSION FORMATION IN HETEROGENEOUS COMBUSTION**

by

**G.L. Borman, P.S. Myers, O.A. Uyehara,  
L. Evers, M. Ingham, and D. Jaasma**

**University of Wisconsin  
Department of Mechanical Engineering  
Madison, Wisconsin 53706**

**Grant No. R803058-01-1**

**EPA Project Officer: John J. McFadden**

Prepared for

**ENVIRONMENTAL PROTECTION AGENCY  
Office of Air and Waste Management  
Office of Mobile Source Air Pollution Control  
Emission Control Technology Division  
Ann Arbor, Michigan 48105**

**February 1977**

This report is issued by the Environmental Protection Agency to report technical data of interest to a limited number of readers. Copies are available free of charge to Federal employees, current contractors and grantees, and nonprofit organizations - in limited quantities - from the Library Services Office (MD-35), Research Triangle Park, North Carolina 27711; or, for a fee, from the National Technical Information Service, 5285 Port Royal Road, Springfield, Virginia 22161.

This report was furnished to the Environmental Protection Agency by the University of Wisconsin, Department of Mechanical Engineering, Madison, Wisconsin 53706, in fulfillment of Grant No. R803058-01-1. The contents of this report are reproduced herein as received from the University of Wisconsin. The opinions, findings, and conclusions expressed are those of the author and not necessarily those of the Environmental Protection Agency. Mention of company or product names is not to be considered as an endorsement by the Environmental Protection Agency.

Publication No. EPA-460/3-77-006

## CONTENTS

	<u>Page</u>
Abstract	ii
List of Figures	iii
List of Tables	vi
Acknowledgements	vii
<u>Sections</u>	
I        Conclusions	1
II       Recommendations	3
III      Introduction	5
IV      The Delayed Mixing Stratified Charge Engine Concept	7
V        The Formation of NO <sub>x</sub> by Liquid Fuel Combustion	12
VI      The Divided Chamber Engine Evaluation and Texaco Engine Projects	51
VII     Publications	104
VIII    Glossary	105
IX      Appendix	107

## ABSTRACT

Three research projects are reported under the grant. The first is an investigation of a stratified engine concept in which spark ignited combustion in an engine with a homogeneous rich charge is completed and then air is injected during the expansion stroke giving a leaner overall fuel-air ratio. The study showed substantial reduction of nitric oxides without increasing other emissions. Combustion efficiency was not increased and, because substantial work was needed to supply the compressed air, the engine efficiency was decreased. The second project is an investigation of nitrogen oxides produced by burning of liquid normal heptane from a fuel wetted porous cylinder in a cross flow of air. Variation of free stream air velocity and cylinder diameter showed the moles of nitric oxide per mole of fuel burned to be a weak function of Reynolds number. Soot produced by the flame and collected downstream has been identified as giving off significant amounts of nitric oxide indicating a carbon, nitric oxide interaction in the flame envelope. The third project consisted of a study of the part load operation of the Newhall divided chamber engine previously developed at U.W., Madison, an emissions and fuel economy evaluation of this engine relative to other engines and initiation of a study of the formation of hydrocarbons in a Texaco engine by utilization of an in-cylinder sampling technique. Reasons for abandonment of the divided chamber engine were its higher hydrocarbons and lower fuel economy relative to other engines and its sensitivity to knock.

This report was submitted in fulfillment of Grant Number R803858-01 by the University of Wisconsin under the partial sponsorship of the Environmental Protection Agency. Work was completed as of February 9, 1977.

FIGURE

<u>No.</u>		<u>Page</u>
1	Schematic Representation of the Experiment.	14
2	Air Supply System.	15
3	Cross Section of Porous Cylinder Model.	17
4	Fuel Supply System.	19
5	Collection System.	20
6	Apparatus for NO Profile Determination.	23
7	Typical NO/NO <sub>x</sub> Concentration Measurement.	27
8	Determination of Noise Source.	28
9	NO Concentration Following Removal of Porous Cylinder Model.	30
10	Results of Experiments With Sooted and Clean Collectors.	31
11	Apparatus Used to Measure Amount of NO <sub>x</sub> in Soot. In 1, Soot is Collected in Inlet Tube and on Filter. In 2, Filter and Tube are Heated to Drive Off NO <sub>x</sub> .	33
12	Appearance of Flame at Different Fueling Rates.	37
13	Effect of Fuel Flow Rate on Molar Emission Indices at Constant Cooling Water Flow Rate for .53 x 1.3 cm Porous Cylinder Model in 32 cm/sec Air Stream.	38
14	Apparatus for Determination of Where NO <sub>2</sub> is Produced.	40
15	Effect of Fuel Center Temperature in NO and NO <sub>x</sub> Emission Indices and Burning Rate. Center Temperature Varied by Changing Cooling Water Flow Rates Air Velocity = 32 cm/sec, .52 x 1.3 cm Cylinder.	41
16	NO Concentration Profile 50° From Stagnation Point of a 1.3 cm Porous Cylinder Model. Air Velocity = 30 cm/sec.	46
17	Molar Emission Indices for Porous Cylinder Models Plotted Against Reynold Number Based on Free Stream Properties. Mean Values are Plotted With Bars Showing Highest and Lowest Measured Values. Numbers Under Lower Bar Indicates Number of Points Averaged.	48

<u>No.</u>		<u>Page</u>
18	Divided Chamber Engine Cylinder Head (Top View) - Final Part Load Hardware Configuration.	60
19	Measured NO Concentration Versus Overall Equivalence Ratio - 105° BTDC Injection.	62
20	Measured NO Concentration Versus Overall Equivalence Ratio 70° BTDC Injection.	63
21	Measured CO Concentration Versus Overall Equivalence Ratio 105° BTDC Injection.	65
22	Measured CO Concentration Versus Overall Equivalence Ratio - 70° BTDC Injection.	66=
23	Measured HC Concentration Versus Overall Equivalence Ratio 105° BTDC Injection.	68
24	Measured HC Concentration Versus Overall Equivalence Ratio - 70° BTDC Injection.	69
25	Calculated Specific Fuel Consumption ISFC Versus Overall Equivalence Ratio 105° BTDC Injection.	70
26	Calculated Specific Fuel Consumption (ISFC) Versus Overall Equivalence Ratio - 70° BTDC Injection.	72
27	Calculated Mean Effective Pressure (IMEP) Versus Overall Equivalence Ratio - 105° BTDC Injection.	73
28	Calculated Mean Effective Pressure (IMEP) Versus Overall Equivalence Ratio 70° BTDC Injection.	74
29	Calculated Specific NO Versus IMEP at Constant Equivalence Ratios 105° BTDC Injection.	76
30	Calculated Specific NO Versus IMEP at Constant Equivalence Ratios - 70° BTDC Injection.	77
31	Calculated Specific CO Versus IMEP at Constant Equivalence Ratios - 105° BTDC Injection.	78
32	Calculated Specific CO Versus IMEP at Constant Equivalence 70° BTDC Injection.	79
33	Calculated Specific HC Versus IMEP at Constant Equivalence Ratios - 105° BTDC Injection.	80

<u>No.</u>		<u>Page</u>
34	Calculated Specific HC Versus IMEP at Constant Equivalence Ratios 70° BTDC Injection.	81
35	Calculated ISFC Versus IMEP at Constant Equivalence Ratios 105° BTDC Injection.	82
36	Calculated ISFC Versus IMEP at Constant Equivalence Ratios 70° BTDC Injection.	83
37	Typical Primary Chamber Combustion Pressure Trace.	85
38	Calculated Specific NO <sub>x</sub> , CO, HC and Fuel Consumption Versus IMEP For Dual Ignition Tests.	87
39	Specific NO <sub>x</sub> Versus IMEP Divided Chamber Engine Comparison.	90
40	Specific CO Versus IMEP Divided Chamber Engine Comparison.	91
41	Specific HC Versus IMEP - Divided Chamber Engine Comparison.	93
42	Specific Fuel Consumption Versus IMEP Divided Chamber Engine Comparison.	94
43	Sampling Valve Design for TCCS Hydrocarbon Study.	99

## TABLES

<u>No.</u>		<u>Page</u>
1	Amounts of NO and NO <sub>x</sub> in Soot and Bulk Gases	35
2	Molar Emission Index Test Data Cylinder Size .36 x 2.1 cm	43
3	Molar Emission Index Test Data Cylinder Size .52 x 1.3 cm	44
4	Molar Emission Index Test Data Cylinder Size 0.52 x 1.3 cm	45
5	Molar Emission Index Test Data Cylinder Size 0.67 x 1.3 cm	46
6	Divided Chamber Engine - Operating Conditions Tested	56

## ACKNOWLEDGEMENTS

We wish to thank Mr. William Tierney, Mr. Edward Mitchell, Mr. Robert Canup and most particularly Mr. Martin Alperstein of Texaco for their continuing support and technical assistance with the TCCS hydrocarbon sampling project.

We are grateful to the U.S. Army TARADCOM for providing the M-151 TCP engine for this project, and we would like to thank Mr. Edward Rambie and Mr. Walter Bryzik of TARADCOM and Mr. Andrew Lennert, Mr. Richard Sows and Major Brian Harwood of the Arnold Research Organization whose efforts were instrumental in obtaining this engine for us.

SECTION I  
CONCLUSIONS

DELAYED MIXING ENGINE CONCEPT PROJECT

- a. Computer comparison of two mixing strategies for stratified charge combustion, i.e., gradually mixing successive portions of the rich products into air or vice versa, indicates that successively mixing portions of the air into the rich products gives reasonable efficiency, low nitric oxide concentration, and high specific power for operation near stoichiometric.
- b. An experimental study of this concept using a laboratory engine with outside compression of the air to be mixed with the rich products verified the low nitric oxide concentration and high specific power but showed relatively poor fuel economy due to the work required to compress the air to be mixed with the rich products.

FORMATION OF NO BY LIQUID FUEL COMBUSTION PROJECT

- a. There is preliminary, but convincing, experimental evidence suggesting that carbon absorbs significant quantities of  $\text{NO}_x$  thus serving as a sink for  $\text{NO}_x$ . Work should be done to conclusively verify this observation and to understand how  $\text{NO}_x$  is absorbed and released since carbon is usually produced during heterogeneous combustion.
- b. Preliminary data indicate that molar emission indices for diffusion type flames surrounding a porous cylinder are relatively insensitive to changes in the Reynolds number based on approach stream properties.

THE DIVIDED CHAMBER ENGINE EVALUATION AND TEXACO ENGINE  
PROJECTS

- a. The divided combustor chamber engine produces lower  $\text{NO}_x$  emissions than conventional engines but has higher specific fuel consumption than competitive hybrid engines having comparable  $\text{NO}_x$  emissions.
- b. Hybrid engines have better fuel economy but their hydrocarbon emissions are high. An in-cylinder sampling study should be conducted on a hybrid engine to determine the mechanism and location of hydrocarbon formation since this could lead to a low emission engine having good fuel economy.

SECTION II  
RECOMMENDATIONS

THE DELAYED MIXING STRATIFIED ENGINE CONCEPT

- a. That no additional work be done on the delayed mixing concept unless a practical method of compressing the required air which requires significantly less compression work than that required in the experimental set up is found.

THE FORMATION OF NO<sub>x</sub> BY LIQUID FUEL COMBUSTION

- a. That sufficient additional research work be done to determine whether particulate emissions from engines and stationary combustion sources carry with them significant amounts of nitric oxide. If the preliminary findings that there is significant transport of NO<sub>x</sub> by particulates are confirmed the mechanisms of formation and/or absorption and release of the NO<sub>x</sub> should be determined.
- b. That the effects of fuel composition and free stream temperature and composition on emission indices be evaluated.
- c. That emission indices be determined for situations simulating multiple droplets (probably multiple porous or absorbent cylinders) with the objective of producing emission criteria for dense and/or dilute sprays.

THE DIVIDED CHAMBER ENGINE EVALUATION AND TEXACO ENGINE PROJECT

- a. That work on HC formation be done on the Texaco engine rather than on the divided chamber engine because of the fuel economy advantage of the Texaco engine.

- b. That samples be taken at different times and locations in the clearance and displacement volumes of of the Texaco engine in an attempt to determine where and how hydrocarbons fail to be oxidized and are consequently emitted through the exhaust.

### SECTION III

#### INTRODUCTION

The work done under this grant consists of three different projects each being the doctoral thesis topic of a graduate student. Dr. L. Evers worked on the project titled, "The Delayed Mixing Stratified Charge Engine Concept" and upon graduation joined the ERDA staff at Bartlesville. Because his project work has been published as a separate report, only a brief discussion of the results are given here. Mr. D. Jaasma is working on the project titled, "The Formation of NO By Liquid Fuel Combustion". This project is concerned with the burning of liquid fuels in a diffusion flame which is supported by a fuel wetted porous cylinder. The cylinder is in a cross flowing air stream. The aim of the project is to produce correlations of moles of NO<sub>x</sub> per mole of fuel burned as a function of porous cylinder diameter, fuel type and flow stream velocity, composition and temperature. Mr. M. Ingham is working on the project entitled, "The Divided Chamber Engine Evaluation and Texaco Engine Project." The first phase of this project was to evaluate the emission and fuel economy performance of the Newhall-U.W. divided chamber engine at part load conditions. After extensive testing and comparisons with other engine data it was concluded in consultation with the EPA Project Officer that continuation of the second phase would be more meaningful if carried out on a more promising engine. The second phase of the project was to deal with an investigation of the sources of unburned hydrocarbons in the engine. It was decided therefore to obtain a Texaco TCCS single cylinder engine and conduct sampling probe studies on it to try to determine the mechanisms resulting in unburned hydrocarbon emissions.

Because of this switch, probe data from the Texaco engine had not yet been obtained at the termination of the grant.

Although all three projects concern heterogeneous combustion they are different enough that presentation of each in a separate section seemed desirable. Thus the following three sections deal with the three projects in turn.

## SECTION IV

### THE DELAYED MIXING STRATIFIED CHARGE ENGINE CONCEPT

One portion of the work conducted under this (and previous) EPA grant was completed during this grant period. (See Section VII of this report.) Five publications have been presented covering the work done. In order that the reader of this report can assess for himself whether or not he wishes to read these publications to obtain a detailed understanding of the work done a brief synopsis of the work done will be presented here.

Computer studies conducted under a previous EPA grant indicated that, in an engine having a stratified charge consisting of a rich mixture plus a lean mixture or, in the limit, air, the method of burning the rich mixture and mixing the resulting products with the remaining air to obtain an overall lean mixture markedly influenced the variation in specific  $\text{NO}_x$  (grams per KW) produced as the air-fuel ratio was varied.

Two strategies were investigated analytically. In both strategies combustion was started in the rich region of the charge. In the first strategy, called instantaneous mixing, as soon as the rich products of combustion of a portion of the mixture were formed they were thoroughly mixed with the lean mixture (air). Especially during the early portion of the process, the resultant product mixture was cool and lean, consequently limiting the nitric oxide formation. This strategy was very effective for very lean overall fuel-air mixtures. As the overall fuel air mixture approached stoichiometric proportion, however, the product mixture temperature increased. Higher temperatures and the presence of excess oxygen resulted in higher nitric oxide concentrations.

The disadvantage of the instantaneous mixing approach was that low nitric oxide concentrations were associated with low specific power because of the lean overall fuel-air mixture. The advantage of this approach was that, assuming burning rates could be maintained, lean overall mixtures resulted in both low nitric oxide concentrations and higher efficiencies.

In the second strategy, called delayed mixing, the rich products of combustion were not mixed with the gas (air) in the lean region until combustion was complete. A major difference, however, was that the lean region was mixed into the rich products instead of vice versa as for the instantaneous mixing concept. Thus the product mixture was initially rich and was gradually diluted to the final overall fuel-air ratio. When the final fuel-air ratio was stoichiometric, the nitric oxide formation was low because of the lack of oxygen in the early high temperature part of the expansion and because of the low temperature in the later part of the expansion. However, if the overall fuel-air ratio was made very lean, high temperatures and excess oxygen would be present early in the expansion stroke and would result in high concentrations of nitric oxide. The disadvantage of the delayed mixing strategy was that high efficiency (lean overall operation) was associated with high nitric oxide concentration. The advantage indicated by the computer model was reasonable efficiency, low nitric oxide concentration, and high specific power for operation near stoichiometric.

When the nitric oxide emissions of various types of internal combustion engines were examined, it appeared that some engines employed a limited mixing concept. The process began with rich combustion followed by a period of limited mixing. The final stage involved mixing of air into the products, or products into the air, or air and products into each other. This group of engines had trends

in nitrogen oxide emissions similar to those of the delayed mixing concept. The nitrogen oxide emissions were low for operation near stoichiometric fuel-air ratios and not sensitive to changes in fuel air ratios.

An experimental program was set up to simulate the combustion processes of the delayed mixing stratified-charge engine concept. The experimental engine was not intended to represent a practical engine configuration, but was simply a means for testing the delayed mixing concept. A single-cylinder spark-ignited carbureted CFR engine was modified to include an air injection valve which could inject air at the desired time in the engine cycle. The experimental engine was operated at a variety of overall fuel air ratios and air injection timings to evaluate the delayed mixing concept.

The high pressures associated with combustion required high pressure air. This air came from storage tanks; through a pressure regulator; through a flow restriction used for metering purposes; through a flow controlling valve; through a surge tank; and finally through a short duration (40 crank angle degrees) variable-timing cam-operated valve to a nozzle and to the combustion chamber.

In general, the engine was operated near 800 rpm at a compression ratio of seven using iso-octane as a fuel with the maximum air flow rate through the carburetor. The spark timing was varied in an attempt to operate at minimum advance for best torque (MBT) but these conditions were not always obtained. The high pressure air was normally introduced after or during the last part of combustion. However some runs had variable injection timing (including well before spark) to show the influence of the entire range of air-injection timings.

To establish a baseline the engine was first operated without air injection over a range of fuel-air ratios with power output, fuel economy and emissions being measured. As

expected, the maximum  $\text{NO}_x$  emissions occurred at slightly lean conditions.

Using air injection into a rich mixture to produce an overall stoichiometric mixture  $\text{NO}_x$  emissions were essentially equivalent to the homogeneous case whenever air injection started before about 30 degrees BTDC but decreased rapidly as air injection was retarded. Starting air injection at TDC or later produced low  $\text{NO}_x$  emissions, i.e., 80-100 ppm. This suggests that when injected before combustion the injected air mixes quickly with the rich mixture to form essentially homogeneous mixture having the equivalence ratio of the overall mixture and producing comparable  $\text{NO}_x$  emissions when burned. When air was injected during the latter part of or after combustion very little  $\text{NO}_x$  was formed from the additional oxidation because of the lower temperatures.

In general, the CO concentrations using air injection were directly comparable to those observed when operating the engine on a homogeneous mixture having an equivalence ratio equal to the overall fuel-air ratio using air-injection. The two exceptions to this were that, when air injection occurred very late (92 degrees ATDC) or during the middle of the combustion period (near TDC), higher CO concentrations were observed. In the first case it was thought that the air was injected too late to destroy the CO from both a time and temperature standpoint. In the second case it appeared that the injected air interfered in some way (possibly by cooling) with combustion and produced excessive CO.

Speaking of HC's, with the exception of an air-injection timing of 8° BTDC, the values observed with air injection were generally lower than those observed with homogeneous combustion at the same overall equivalence ratio. The high observed values at 8° BTDC are undoubtedly the result of disturbing combustion by air injection and are probably

related to the high CO observed with this air injection timing.

The indicated efficiency with air injection (not taking into account the work of compressing the air) increased when using leaner overall mixtures partly for thermodynamic reasons and partly because more compressed air was put into the cylinder. When the work of compressing the required high pressure air was taken into account, the indicated efficiency decreased as the overall equivalence ratio decreased, i.e., became leaner. This indicates that the work used in this set up to compress the air was large and required more energy than could be obtained from the additional burning of the rich mixture. While a practical engine might not use air compression outside the cylinder and certainly would not include a metering system, these data raise serious questions as to the viability of the process from a fuel economy standpoint.

Speaking of engine power, when the IMEP was corrected by subtracting the estimated work required to compress the injected air, the magnitude of the corrected IMEP is equal to or less than the corresponding homogeneous operation. Thus again emphasizes the importance of the work of compressing the air.

In summary, the delayed mixing stratified-charge engine concept was an effective method of controlling the nitric oxide emissions. The carbon monoxide emissions were equivalent to those of homogeneous engines and the HC's were lower. The disadvantage of the delayed mixing concept was its low efficiency brought about primarily because of the large amount of work required to produce the injected air.

## SECTION V

### THE FORMATION OF $\text{NO}_x$ BY LIQUID FUEL COMBUSTION

#### INTRODUCTION

Liquid fuel diffusion flames are common phenomena occurring in oil fired burners such as home furnaces, gas turbine combustors, and utility boilers. Oxides of nitrogen ( $\text{NO}$  and  $\text{NO}_2$ , hereinafter termed  $\text{NO}_x$ ) are produced in such flames, and because of their environmental impact there is interest in reducing the amount of  $\text{NO}_x$  which is formed in combustion processes.

One solution to the problem is to find ways to burn fuels so that minimal amounts of  $\text{NO}_x$  are formed. In the case of premixed flames  $\text{NO}_x$  formation is a post flame occurrence. This has allowed analytical models to be used to seek out ways of burning fuels in an environmentally acceptable manner. Models are also being used to study the effects of parameters on  $\text{NO}_x$  formation in liquid fuel diffusion flame devices, but this type of work is hindered by the fact that these systems are heterogeneous in nature and analytical solutions for the space and time dependent temperatures and concentrations are not easily obtainable. Even the case of a single drop of fuel under many simplifying assumptions is difficult to solve for the amount of  $\text{NO}$  produced.

Due to the desirability of using an analytical approach to find cleaner ways to burn liquid fuels as diffusion flames and the difficulties involved in applying such an approach, it was deemed reasonable to follow the same procedure used in heat transfer and fluid dynamics when the analytical problems become intractable, namely, to form an empirical correlation. The work reported herein represents the first steps of an effort to experimentally correlate the molar emission index (molar emission index = gram mol of pollutant

formed/gram of fuel burned) for burning droplets as a function of independent variables such as fuel, drop size, velocity of air relative to the drop, composition of the air around the drop, and temperature of the air stream around the drop. Such a correlation is of interest over a range of Reynolds numbers from 0 to the point where transition to wake flame occurs.

### EXPERIMENTAL APPARATUS

Figure 1 shows a schematic diagram of the experimental apparatus used in this investigation. The air supply system provides a jet of air in which the experiments are performed, and a porous cylinder model is used to simulate the burning droplet. The collection system is used to catch all of the products of combustion from the experiment, along with the inevitable dilution air from the surroundings. The systems are described separately in detail.

#### Air Supply System

The purpose of the air supply system is to provide a region of uniform air velocity, the temperature of which can be varied over a range of 20-1100°C. The design of the system includes a cross flow heat exchanger and is shown in Figure 2. The amount of air to be heated is determined by varying the pressure upstream of a critical flow orifice, which was calibrated using a positive displacement gas meter. The metered air enters the steel shell of the heat exchanger at one end, is forced by baffles to pass through a series of fourteen cross flow core sections, and passes out of the shell through a vertically oriented converging nozzle with a rectangular outlet of size 5.6 x 4.9 centimeters. An industrial burner using propane as fuel provides hot products of combustion which pass in a straight line through the fourteen core sections and then out an exhaust pipe at the other end of the exchanger. All internal

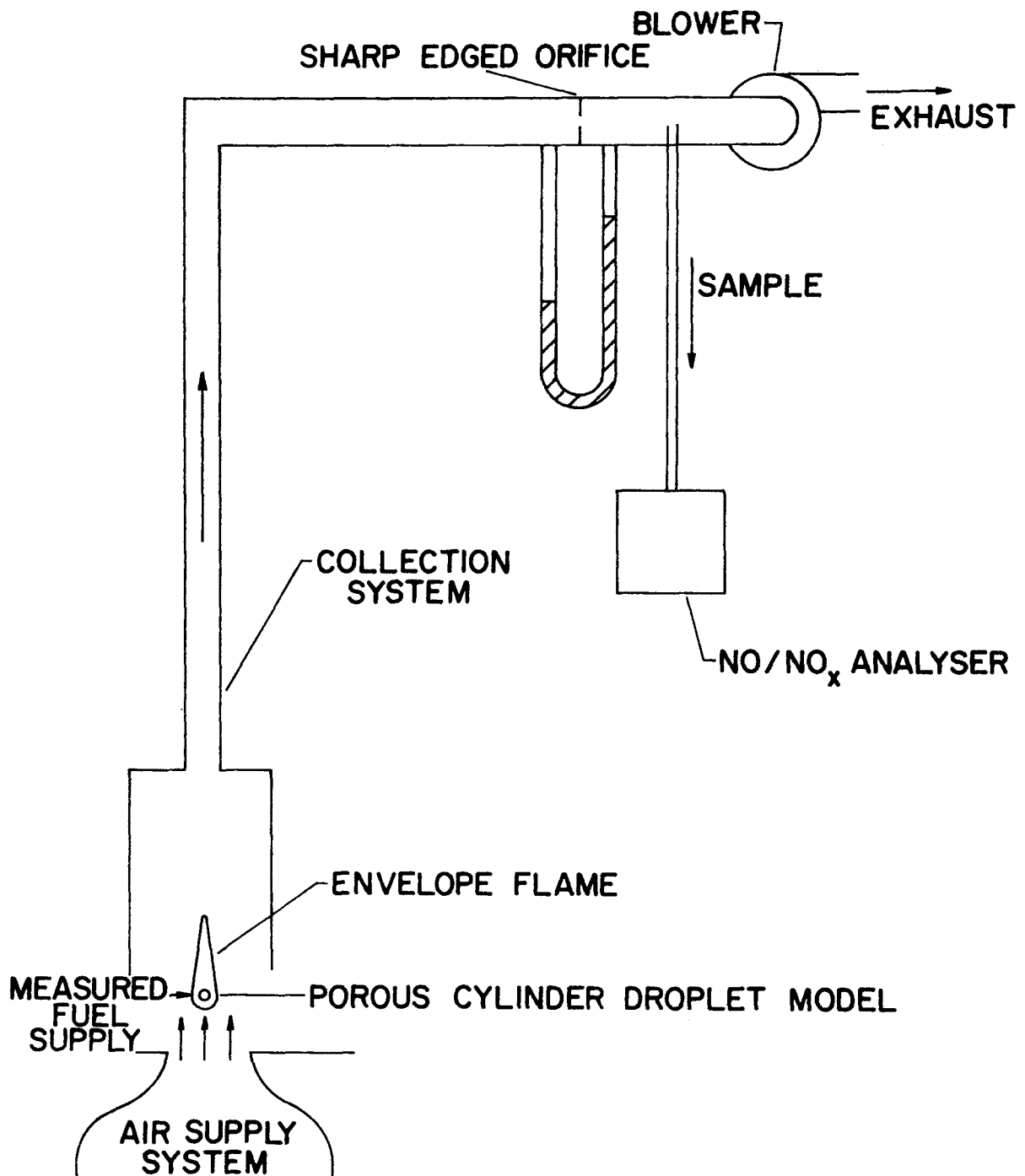


Figure 1. Schematic Representation of the Experiment.

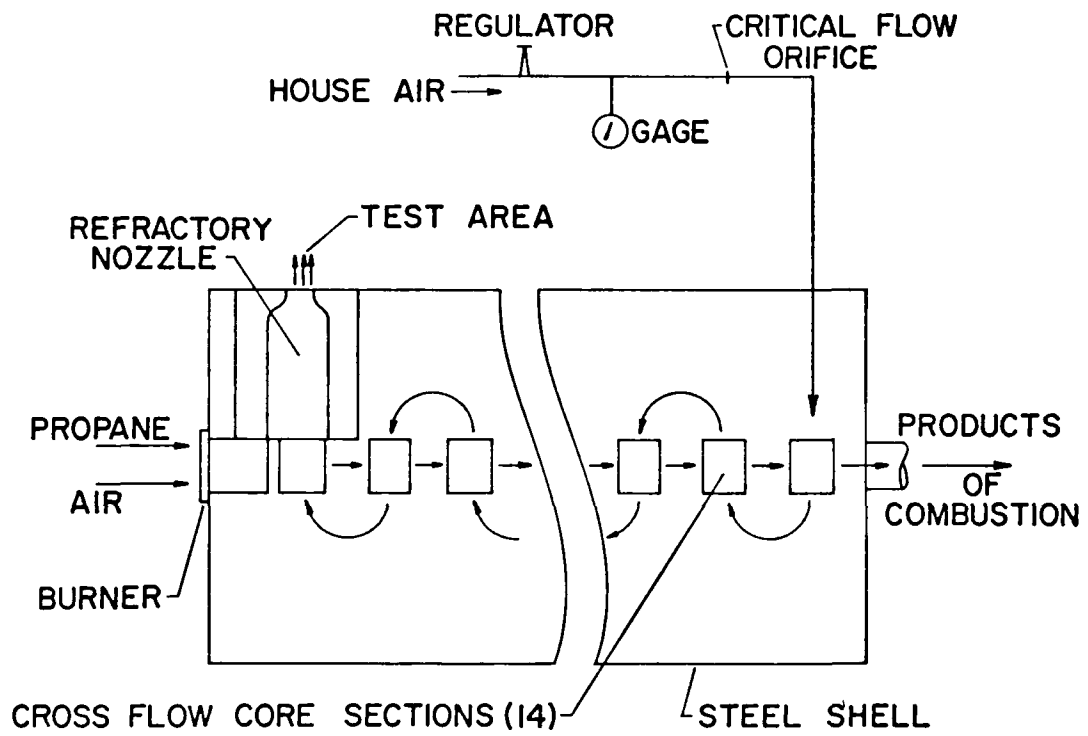


Figure 2. Air Supply System.

parts of the heat exchanger are made of refractory materials, with insulating fire brick being used for the support and baffling materials. The brick is coated with refractory mortar to reduce its porosity, and the air outlet nozzle is a refractory casting. The steel shell of the heat exchanger is supported by a steel angle frame and made air tight, the only inlets and outlets being for the air and propane products. A great deal of effort was spent trying to produce acceptable sealing between the air and products side of the heat exchanger, but the internal leakage was never reduced to acceptable levels. Consequently, it was decided to operate the heat exchanger as a heat storage device by first capping off the air inlet and outlet and running the propane burner long enough to heat up the core sections and surrounding bricks to a very high temperature. The burner inlets and exhaust could then be sealed off and the air supply turned on to flush out the products of combustion of the burner and to provide the hot air for the experiments. Using this technique, an air outlet temperature of over 500°C at 7.8 kilograms per hour was achieved, with the temperature of the air falling off so slowly that it could be assumed constant for data taking purposes. Due to problems with warpage of the stainless steel at the nozzle outlet, the system has not yet been tested to determine the maximum possible air temperature it can deliver. As mentioned previously, the design condition has an outlet temperature of 1100°C, and it is expected that temperatures in this range can be achieved once the nozzle outlet problem is solved.

#### Experimental Models of Burning Droplets

A cross section of the porous cylinder experimental model of the burning droplet is shown in Figure 3. The porous section is made of a sintered bronze material which is commonly impregnated with oil and sold as a pre-lubricated bearing. Some sizes used were available off the shelf, while

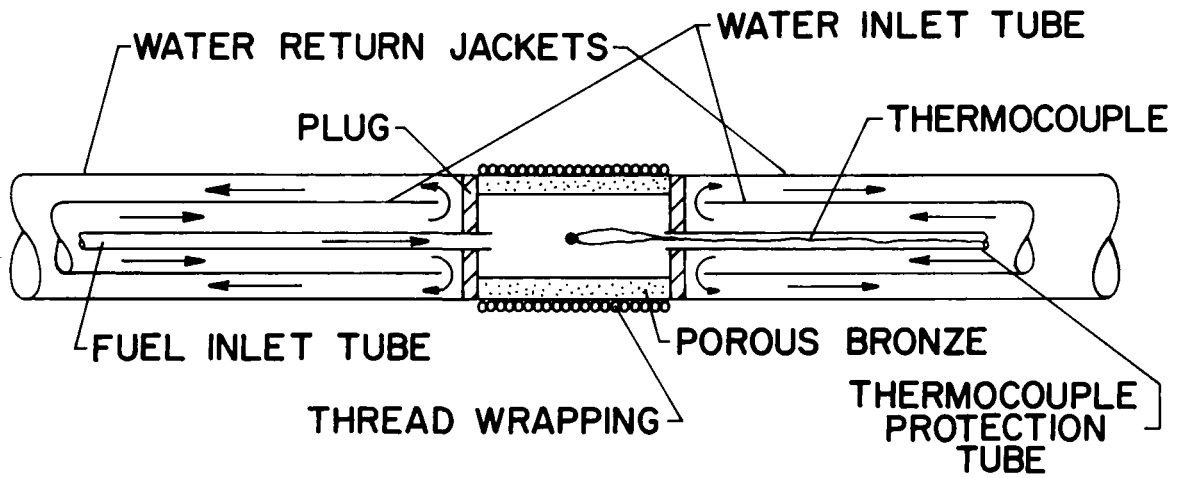


Figure 3. Cross Section of Porous Cylinder Model.

the others were machined from bars of this material. The cylinders are washed thoroughly in trichlorethylene to remove the oil, and then soft soldered at the ends to four tubes, two for cooling water return, one for a fuel feed, and another to insert a thermocouple for measurement of the fuel temperature at the center of the cylinder. The larger diameter cylinders also require end plugs as shown to keep the water and fuel separated. An additional tube is inserted from each end around the innermost tube and inside the water return tube. Cooling water is fed down the additional (water feed) tubes, turns around at the ends of the porous cylinder, and exits through the water return tubes. The cooling water is necessary to allow the fuel to reach the cylinder in a liquid condition, particularly when the cylinder is placed in a high temperature air stream. Cooling water flow through each side is separately controlled and measured by means of rotameters. In order to insure that the entire porous cylinder is fuel covered, a .2 mm diameter cotton thread is wrapped around the cylinder and secured at each end by a small amount of epoxy cement. The capillary action of the thread is sufficient to cause the entire cylinder to be wetted with the fuel.

#### Fuel Supply System

The fuel supply system for the experimental models is shown in Figure 4. Fuel flow is controlled by varying the air pressure above the fuel and is measured using a rotameter which was calibrated using a knife edge balance to weigh the amount of fuel passed in a given amount of time.

#### Collection System

The products of combustion from the droplet model are collected by a water cooled system as shown in Figure 5. The cooling is required primarily for the heated air experiments. The products of combustion enter at the bottom of

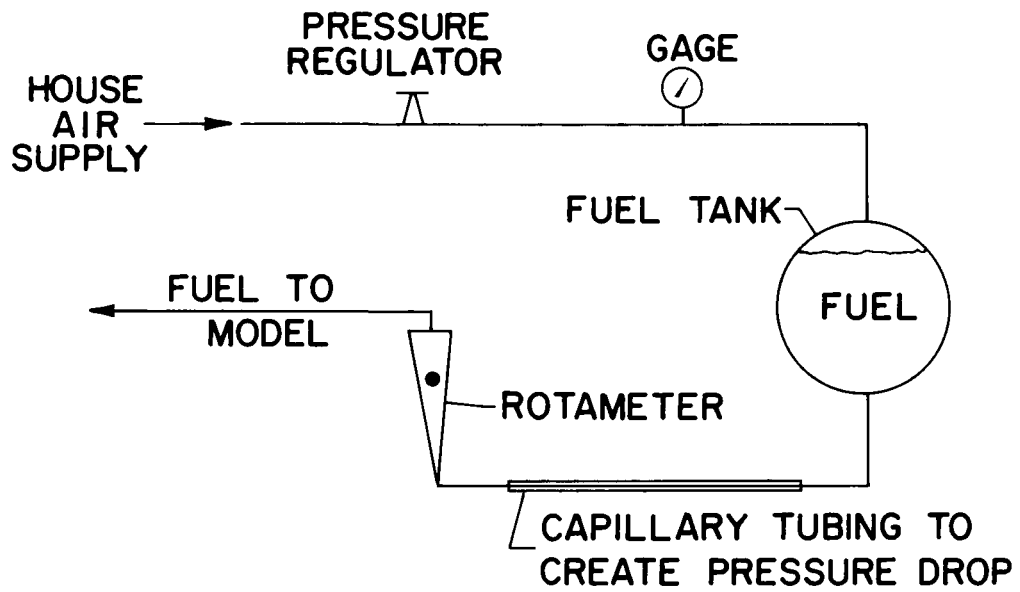


Figure 4. Fuel Supply System.

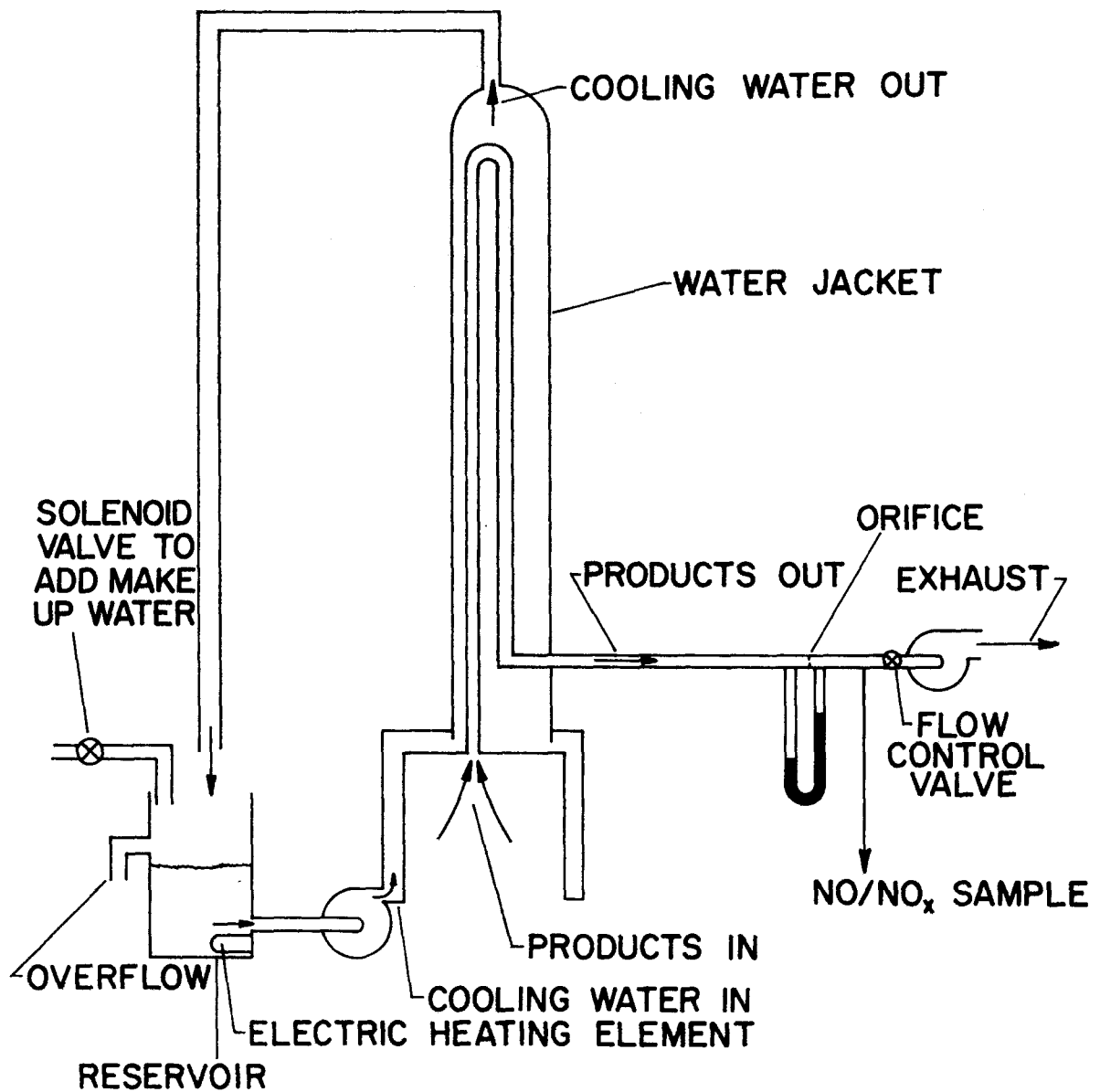


Figure 5. Collection System.

the cooler and pass through 4 meters of copper tube which is surrounded by cooling water. Problems with condensation of products in the cooler led to installation of an electric heating element to keep the cooling water at a minimum of 49°C. The temperature is controlled by a sensor which turns on a solenoid operated valve when the cooling water reaches the preset temperature level, adding room temperature water to the system. In this way the cooling water temperature is maintained to within  $\pm 2^\circ\text{C}$  of the nominal set point, which can be anywhere from 49 to 80 °C. The cooled products and excess air pass through a sharp edged orifice which had been calibrated using a positive displacement gas meter. A blower is used to pull the products through the system, and the gas sample is drawn off downstream of the orifice.

#### Instrumentation

The independent variables in the experiment are the physical description of the porous cylinder (diameter and length), air stream velocity, air stream temperature, cooling water flow rate (through the porous cylinder supports), and collector flow rate. The air stream velocity is calculated from a knowledge of the pressure upstream of the critical flow orifice and the temperature of the air at the nozzle exit. The pressure is measured with a bourdon tube gage, and the temperature is measured with a chromel alumel thermocouple located in the exit plane of the nozzle. Cooling water flow is varied by use of needle valves and measured with rotameters. The temperature of the fuel at the center of the cylinder depends on the amount of cooling, and can be varied over the range 50-95°C. The collector flow is measured using a sharp edged orifice and a water manometer. A positive displacement gas meter was used to calibrate several different size orifice plates so that no matter what the collector flow rate is the differential pressure read on the manometer is in the range of 6-50 centimeters of water when the appropriate orifice is used.

The dependent variables are the concentrations of NO and NO<sub>x</sub> in the collector stream, the burning rate of the fuel, and the temperature and pressure of the product stream as measured at the orifice. Concentrations of NO and NO<sub>x</sub> are measured continuously using a chemiluminescent analyzer, with the sampling probe location downstream of the orifice as shown in Figure 1. The sampling probe is located in this position because it was believed that the products/air mixture entering the cooler could be somewhat stratified, but would be well mixed by the time it got to the sample point. The accuracy of the reading is limited to ± 5%, since the calibration gas is known only to this accuracy. A strip chart recorder is used to record the readings as a function of time. A thermocouple is located near the orifice, and the manometer used for measuring the differential pressure could also be used to measure the difference between the upstream pressure of the orifice and the ambient. This difference is small enough to be neglected in the subsequent computations of emission indices.

The chemiluminescent analyzer is also used to obtain nitric oxide concentration profiles by sampling flame gases directly into the analyzer through a quartz microprobe. A vacuum pump is used in place of the low pressure bypass pump and the sample pressure regulator is adjusted so that a choked flow condition is maintained at the probe inlet. The set up is shown in Figure 6.

#### EXPERIMENTAL TECHNIQUE

In most of the tests a single independent parameter is varied through its range of interest, while all the other independent variables are held constant. The sequence of events for a run is as follows.

The collector-cooler is warmed up to at least 49°C to prevent condensation of products before they become well

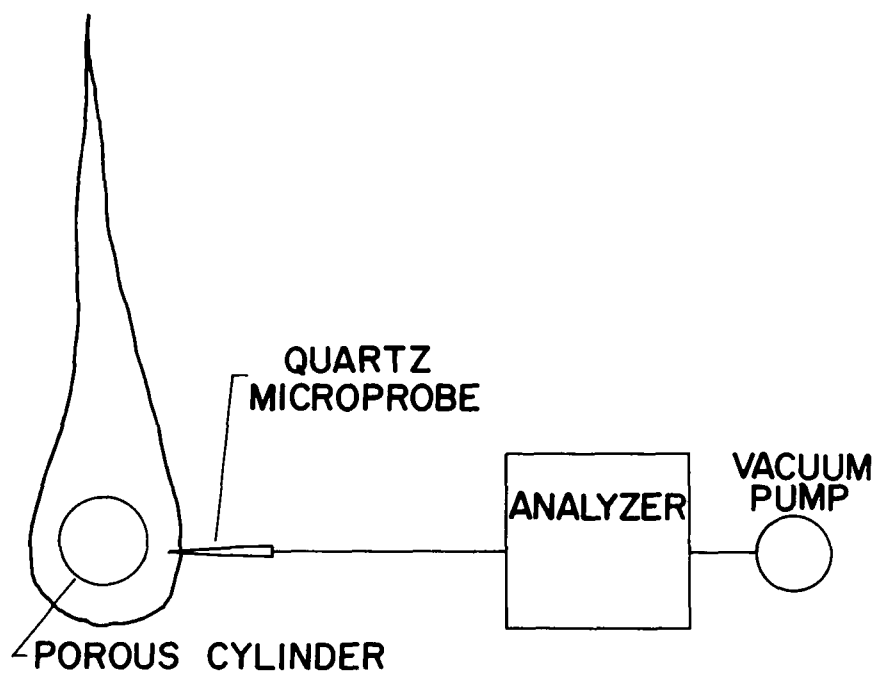


Figure 6. Apparatus for NO Profile Determination.

mixed with excess air. A porous cylinder model is placed over the outlet of the air nozzle and the dimensions are noted. The blower is then turned on and the collector flow rate adjusted by means of a valve. Air stream velocity and the cooling water flows for the porous cylinder model are then adjusted. The fuel supply is turned on and the cylinder is lit with a match when the fuel appears on its surface. The air pressure in the fuel tank is then adjusted so that the thread appears wet with fuel. Readings of NO or NO<sub>x</sub> concentrations, fuel flow, collector flow, and product gas temperature downstream of the orifice are made after the strip chart recorder shows a constant signal level for 1-2 minutes. Noise in the recorder signal necessitates a visual interpretation of the average signal level during this time. The parameter which is under study for the particular test run is then changed and new readings are taken after the NO and NO<sub>x</sub> readings are again stabilized. When the air velocity and amount of cooling are varied, a readjustment of the fuel flow is required following each change, since the mass burning rate of the fuel is dependent on these parameters.

In the NO profile determination, the quartz probe is adjusted to the desired position by means of a micromanipulator. The flow rate through the analyzer is very low in this situation due to the small size of the probe orifice (about 50 micrometers), and it takes up to 5 minutes for the instrument to respond completely to a change in probe position.

#### COMPUTATION OF EMISSION INDICES

In order to compute the molar emission indices for a given set of experimental conditions, it is necessary to know the mass burning rate of the fuel and the molar rate of formation of NO and NO<sub>x</sub>. The mass flow of fuel is known by means of the calibrated rotameter, while the net molar rate of formation of NO and NO<sub>x</sub> is obtained from measurements of the

total volumetric flow rate through the system (using the sharp edged orifice) and concentration measurements for NO and NO<sub>x</sub> downstream of the orifice. This information may be converted to a molar rate of NO<sub>x</sub> by the equation

$$\dot{M}_{NO_x} = Q \cdot n \cdot Y_{NO_x}$$

where

$\dot{M}_{NO_x}$  = molar rate of NO<sub>x</sub>, mols/second

Q = volumetric flow rate through orifice,  
liters/second

n = molar density of gases at the orifice,  
mols/liter

$Y_{NO_x}$  = mol fraction of NO<sub>x</sub>

The molar emission index for NO<sub>x</sub> is then given by

$$EI_{NO_x} = \dot{M}_{NO_x} / \dot{m}_{fuel}$$

where

$EI_{NO_x}$  = molar emission index of NO<sub>x</sub>, (gram mols NO<sub>x</sub>/gram fuel)

$\dot{m}_{fuel}$  = mass rate of fuel burned, grams/second

The molar emission index for NO may be computed from the same formulas, if the mol fraction of NO is substituted for the mol fraction of NO<sub>x</sub>. Thus we have

$$\dot{M}_{NO} = Q \cdot n \cdot Y_{NO}$$

where

$\dot{M}_{NO}$  = molar rate of NO formation

There are at least two reasons for using molar emission indices (mols of pollutant/mass of fuel) instead of mass emission indices (mass of pollutant/mass of fuel). The environmental impact of the emission of one mol of NO is the same as

the impact of a mol of  $\text{NO}_2$ . The molar emission index gives the same index to a drop which produces a mol of NO as to a drop that produces a mol of  $\text{NO}_2$ . The second reason is that the molar emission index allows the relative amounts of NO and  $\text{NO}_2$  produced by a given flame condition to be compared by looking at the emission indices for NO and  $\text{NO}_2$ . If the mass emission index is used, one must do one of two things to compare relative amounts of NO and  $\text{NO}_2$ . Either one of the emission indices must be divided by the ratio of the molecular weights of NO and  $\text{NO}_2$ , or the emission index for NO could be computed using the molecular weight of  $\text{NO}_2$ . The use of the molar emission index thus eliminates ambiguity and lends itself to easy evaluation of what is happening in the flame.

## DISCUSSION

Preliminary tests using unheated air gave NO and  $\text{NO}_x$  concentrations on the order of 2-10 parts per million (PPM). A typical trace on the strip chart recorder appears as shown in Figure 7. Two tests using calibration gas and with no flame were run to determine the cause of the noise in the signal, and the resulting strip chart recordings are shown schematically in Figure 8. The results indicate that the cause of the fluctuations is in the fluid dynamics of the product gases as they enter the cooler, rather than being associated with the flame itself or a pulsation induced by the blower.

During the course of one of the early experiments, the following sequence of events occurred:

1. The experiment was run for about a half hour at various conditions.
2. The flame was blown out and fuel supply turned off.
3. The blower unit was turned off, while the  $\text{NO}_x$  analyzer was left on.

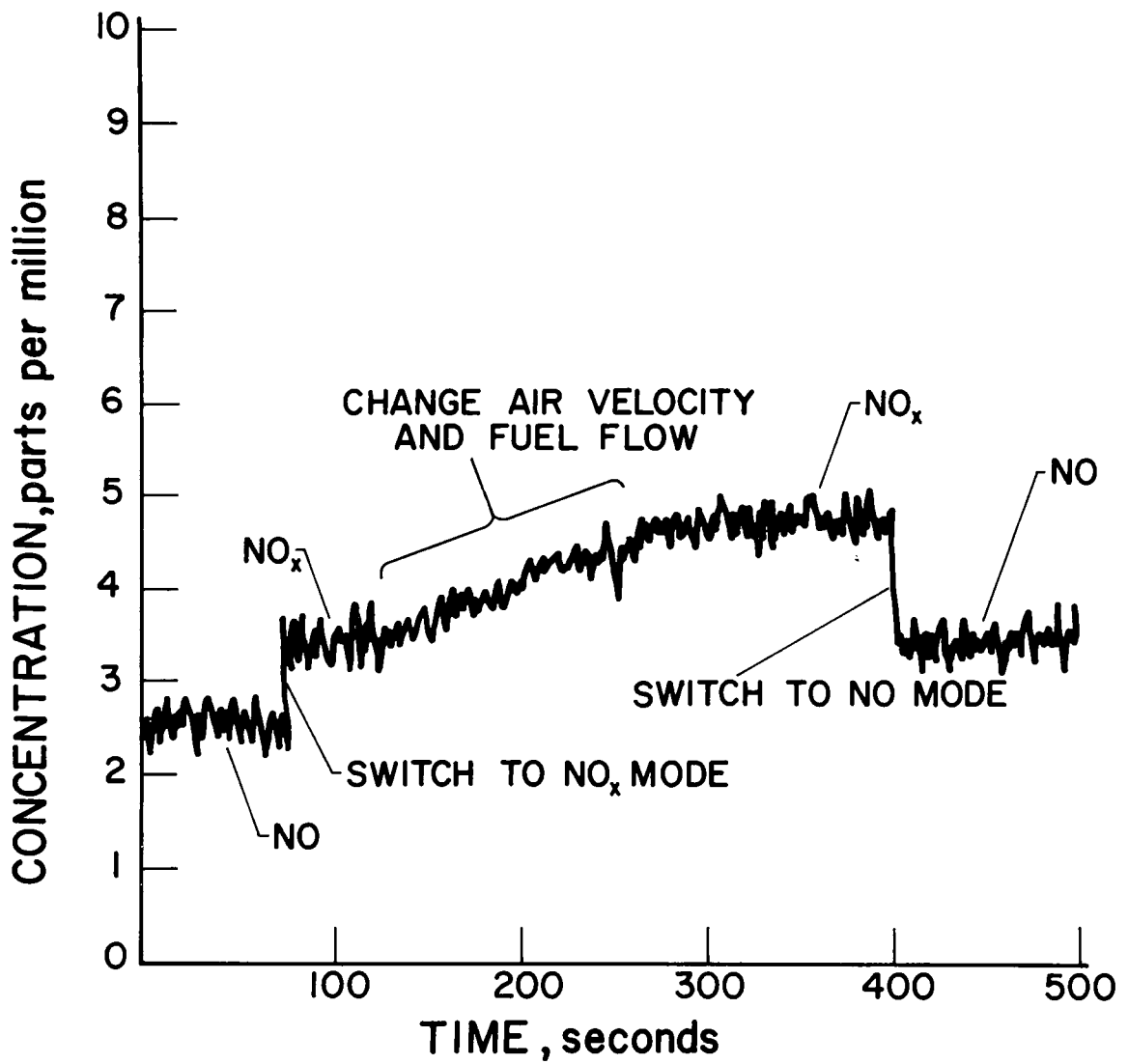


Figure 7. Typical NO/NO<sub>x</sub> Concentration Measurements.

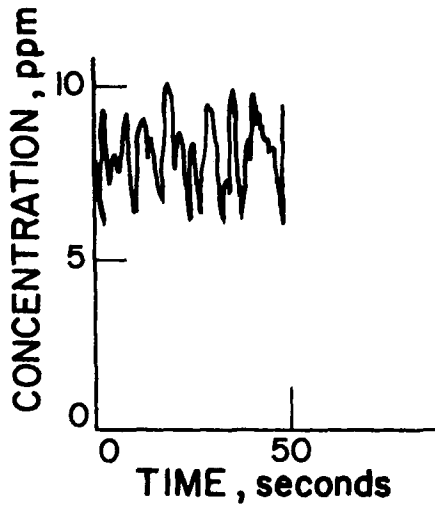
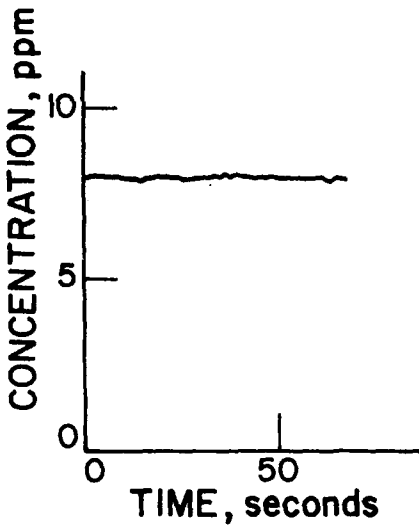
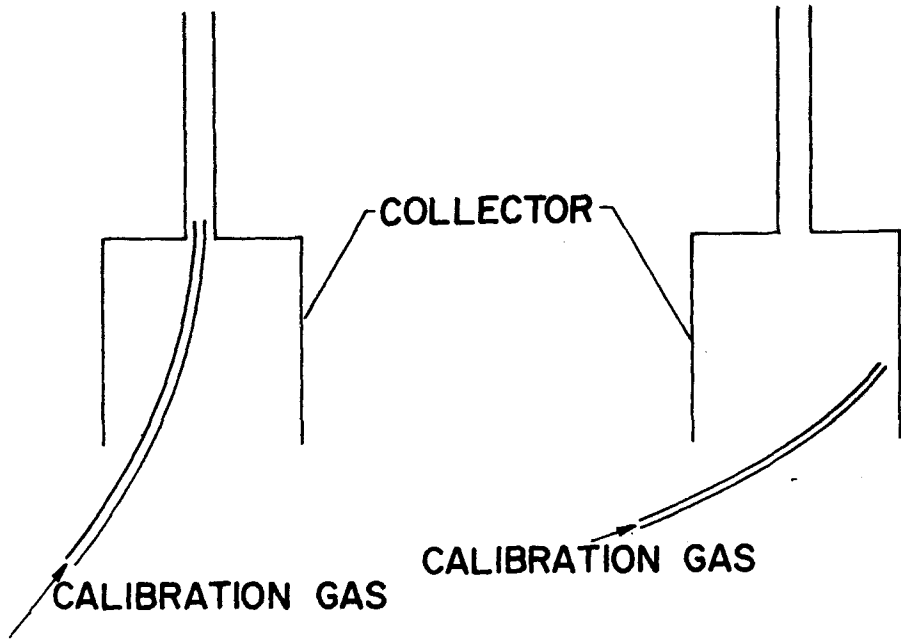


Figure 8. Determination of Noise Source.

This produced the strip chart recording shown in Figure 9. The measured concentration of NO decreased to near zero shortly after the removal of the flame, but then increased following shut down of the blower which had been pulling fresh air through the collection system. In fact, the measured concentration of NO increased to levels which were much greater than those measured during the actual running of the experiment. It became apparent that somewhere in the system NO was being released and that this occurred over a period of hours, as evidenced by letting the system sit for an hour, purging the system with the blower, shutting off the blower, waiting five minutes, and then sampling the collector-cooler gases. Inspection of the system revealed condensed water in the cooler and orifice tubing (unexpected) and that the entire system was coated with soot (expected). It appeared that there were three possible causes of this "residual NO", namely, the water, the soot, or the copper tubing from which the collector-cooler was made. Since NO is insoluble in water, the water was considered as a highly unlikely source. Rerunning the experiment with higher collector flow rates (to collect enough excess air to prevent condensation) ruled out the water hypothesis, as the qualitative behavior of the system was the same.

In an attempt to determine whether the soot or the copper was the cause of the residual NO, a mock up was made of the collector-cooler system using clean copper tubing. The two experiments shown schematically in Figure 10 with their resulting strip chart outputs were then conducted. The first experiment used the sooted collector-cooler and a porous cylinder flame, while the second experiment used the clean collector and a premixed propane-air nonsooting flame. In the first experiment, the sooted collector was purged with room air until there was no longer any residual NO being measured. The porous cylinder model

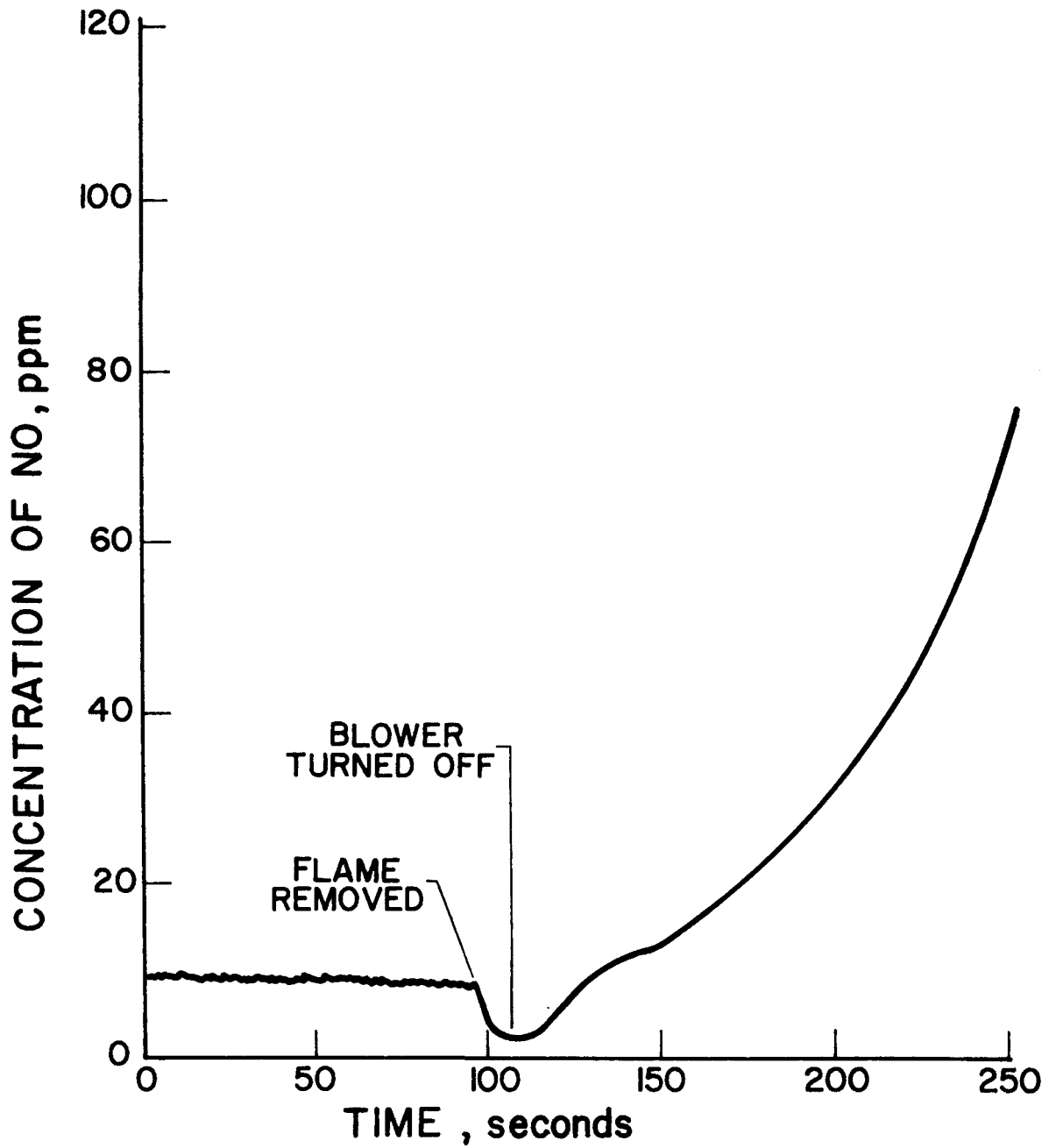


Figure 9. NO Concentration Following Removal of Porous Cylinder Model.

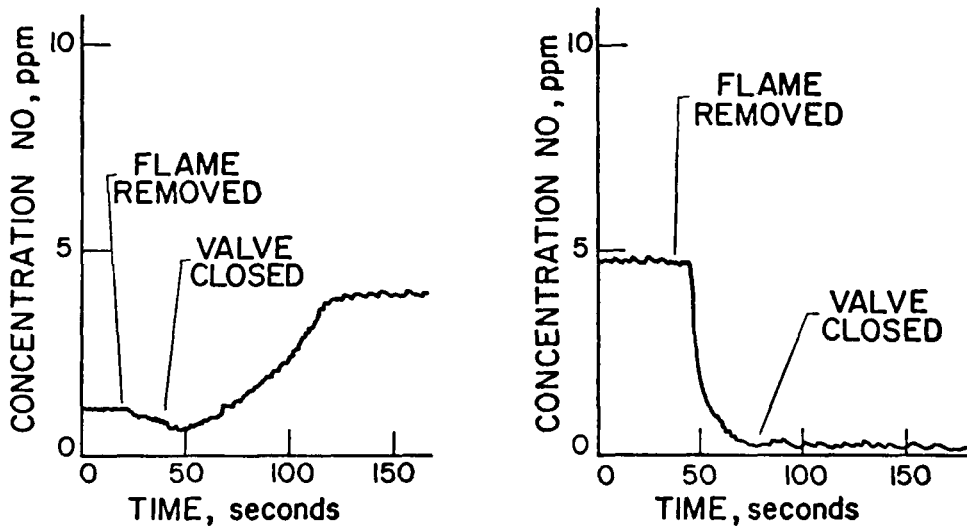
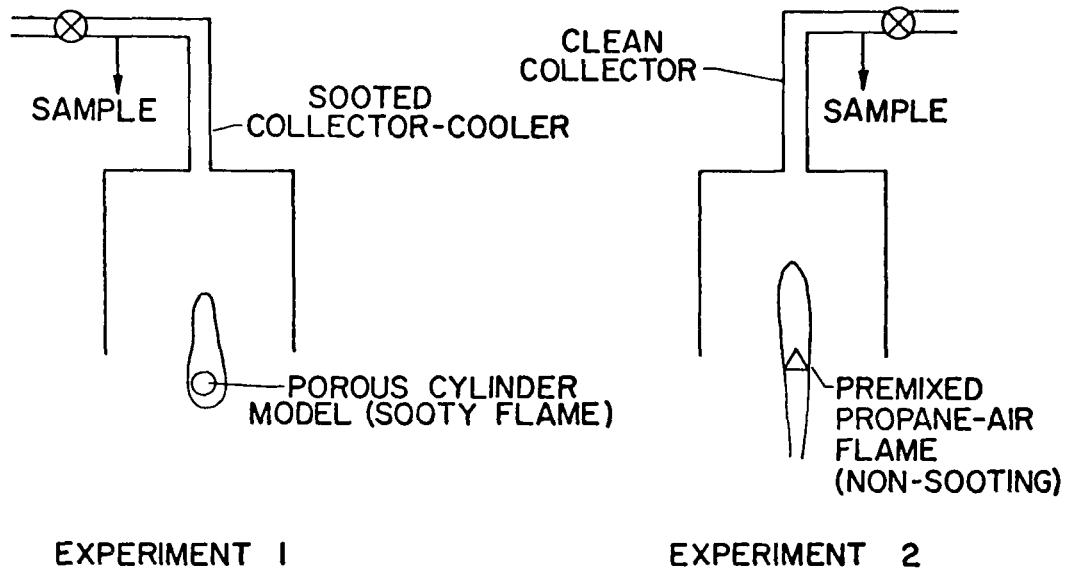


Figure 10. Results of Experiments With Sooted and Clean Collectors.

was then used to give a bulk gas concentration of NO  $\approx$  .5 PPM for a period of 15 minutes with the blower running. Removal of the flame was followed by a drop in the measured concentration of NO, and at the end of 20 seconds the blower inlet valve was closed. The measured concentration of NO then increased to a value approximately seven times higher than it had been when the porous cylinder was burning.

In the second experiment, the clean collector system was run for 15 minutes with a propane air (non sooting) flame at a collector flow which gave a measured concentration of NO around 5 PPM. The flame was removed, and 20 seconds later the valve controlling collector flow was again closed. The measured concentration of NO remained very close to zero.

Comparison of the results of these two experiments indicates that the residual NO is associated with the soot, and not the material of the collector cooler. The fact that the measured residual NO concentrations exceeded the NO concentrations during the experiment is not evidence that more NO is associated with the soot, since the concentrations alone do not give a measure of total amount of a specie present. Since it is of great interest to know how much NO is bound to the soot (and hence escapes measurement by the chemiluminescent analyzer) compared to how much NO is in the gas phase, an experiment was performed to estimate the ratio of the NO in the soot to the NO in the gas phase.

The experiment is shown schematically in Figure 11. An uncooled collector was set up which allowed sampling of the product gases 13 centimeters above the point where the collector is attached to the product gas piping. The sample line had a 7 micrometer filter at the end of it which seemed adequate to trap all of the soot which entered the sampling system. The .52 cm diameter cylinder was used to provide a flame for 30 minutes, during which time NO and NO<sub>x</sub> measurements were made in the manner described earlier. Since the

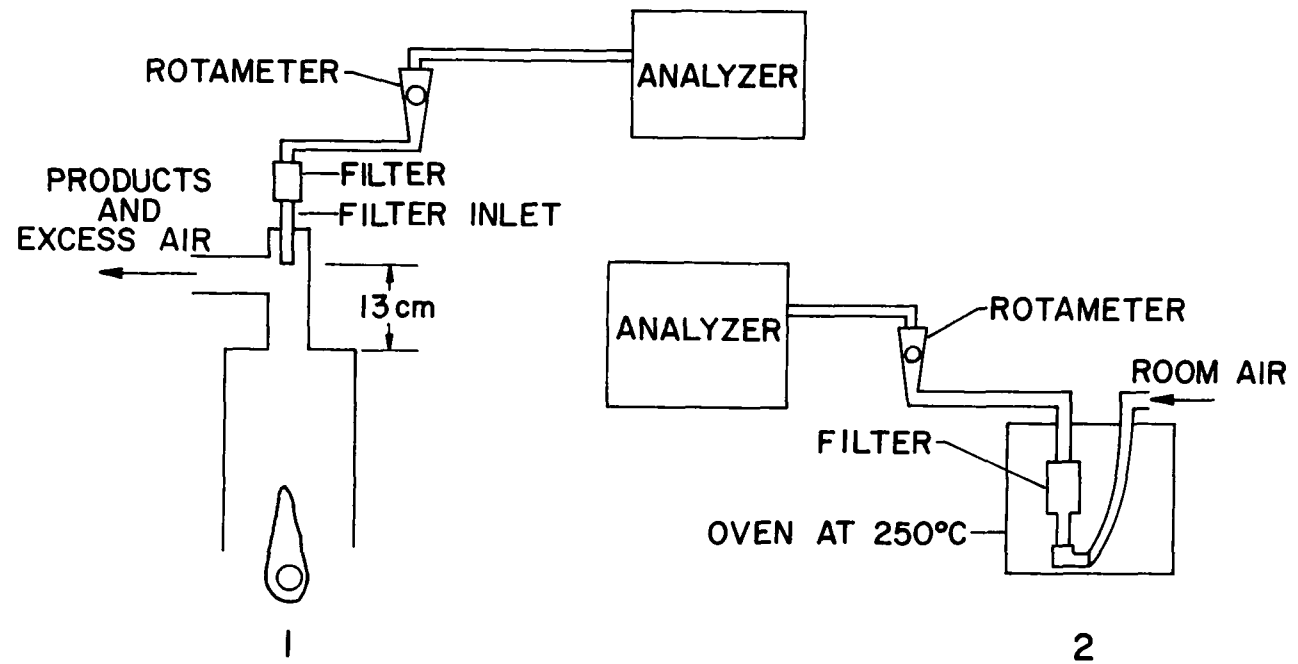


Figure 11. Apparatus Used to Measure Amount of  $\text{NO}_x$  in the Soot. In 1, Soot is Collected in Inlet Tube and on Filter. In 2, Filter and Tube are heated to Drive Off  $\text{NO}_x$ .

filter and filter inlet tube were initially clean, the soot which accumulated in them was due entirely to the combustion gases which were pulled through the sampling system. The sampling system flow rate was measured by rotameter to be 43 liters per hour, and the concentrations of NO and NO<sub>x</sub> were 5.2 and 7.1 parts per million. The amount of NO and NO<sub>x</sub> which is associated with the gas portion of the sample stream can then be calculated, and is given in Table 1. The sooted filter was then placed in an oven and raised to a temperature of 250°C, during which time a flow of 40 liters/hour of room air was passed through the filter and the concentration of NO<sub>x</sub> was measured by the strip chart recorder. The concentration reading rose to a maximum of 4 PPM and fell to room level in about two hours.

The resulting curve was integrated over time to yield the amount of NO<sub>x</sub> which was associated with the soot, and this value is also given in Table 1. The amount of NO shown in the table is an estimate based on the fact that in this type test the ratio of concentrations of NO/NO<sub>x</sub> appeared to be about .9. Since it was only possible to monitor either NO or NO<sub>x</sub> as a function of time, spot checks of the second specie (NO) are the basis of the estimate.

It may be argued that not all the NO<sub>x</sub> was driven off of the soot by heating it to 250°C, but for lack of a hotter oven this is the temperature the data are for. Assuming that the sum of the measured gas phase NO<sub>x</sub> and the measured soot bound NO<sub>x</sub> accounts for all the NO<sub>x</sub> produced by the flame, the percentage of the total NO<sub>x</sub> which is "missed" by using the gas phase estimates alone is 16%. Since the measurements in this report are based on measured gas phase NO/NO<sub>x</sub> only, it is clear that they would need to be adjusted upwards by about 19% to account for all the NO produced. This assumes that the ratio NO gas phase/NO soot is a constant over all experimental conditions measured, which is not known to be true at this time.

Table 1. AMOUNTS OF NO AND NO<sub>X</sub> IN SOOT AND BULK GASES

	NO	NO <sub>X</sub>
g mols from gas phase measurements	$5.0 \times 10^{-6}$	$6.8 \times 10^{-6}$
g mols from sooted filter and inlet tube	$1.2 \times 10^{-6}$ (ESTIMATE)	$1.3 \times 10^{-6}$

Several tests were run to verify whether the parameters which are assumed to be immaterial to the experiment did indeed have negligible effects on the measured emission indices. These tests are discussed in this section.

The flow rate through the collector-cooler was varied by means of a valve shown in Figure 5 which was located between the blower inlet and the sharp edged orifice. If this flow rate is very small, it seems clear that not all the products of combustion will be pulled into the collector, and the measured emission indices will be too low. As collector flow is increased it is expected that less of the products will escape the collector, and the measured index will increase. Assuming that the collector flow rate does not affect the amount of NO and NO<sub>2</sub> produced by the flame, the emission index should become constant with respect to collector flow rate as the flow rate is increased to the point where all the products are collected. This behavior was observed and periodic checks were made during data taking to insure that the apparatus was operating on the flat portion of the curve.

A second parameter which could conceivably influence the emission index was the rate at which fuel was supplied to the cylinder. Three conditions could be qualitatively identified when cooling water flows to the model were held constant and are shown in Figure 12. In the underfueled condition, the thread appeared dry and the flame did not cover the entire cylinder. The correct fueling rate caused the thread to appear wet and the flame to cover the entire cylinder. In the overfueled condition, the fuel and flame spread out onto the water return jackets. Measurements of the emission indices for these conditions gave the results shown in Figure 13. The NO<sub>x</sub> emission index was virtually unaffected by the fuel flow, but the NO emission index decreased markedly with increasing fuel flow. As far as

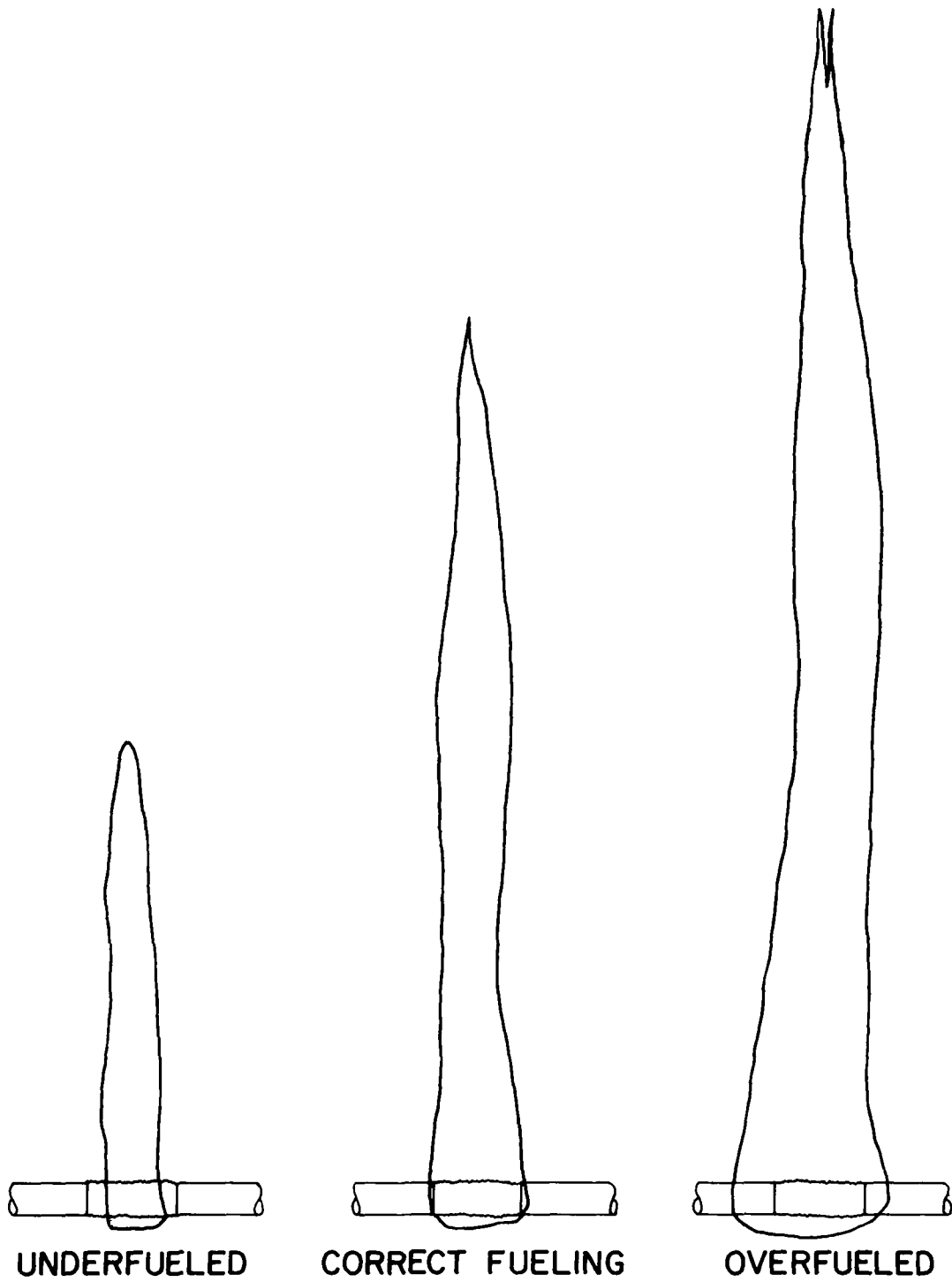


Figure 12. Appearance of Flame at Different Fueling Rates.

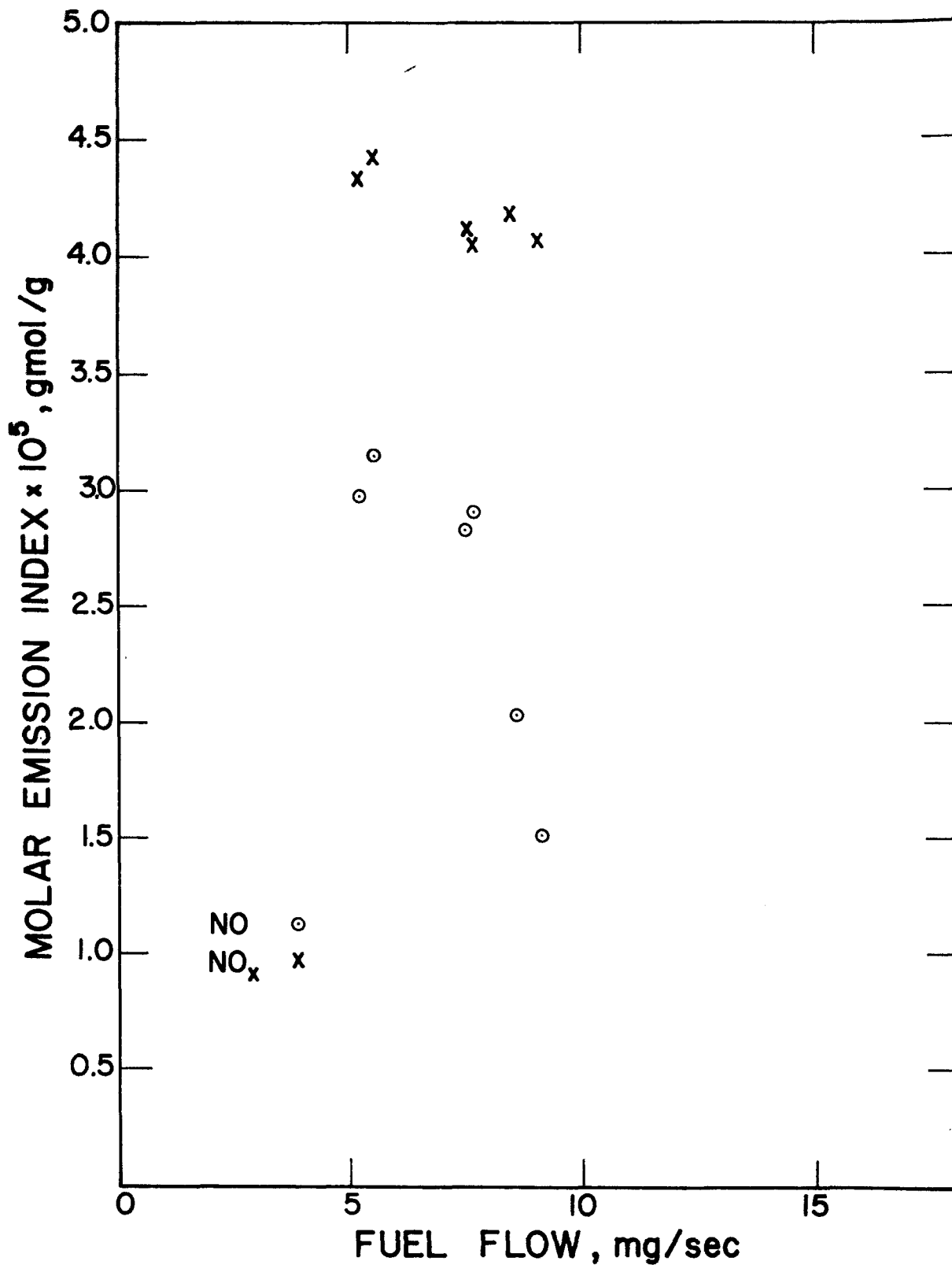


Figure 13. Effect of Fuel Flow Rate on Molar Emission Indices at Constant Cooling Water Flow Rate For .53 x 1.3 cm Porous Cylinder Model in 32 cm/sec Air Stream.

environmental considerations go, it is not very important whether NO or NO<sub>2</sub> is produced, and so it can be argued that the sensitivity of NO emission index to fueling rate is not a reason to abandon the use of experimental models of this type.

It was considered to be of interest to determine where the NO<sub>2</sub> is being formed, and to this end the experiment shown in Figure 14 was performed. A baseline condition was established with the 5.2 x 12.7 mm porous cylinder, and concentration readings of NO and NO<sub>x</sub> were taken. The experiment was repeated as case 1 with a measured flow of calibration gas (NO in N<sub>2</sub>) being added to the collected products at the inlet to the cooler. The measured values of NO and NO<sub>x</sub> both increased by the same amount, indicating that none of the added NO was converted to NO<sub>2</sub> between the cooler inlet and the analyzer. Moving the tube to a position near the bottom edge of the collector gave a similar result, leading one to believe that the production of NO<sub>2</sub> was associated with the flame or the gases immediately surrounding the flame.

The amount of cooling due to the water jacket on each end of the porous cylinder was another parameter which could conceivably affect the results of the experiment. To determine what effect the cooling has, the flow of cooling water was varied and the temperature of the fuel at the center of the porous cylinder was measured with an iron constantan thermocouple. The results are shown in Figure 15. Although the burning rate of fuel increases with temperature as would be expected, the emission indices of NO and NO<sub>x</sub> were virtually unaffected at the cooling rates which gave these fuel temperatures.

The results of the tests on the porous cylinder models using N-Heptane as fuel at ambient air temperatures with no correction for soot bound NO are presented graphically in Figure 16 and in tabular form in Tables 2-5. The averages

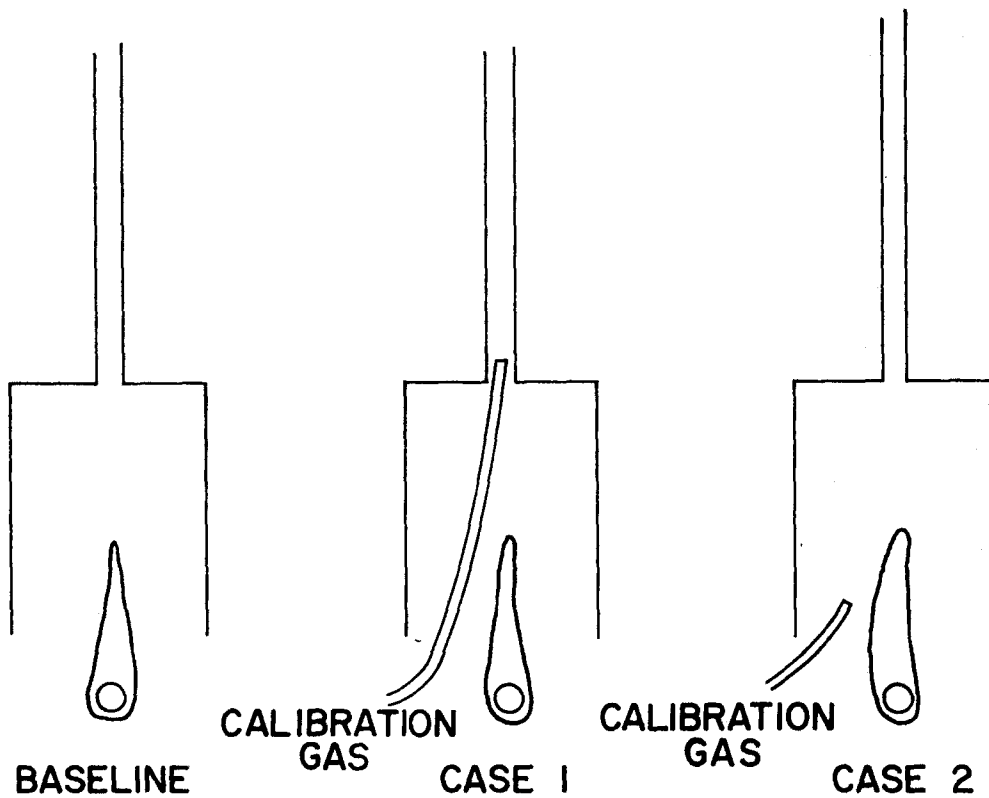


Figure 14. Apparatus for Determination of Where  $\text{NO}_2$  is Produced.

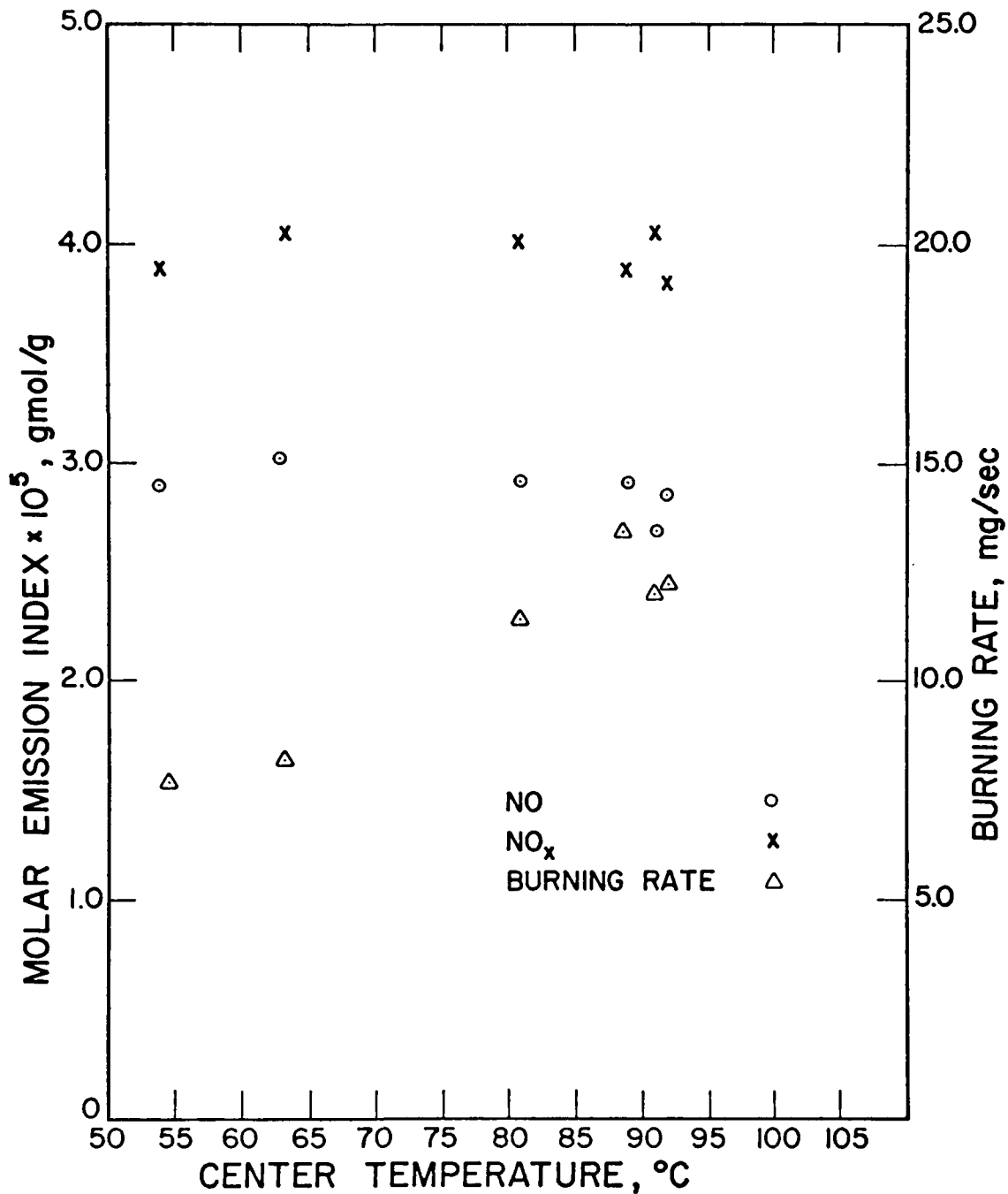


Figure 15. Effect of Fuel Center Temperature on NO and NO<sub>x</sub> Emission Indices and Burning Rate. Center Temperature Varied by Changing Cooling Water Flow Rates. Air Velocity = 32 cm/sec, .52 x 1.3 cm Cylinder.

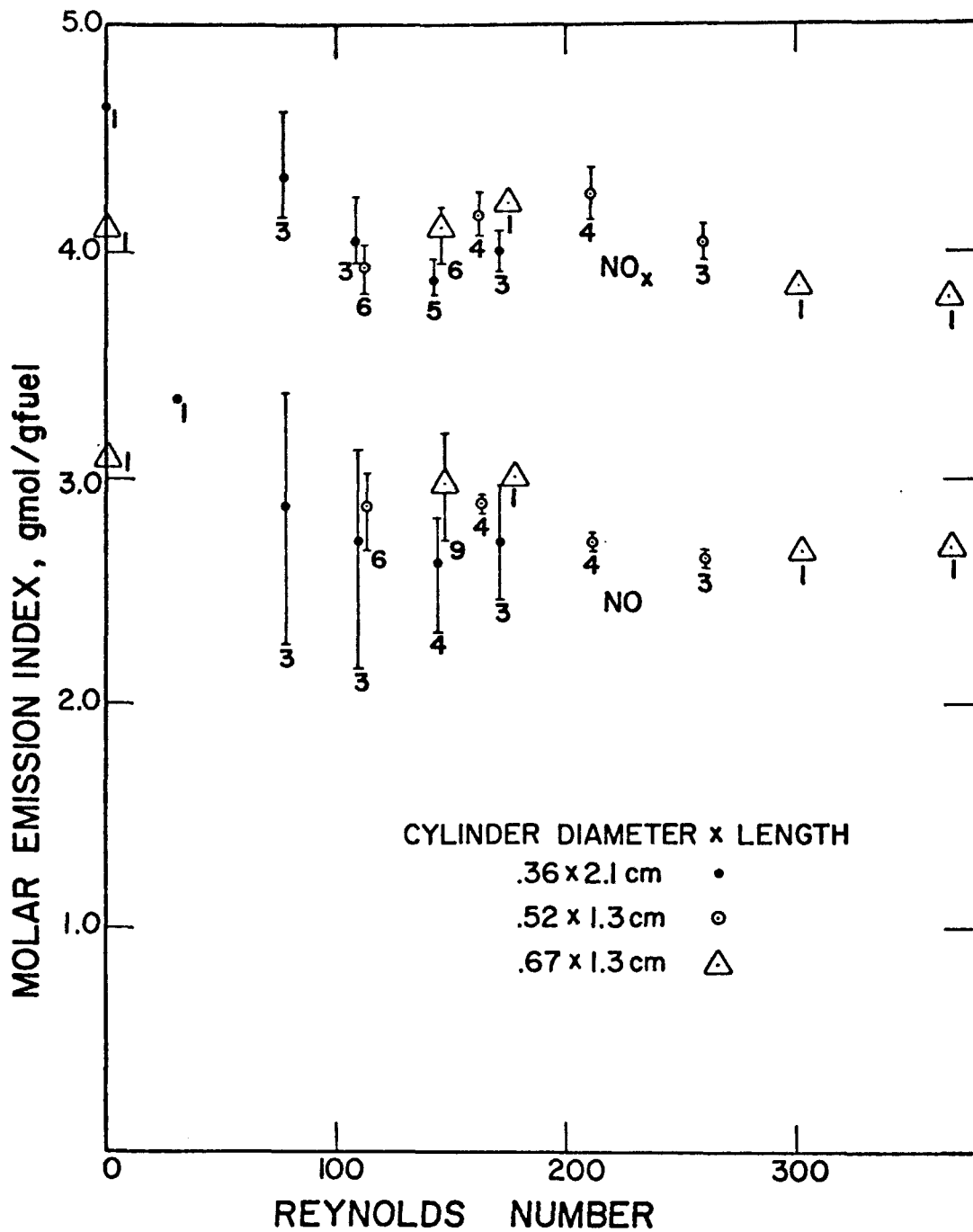


Figure 16. Molar Emission Indices for Porous Cylinder Models Plotted Against Reynolds Number Based on Free Stream Properties. Mean Values are Plotted with Bars Showing Highest and Lowest Measured Values. Number Under Lower Bar Indicates Number of Points Averaged.

Table 2. MOLAR EMISSION INDEX TEST DATA  
CYLINDER .36 x 2.1 cm.

Air Velocity, cm/sec	Reynolds Number	Fueling rate, mg/sec	EI <sub>NO</sub> , gmol/g	EI <sub>NOx</sub> , gmol/g
0	0	8.3	3.56 x 10 <sup>5</sup>	4.64 x 10 <sup>-5</sup>
32	79	11.4	2.26	4.23
32	79	10.2	3.38	4.62
32	79	10.4	3.00	4.15
46	112	12.5	2.15	3.95
46	112	11.7	3.12	4.25
46	112	12.0	2.89	3.96
60	146	14.4		3.85
60	146	13.7	2.32	3.92
60	146	14.0	2.63	3.79
60	146	14.0	2.83	3.97
60	146	14.0	2.68	3.82
71	173	14.4	2.46	3.92
71	173	13.1	2.98	4.09

Table 3. MOLAR EMISSION INDEX TEST DATA  
CYLINDER SIZE .52 x 1.3 cm.

	Air Velocity, cm/sec	Reynolds Number	Fueling rate, mg/sec	Fuel temperature, °C	EI <sub>NO</sub> , gmol/g	EI <sub>NO<sub>x</sub></sub> , gmol/g
	32	114	7.7	54	2.90 x 10 <sup>-5</sup>	3.89 x 10 <sup>-5</sup>
variable cooling	32	114	8.3	63	3.02	4.03
water flows	32	114	11.4	81	2.92	4.01
with "correct"	32	114	13.4	89	2.90	3.88
fuel feeds	32	114	12.2	92	2.85	3.82
	32	114	12.0	91	2.68	4.03
cooling water	32	114	7.7	-	2.55	4.05
flow constant,	32	114	9.1	-	1.50	4.03
variable	32	114	5.2	-	2.97	4.34
fuel feed	32	114	7.5	-	2.82	4.12
	32	114	8.6	-	2.02	4.16
	32	114	8.6	-	2.02	4.16
	32	114	5.5	-	3.15	4.43

Table 4. MOLAR EMISSION INDEX TEST DATA  
CYLINDER SIZE 0.52 x 1.3 cm.

Air Velocity, cm/sec	Reynolds Number	Fueling rate, mg/sec	EI <sub>NO</sub> , gmol/g	EI <sub>NO<sub>x</sub></sub> , gmol/g
46	165	8.1	$2.93 \times 10^{-5}$	$4.26 \times 10^{-5}$
46	165	8.1	2.86	4.07
46	165	8.1	2.86	4.10
46	165	7.9	2.92	4.21
60	214	9.3	2.72	4.25
60	214	9.3	2.71	4.28
60	214	9.3	2.73	4.14
60	214	9.3	2.73	4.37
73	263	10.2	2.62	4.03
73	263	10.2	2.67	3.96
73	263	10.2	2.62	4.12

Table 5. MOLAR EMISSION INDEX TEST DATA  
CYLINDER SIZE 0.67 x 1.3 cm.

Air Velocity, cm/sec	Reynolds Number	Fueling rate, mg/sec	EI <sub>NO</sub> , gmol/g	EI <sub>NO<sub>x</sub></sub> , gmol/g
0	0	5.8	$3.11 \times 10^{-5}$	$4.11 \times 10^{-5}$
32	146	6.7	3.02	4.20
32	146	9.1	2.91	4.17
32	146	9.3	2.85	4.01
32	146	9.5	2.88	4.11
32	146	9.5	3.16	-
32	146	9.5	2.88	-
32	146	9.5	3.16	-
32	146	9.3	3.19	4.20
32	146	16.1	2.72	3.95
39	178	9.3	3.00	4.23
66	303	11.0	2.67	3.84
80	366	11.7	2.69	3.79

of the data are plotted against a Reynolds number based on the properties of air at the approach stream condition. Within the range and repeatability of the data, the emission indices are relatively unaffected by Reynolds number and do not seem to vary significantly due to diameter or air stream velocity alone.

It is regrettable that due to equipment problems with the air heating system we were unable to obtain data for the high temperature air stream. The emission index measurements to date do not seem to be highly sensitive to the independent parameters varied during our investigation. It will be of great interest to see if the sensitivity to ambient temperature (predicted by simple analytical models) can be demonstrated experimentally, and also to see what effect the addition of product gases to the ambient air stream has on emission indices.

Attempts to obtain concentration profiles for NO around porous cylinder models produced unexpected results. The profiles appear to have two maxima, one near the surface of the model and the other on the air side of the luminous zone, as shown in Figure 17. This type of profile has also been reported by Hart et al.<sup>1</sup> for measurements along the stagnation line of porous cylinders burning N-Heptane doped with pyridine. If the data are correct, then there is production of NO in the cool and relatively oxygen free region near the surface of the simulated droplet. The dip in concentration between the two maxima then indicates that a destruction reaction or absorption mechanism exists. Both these phenomena are not predicted by the familiar Zeldovich kinetics and leads one to question whether the dip in the profile is an artifact due to the disturbance introduced by the probe. However, the discovery of the interaction between soot and NO provides a possible basis for a NO gas phase concentration reduction mechanism, since soot formation and the reactions leading up to it may be expected to

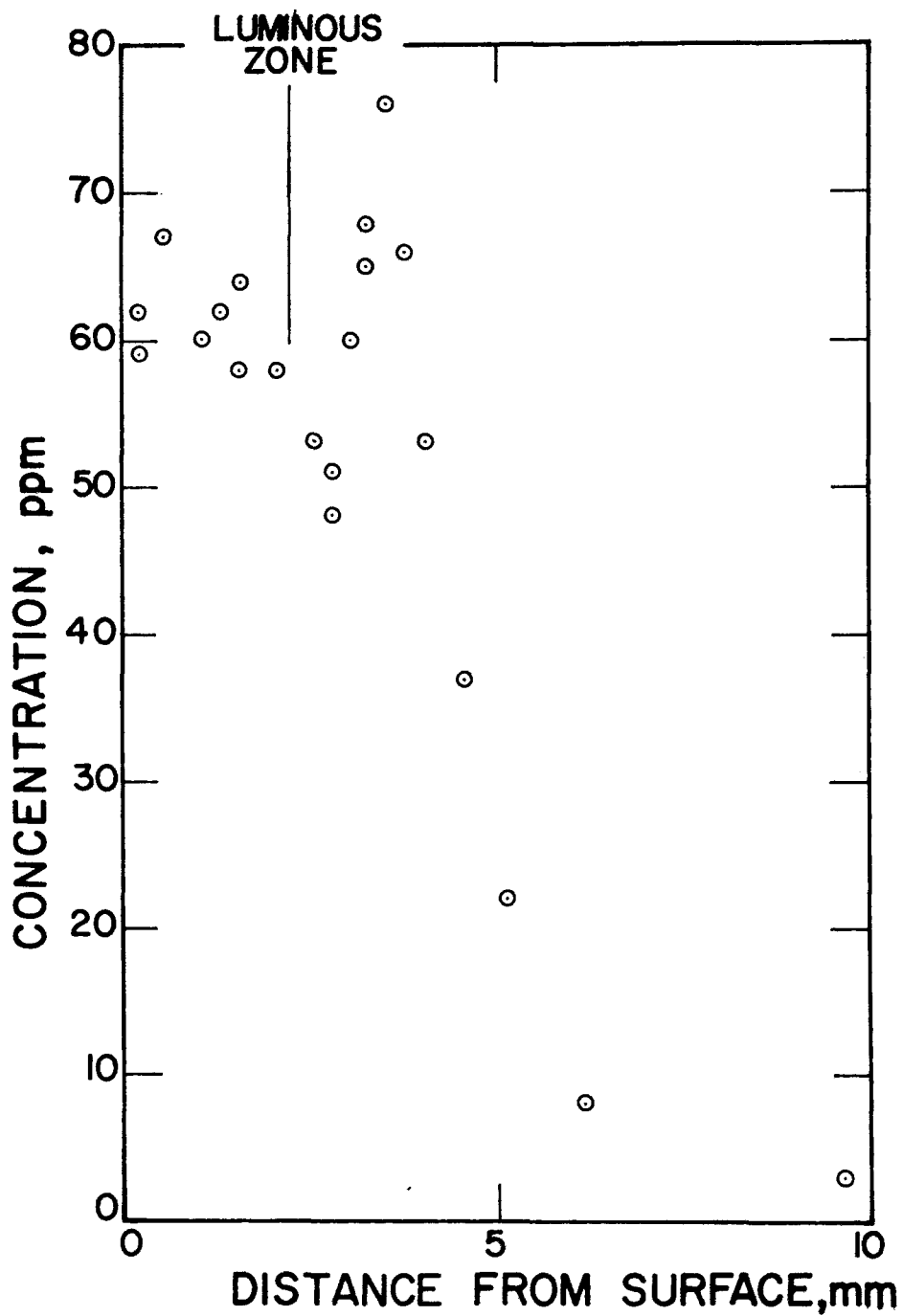


Figure 17. NO Concentration Profile 90° From Stagnation Point of a 1.3 cm Porous Cylinder Model. Air Velocity = 30 cm/sec.

take place in the region of the minimum. If this is true, the soot may then be thought of as a "sink" for gas phase NO in the region where the minimum in NO concentration occurs, and such a dip in the profile would be expected to occur. Some portion of the NO trapped by or reacted with the carbon may be driven off as the carbon goes through the wake region and is oxidized and/or heated. The NO remaining with the carbon that escapes from the flame may thus be only a small portion of the NO which has reacted with carbon inside the flame envelope. Clearly the entire area of carbon NO interaction within the flame and its resulting products deserves considerably more study.

## REFERENCES FOR SECTION V

1. Hart, R., M. Nasralla, and A. Williams. The Formation of Oxides of Nitrogen in the Combustion of Droplets and Sprays of Some Liquid Fuels. Combustion Science and Technology. 11:57-65, July 1975.

SECTION VI  
THE DIVIDED CHAMBER ENGINE EVALUATION AND  
TEXACO ENGINE PROJECTS

INTRODUCTION

Recent years have seen the expenditure of large quantities of research time and money in the quest for alternative internal combustion engine configurations. The primary motivation for these efforts has been the ever increasing pressure of federal legislation for cleaner and more fuel efficient personal transportation. Proposed standards for exhaust emissions and fuel economy were straining the capability of conventional homogeneous charge and diesel engines, prompting the search for hybrid combustion systems.

The original purpose of the research carried out under the current grant (R-803858-01-1) was to complete the analysis of one such hybrid, the divided combustion chamber engine, and to begin a study of the mechanism of unburnt hydrocarbon formation peculiar to the divided chamber combustion system.

Prior research on the divided chamber concept, carried out at the University of Wisconsin, demonstrated its ability to reduce emissions of the oxides of nitrogen ( $\text{NO}_x$ ) and carbon monoxide (CO) to levels below those of conventional engines. However, its emission of high concentrations of unburnt hydrocarbons (HC), and its high specific fuel consumption demanded further attention.

All of this prior divided chamber work had been run under naturally aspirated unthrottled intake conditions and consequently over a limited load range. In order to gain a more complete picture of the engines overall flexibility, as well as its future potential, part load testing was initiated. Three methods for achieving a broader load

range were tried: fuel stratification within the prechamber, reduction of prechamber volume and intake air throttling. As will be explained in the report, the first two approaches proved unsatisfactory while intake throttling, in conjunction with fuel injection and ignition parameters, enabled a reasonably broad range of operation.

Emissions and fuel consumption data from these tests, (to be presented later in this report) along with the unthrottled test results, were compared with available data for a number of other promising hybrid engines as well as data from conventional homogeneous charge spark ignition and diesel engines. This comparison showed that while emissions from the divided chamber engine are comparable to those from other hybrid combustion systems such as the Ford PROCO and the Texaco TCCS, its specific fuel consumption is 20 to 50 percent greater throughout its useable load range. The comparison also brought out the fact that the upper output limit (IMEP) available from the divided chamber engine in its naturally aspirated form was substantially lower than conventional homogeneous charge and diesel engines and most of the hybrid engines as well.

Further tests (presented in a later section of this report) using a modified ignition system showed the fuel consumption picture somewhat improved at light to medium loads but still some 15 to 30 percent higher throughout the load range than the other engines studied in the comparison. In addition to these tests, a number of unthrottled runs were conducted using fuel blends having octane numbers in the range of currently available motor fuels. These tests indicated a degree of octane sensitivity in the divided chamber engine, and examination of combustion pressure traces showed what appeared to be incipient knock. This condition seemed to preclude turbocharging as a means for extending the output limit of the divided chamber engine.

The results of all of these tests, as well as the comparison study, were presented to the EPA grant monitor at the grant review meeting. The merits of further study of the divided chamber engine were weighed and it was decided that because of its poor fuel consumption characteristics and its limited load range, the divided chamber engine held limited prospect as an alternative vehicle powerplant. Accordingly, it was concluded that there would be minimal interest in a study of the mechanism of unburnt hydrocarbon formation peculiar to the divided chamber engine and that the intent of the grant would be better served by a study of the origins of unburnt hydrocarbons in a stratified charge combustion system of recognized potential.

It was suggested that the Texaco TCCS stratified charge engine be given serious consideration as a candidate for this study. Vehicle applications of the TCCS had clearly demonstrated its excellent fuel economy and low emissions qualities as well as its multifuel capability.

An extensive search of heterogeneous combustion literature was conducted to determine the extent of knowledge of hydrocarbon formation in such systems. Literature dealing with sampling techniques which might lend themselves to such a study were also reviewed.

Because of the rapid spatial and temporal variation of burning stoichiometry occurring in heterogeneous combustion systems, it was felt that the most informative technique by which some understanding of unburnt hydrocarbon formation occurring in such systems might be obtained would be a high resolution, in-cylinder sampling device which was not limited to use solely in the clearance volume of the engine. In order to obtain the degree of resolution desired and avoid the possible masking effect of quench layer formation at the sampling orifice, it was felt that such a device should utilize the continuous flow concept first developed by Rhee.<sup>1</sup> It was agreed that the development of such a device could

proceed in conjunction with and as a means to enable the study of hydrocarbon formation in the Texaco combustion process.

The next step taken was to contact the U.S. Army TACOM and seek their assistance in determining the feasibility of using a TCCS engine for the hydrocarbon study. They provided detailed drawings of two versions of the TCCS engine which were then studied with a view to accessibility for installation of the proposed sampling device. It was found that the original single cylinder M-151-TCP engine, designed by Texaco for TACOM and based on the L-141 cylinder block, held the most promise for our purposes.

TACOM was contacted again and queried about the possibility of obtaining one of these engines. After a series of negotiations, a single cylinder M-151-TCP engine was transferred from TACOM to the University of Wisconsin.

The engine has since been completely overhauled. An engine support stand has been fabricated and the engine has been installed into an engine test cell and coupled to an electric dynamometer. The installation and instrumentation of the engines' peripheral systems is nearing completion as of this writing and initial run in of the engine will begin shortly.

#### EXPERIMENTAL APPARATUS FOR DIVIDED-COMBUSTION CHAMBER ENGINE STUDIES

The design and construction of the experimental set up used for the divided chamber engine tests has been described in detail by El-Messiri<sup>2</sup>. However, since a number of hardware changes were subsequently incorporated, a brief description will be given here. The engine used for these tests was a Waukesha CFR-48 cetane engine. The secondary "quench" volume for the divided chamber design was created by inserting a surface ground spacer plate of appropriate thickness between the cylinder block and head. The thickness of this plate was calculated after selecting the

desired compression ratio and the ratio of primary to total combustion chamber volume. For all of the part load testing these values were set at 8:1 and 0.65:1 respectively. These values were selected as a judicious compromise between desired emissions levels versus fuel economy and power output. They do not reflect a truly optimized configuration. The orifice connecting the quench region with the standard cetane combustion chamber, hereafter designated the primary chamber, was enlarged by El-Messiri to an orifice to piston diameter ratio of 0.10. El-Messiri's tests were run with a Bosch model ADN-30-S3 Pintle type nozzle mounted in the standard cetane engine location. A standard CFR ignition system was used in conjunction with an extended tip 14 mm spark plug mounted in a sleeve designed to replace the variable compression plug assembly.

The following hardware changes were made prior to the final part load test program. The Bosch injection nozzle was replaced with a proprietary "soft spray" vibrating pintle nozzle having a spray cone angle of  $80^\circ$  and an injection pressure of  $\sim 1700$  kPa. The nozzle was moved from its original location to the opposite end of the primary chamber in place of the spark plug. The ignition system was replaced with a high energy capacitive discharge unit in order to accommodate the use of larger spark plug gaps ( $\sim 1$  mm) and provide a more reliable source of ignition. An adaptor was built to permit installation of a 10 mm motor-cycle spark plug in the original injection nozzle location. The once through cooling system used by El-Messiri was replaced with the standard CFR evaporative cooling tower so that a more stable coolant temperature could be maintained.

All results reported here were obtained with the engine configuration just described. Table 6 summarizes the engine operating conditions maintained during the tests except as noted, all tests were run with iso octane as the engine fuel.

Table 6. DIVIDED CHAMBER ENGINE - OPERATING  
CONDITIONS TESTED

Compression Ratio	C.R. = 8:1
Primary to Clearance Volume Ratio	$\beta = 0.65$
Orifice to Piston Diameter Ratio	$\alpha = 0.10$
Speed	900 RPM
Ignition Timing	MBT
Injection Timing	105° & 70° BTDC
Overall Fuel-Air Equivalence Ratio	0.5 - 1.0
Degree of Air Throttling	0 - 60%

## TEST RESULTS FROM PRELIMINARY PART LOAD CONFIGURATIONS

Three methods of achieving part load operation were examined during the exploratory phase of the testing program. Charge stratification within the primary chamber was believed to be a possible approach because earlier undocumented testing by El-Messiri had implied that this phenomena was occurring. The engine configuration selected for the part load evaluation was essentially the same as that used by El-Messiri at the time he noted apparent stratification, so it seemed expedient to examine this approach first. The Bosch Pintle injection nozzle was retained in its original location and the spark gap was positioned in the location specified by El-Messiri. The engine was run unthrottled over a range of speeds (800-1800 RPM) and equivalence ratios but the resulting data were not indicative of the type of stratification sought. The experiences of Ford and Texaco with stratified charge engines have shown that stratification is extremely difficult to maintain over the range of operating loads imposed on a vehicle powerplant. Accordingly, it was decided to abandon this approach and explore more conventional methods of part load operation.

The second technique tried was throttling of the intake air. The procedure was to set the throttle for the desired degree of air flow restriction and to vary the injection pump rack setting to obtain a spread of fuel-air equivalence ratios. Again the results proved somewhat disappointing. As the degree of throttling was increased, misfiring occurred with greater frequency causing extremely high concentrations of unburnt hydrocarbons in the exhaust. Examination of the spark plug insulator and the surrounding combustion chamber surfaces showed a large build up of soot. What appeared to be happening was that the reduced air density in the primary chamber due to throttling was allowing increased penetration of the injection spray with subsequent wetting of the chamber walls and the spark plug.

Hardware changes were indicated, but it was decided to proceed with the third approach before altering any equipment.

The third method used to achieve part load operation was to reduce the volume of the primary combustion chamber while maintaining the secondary "quench" volume constant. The net effect was to increase the compression ratio while reducing the relative proportion of combustible mixture. This was accomplished by increasing the depth of the spark plug mounting sleeve. It was hoped that the increase in compression ratio would alleviate some of the fuel spray penetration problem, but the test results indicated that this effect was more than offset by the shorter distance between the spark plug and the injection nozzle. The misfire problem was more severe than it had been with air throttling resulting in loss of power, increased specific fuel consumption and high hydrocarbon emissions. It was decided to discard this technique altogether since it was, from the viewpoint of practicality, the least feasible of the three methods and to concentrate on the throttling approach to part load operation.

The hardware changes made in an effort to cure the problems encountered during the throttling phase of the initial testing program were detailed in the section on experimental apparatus. However, in the interest of continuity, they will be reviewed again briefly. In order to reduce fuel spray penetration related problems, a nozzle having both a lower operating pressure and a broader spray cone angle was needed. The Ford Motor Company was kind enough to loan us a proprietary vibrating pintle nozzle having both a low operating pressure and good quality of atomization as well as a broad spray cone angle. In order to improve fuel spray distribution, this nozzle was mounted on the primary chamber centerline axis at the end of the chamber opposite the original injector nozzle. The spark plug was mounted in the original injector location, directly over the connecting orifice, and the ignition system was

replaced with a high-energy, long-duration capacitive discharge unit. Figure 18 shows the general hardware layout used for the remainder of the part load testing. Initial tests after these modifications indicated improved consistency of combustion and generally smoother operation.

The final test procedure was worked out during the initial testing sequence on the engine. It was decided to run tests at five different throttle settings and two different injection timings. Table 6 lists the operating conditions selected. The procedure was to start the engine and allow it to run unthrottled at the desired test speed until conditions stabilized, i.e., coolant and lubricating oil temperature and ambient air temperature. At this point, the atmospheric pressure and wet and dry bulb temperature in the test cell were measured and recorded. The rate of air consumption of the engine was measured using a Meriam laminar flow element and the throttling valve was then set to give the desired degree of throttling. For example, if the test was to be run with the engine 30 percent throttled, the throttling valve was set to achieve a rate of air consumption equal to 70 percent of the unthrottled rate at the same speed. This done, the throttle was locked in place and the injection pump rack was adjusted to determine the leanest operating point. The ignition timing was adjusted to obtain the best torque at this rack setting and the engine was allowed to stabilize at this condition.

Fuel consumption was measured using an electro-optical gravimetric weighing system. Engine RPM and load were recorded as were emissions data. Exhaust samples were taken downstream of an exhaust mixing tank having a volume of approximately ten times the cylinder displacement. The sample was first run through a particulate filter, thence through an ice bath and finally through a dessicant tube before entering the emissions analysis equipment.

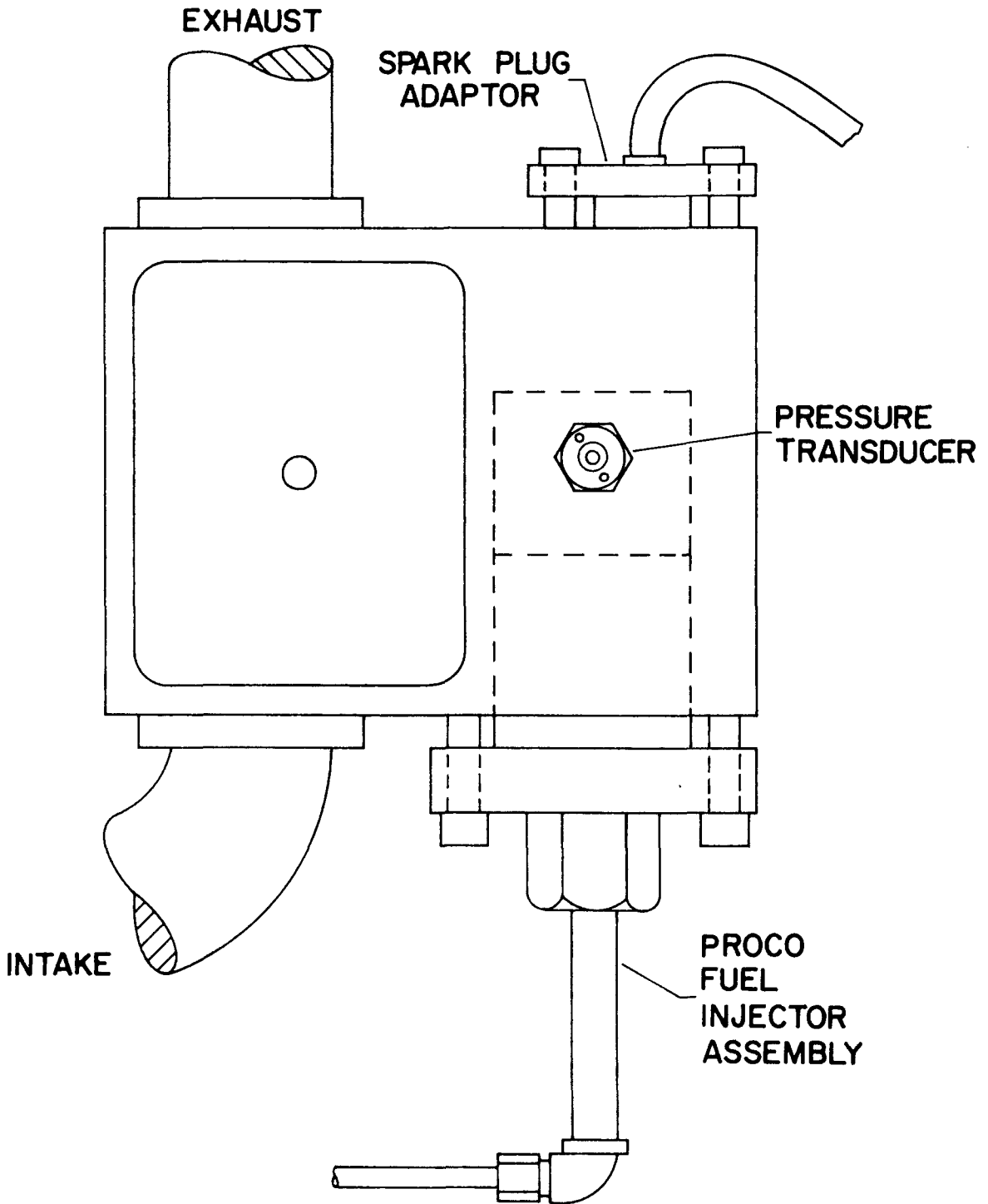


Figure 18. Divided Chamber Engine Cylinder Head (Top View) Final Part Load Hardware Configuration.

Hydrocarbon concentration was measured with a Beckman Model 109A unheated flame ionization detector (FID), carbon monoxide was measured using a Beckman model IR-15A non dispersive infrared detector with a 0 to 3 percent range and a Thermo-Electron Model 10A chemiluminescent analyzer was used to measure NO and NO<sub>x</sub>.

Once the data points were recorded, the injection pump rack was reset to give a slightly richer fuel-air ratio and the ignition-timing was adjusted to give maximum torque. After stabilization, a new set of data were recorded. This procedure was repeated to yield a spread of fuel-air equivalence ratios from 0.5 to 1.0.

Each set of data were processed by means of a computer program to obtain specific fuel consumptions, mean effective pressures, specific emissions rates and other quantities of interest for purposes of plotting and final analysis.

#### PRESENTATION AND DISCUSSION OF TESTS OF FINAL PART LOAD CONFIGURATION

Figures 19 through 28 are plots of recorded emissions concentrations of NO, CO and HC and calculated values of specific fuel consumption (ISFC) and mean effective pressure (IMEP) versus overall fuel-air equivalence ratio  $\phi$ .

Figures 19 and 20 show the variation of NO with both  $\phi$  and throttle for the 105° and 70° BTDC start of injection respectively. Recall that the region of the combustion chamber to which fuel is initially introduced constitutes only the fraction  $\beta$  (0.65 for these tests) of the total combustion chamber volume. If it can be assumed that the fuel-air equivalence ratio in the primary chamber can be reasonably approximated by  $\phi_{\text{primary}} = \phi_{\text{overall}}/\beta$ , then an interesting point about these graphs can be noted. (It is recognized that this assumption is not strictly correct. In all probability, a larger fraction of residuals remains in the pre-chamber than in the main chamber. Hence, the resulting fuel air mixture in the prechamber will be slightly richer than that predicted by the above assumption. However, it is

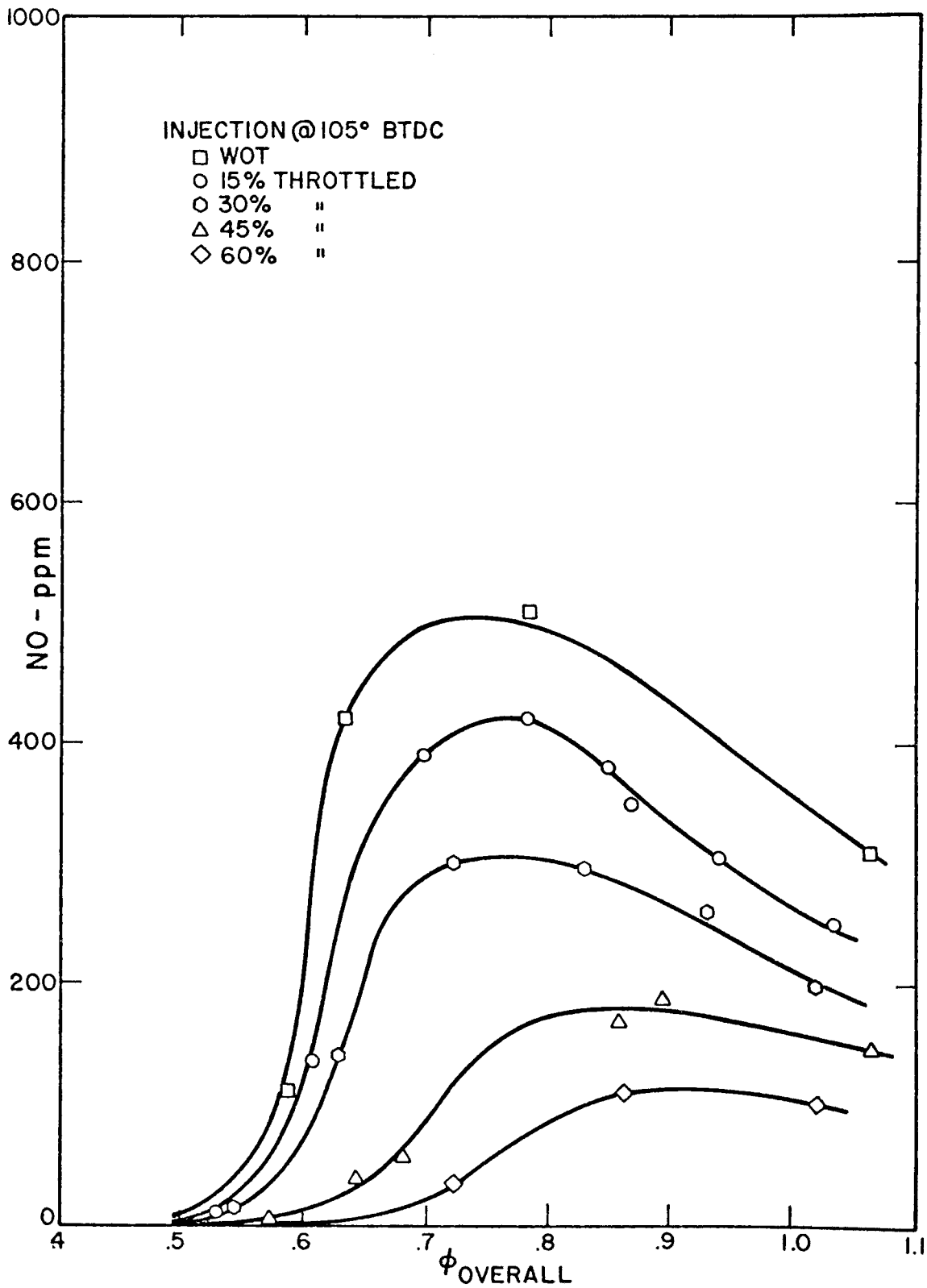


Figure 19. Measured NO Concentration Versus Overall Equivalence Ratio - 105° BTDC Injection.

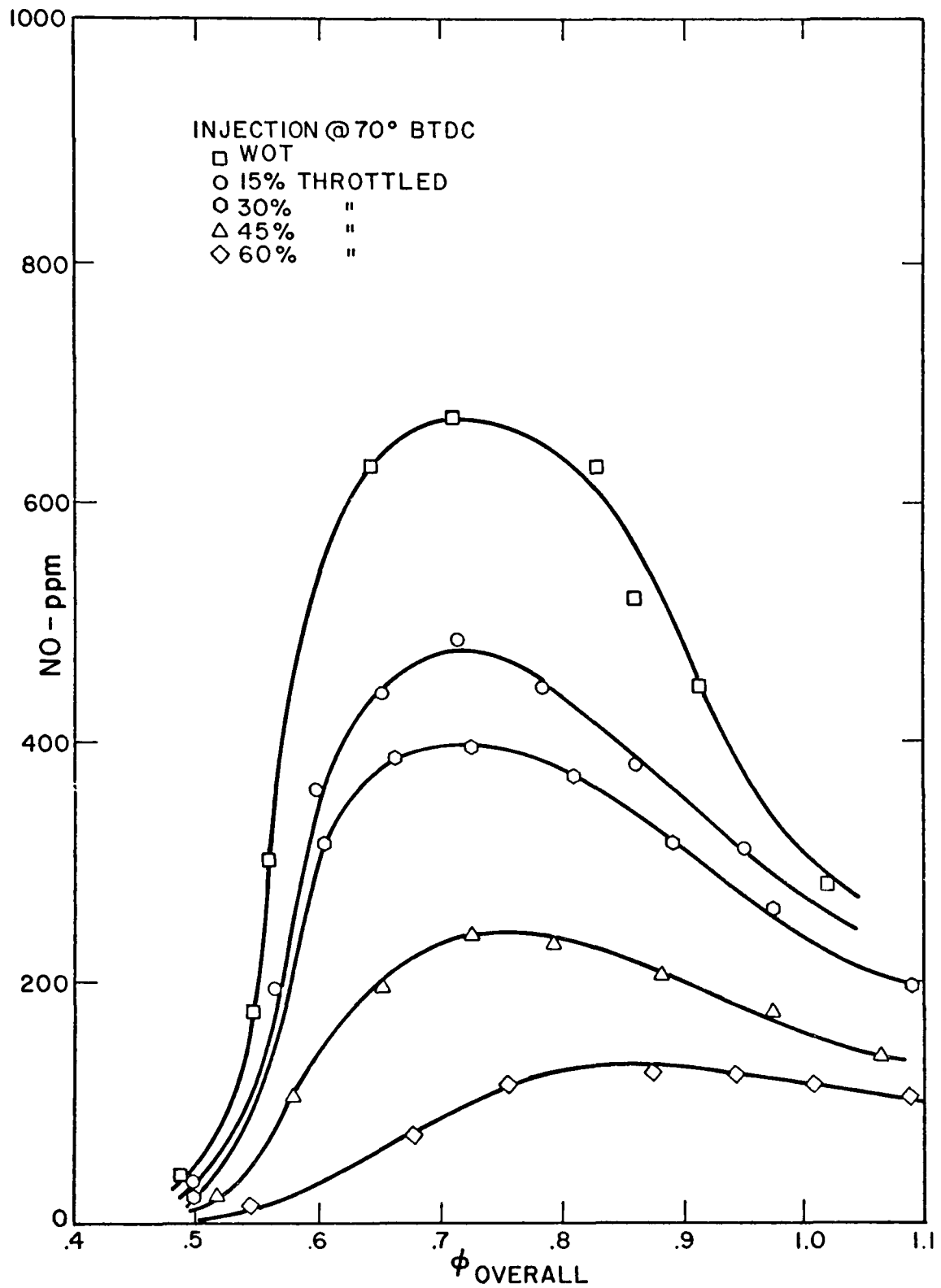


Figure 20. Measured NO Concentration Versus Overall Equivalence Ratio 70° BTDC Injection.

believed that this shift will be quite minor and will not significantly alter any of the results presented here.) Unlike homogeneous charge engines, the peak in NO concentration for the divided chamber occurs slightly on the rich side of stoichiometric. This seems to indicate that NO formation is occurring in the secondary chamber. A reasonable explanation for this behavior can be offered. As the hot products leave the primary chamber and begin to mix with the secondary air a mixing interface is formed. It seems reasonable to expect that NO formation reactions will occur at this interface, at least early in the expansion. If we were able to correctly calculate the portion of air in the secondary chamber which takes part in these NO reactions, we expect that a plot of NO concentration versus fuel-air equivalence ratio, calculated for the primary chamber plus this additional air, would show that the peak NO concentration would occur on the lean side as it does in the homogeneous engine.

We note too that the concentration of NO increased with the later injection timing. This rise is due to an increase in power output which resulted from the later timing. It is believed that less of the injected fuel was sprayed on the chamber walls at the later timing due to the higher air density. Figures 23 and 24 show that hydrocarbon emissions decreased as a result of the retarded timing, which seems to bear out this theory. Therefore, more of the fuel burned during the early part of the combustion process with the later timing producing higher pressures and temperatures which resulted in increased NO formation.

Figures 21 and 22 display measured percent CO versus  $\phi$  and degree of throttling for the two injection timings. We note that the minimum percent CO occurs at roughly the same equivalence ratio for both timings and that the shape and position of the curves are approximately the same also. This seems to agree with the general consensus that CO is a function primarily of fuel-air ratio alone.

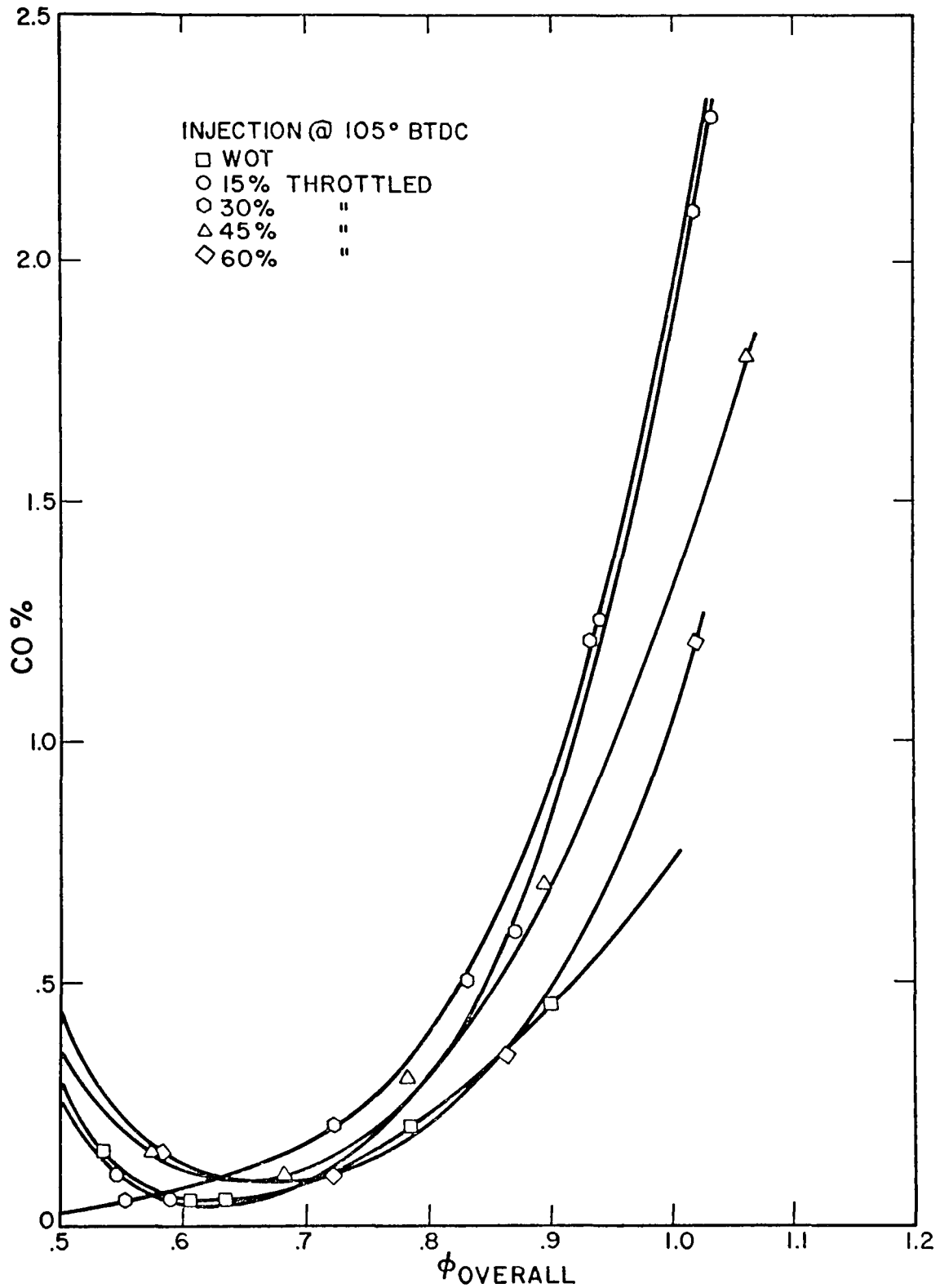


Figure 21. Measured CO Concentration Versus Overall Equivalence Ratio 105° BTDC Injection.

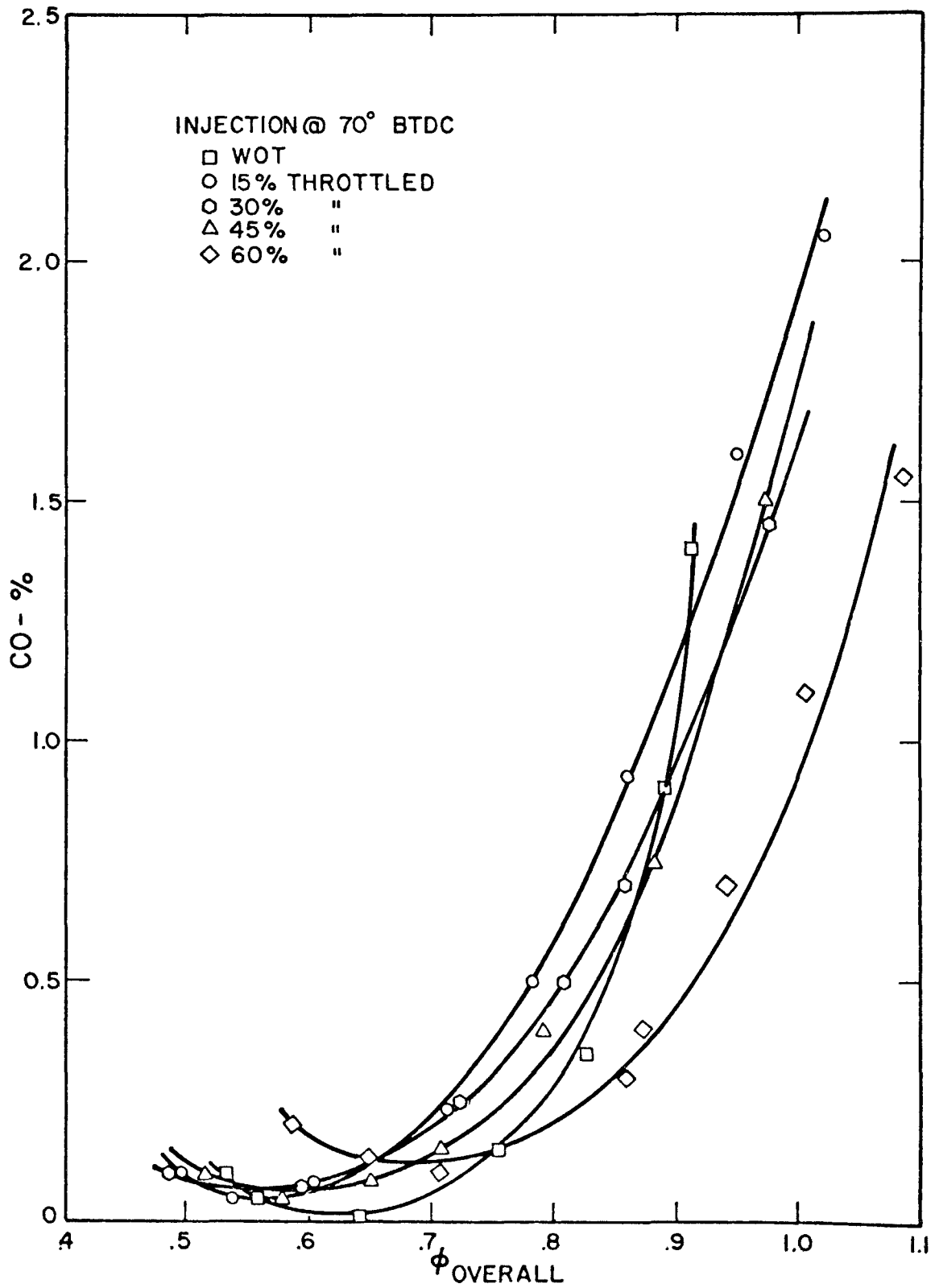


Figure 22. Measured CO Concentration Versus Overall Equivalence Ratio - 70° BTDC Injection.

If we again assume that the equivalence ratio in the primary chamber can be approximated by the overall ratio divided by the volume fraction  $\beta$ , we can note another measure of the reactions occurring in the secondary chamber. At an overall equivalence ratio of 0.8, the ratio in the primary chamber would be 1.23. Reference to Obert<sup>3</sup> shows that for iso octane there should be about 5.5 percent CO in the products entering the secondary chamber. This is more than ten times the value measured in the exhaust from the divided chamber engine. Clearly, substantial oxidation is occurring in the secondary chamber as intended.

One last point might be mentioned. As the fuel-air ratio is leaned beyond the minimum CO point, the percent CO begins to rise. It is thought that this is due to reduction in the destruction of CO in the quench region caused by lower overall gas temperatures resulting from combustion. This occurs because the already slow burning rate of the lean mixtures is further slowed by dilution of the combustible mixture with the residual fraction of exhaust products remaining in the primary chamber from cycle to cycle.

Figures 23 and 24 present measured HC concentration versus overall equivalence ratio as a function of throttling. We can see that at all throttle settings, HC emissions increase rapidly as  $\phi$  is decreased from 0.7 to 0.5. It is thought that this increase in HC is due primarily to the decreasing average gas temperature resulting from combustion and the attendant slowing of hydrocarbon oxidation reaction rates. Note also that the equivalence ratio at which this rapid increase in HC begins increases with decreasing intake manifold pressure. This occurs because the exhaust residual fraction increases with decreasing intake pressure, lowering the flame temperature and slowing down the oxidation reactions. As the overall fuel-air ratio is increased and approaches stoichiometric, HC emissions again begin to rise. It is believed that this is due to increased deposition of fuel on the surface of the primary chamber and resultant wall

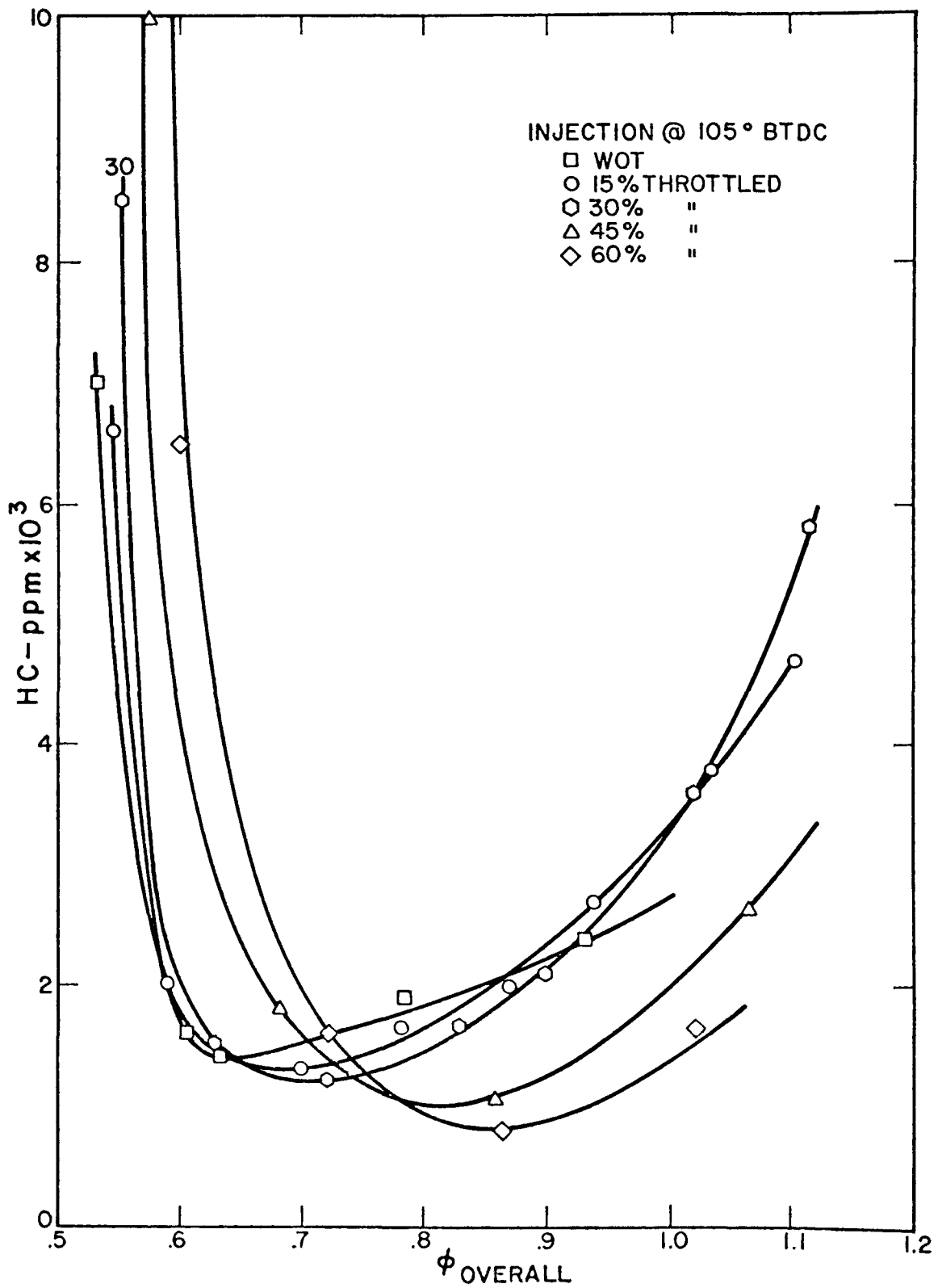


Figure 23. Measured HC Concentration Versus Overall Equivalence Ratio 105° BTDC Injection.

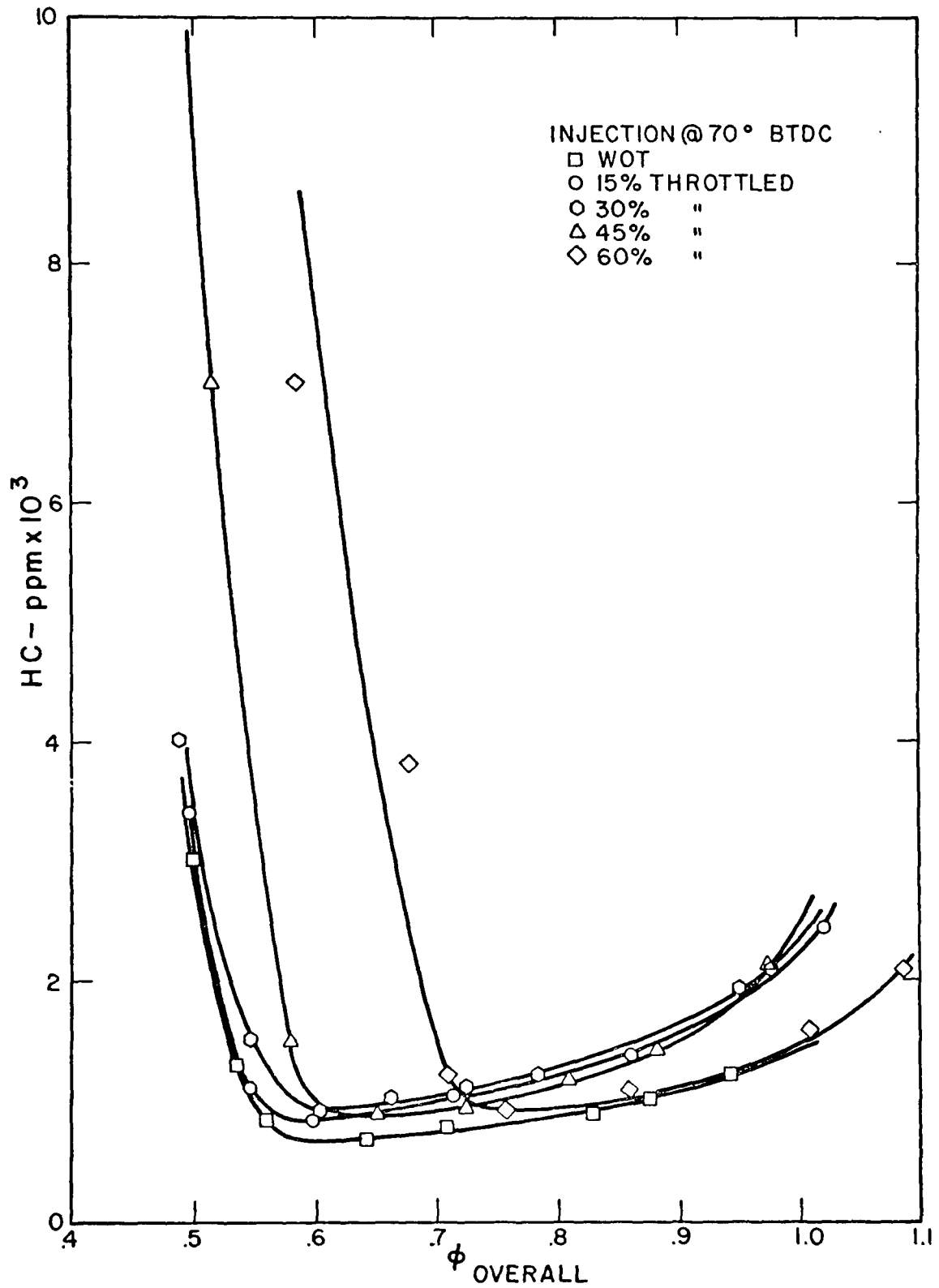


Figure 24. Measured HC Concentration Versus Overall Equivalence Ratio 70° BTDC Injection.

quenching phenomena. Lastly, note that retarding the injection timing resulted in a decrease in HC emissions throughout the operating range. This is probably a result of the generally improved combustion regularity noted at this setting, as evidenced by the increase in mean effective pressure at all equivalence ratios as shown in Figure 28.

Figures 25 and 26 are plots of indicated specific fuel consumption (ISFC) versus  $\phi$  for the two injection timings. We note that ISFC is extremely sensitive to overall fuel-air ratio, much more so than conventional homogeneous charge engines. As  $\phi$  is increased from 0.5 to the value corresponding to the minimum ISFC at any given throttle setting, ISFC decreases almost linearly. Figures 27 and 28 show us that the reason for this is that the power output of the engine increases almost linearly over this same range of equivalence ratios. As  $\phi$  is increased beyond this minimum ISFC point, ISFC again begins to rise sharply. Figures 27 and 28 show that the power output of the engine begins to flatten as  $\phi$  is increased. It is believed that increasing quantities of fuel end up on the primary chamber walls, vaporizing slowly and taking part in wall quenching reactions which lead to increased hydrocarbon emissions rather than useful power output.

Lastly, Figures 27 and 28 present calculated values of indicated mean effective pressure (IMEP) versus  $\phi$  for the various throttle settings. Note the increase in power at the leaner fuel-air ratios which occurred when the fuel injection timing was retarded from  $105^\circ$  to  $70^\circ$  BTDC. The increased air density in the chamber at the later timing reduces the fuel spray penetration, cutting down on the amount of fuel sprayed directly onto chamber surfaces. Such fuel vaporizes at a rate determined by the chamber surface temperature and takes part in wall quenching phenomena leading to increased hydrocarbon emissions, but making little contribution to power output.

An injection timing of  $50^\circ$  BTDC was tried, but combustion became erratic and hydrocarbon emissions rose

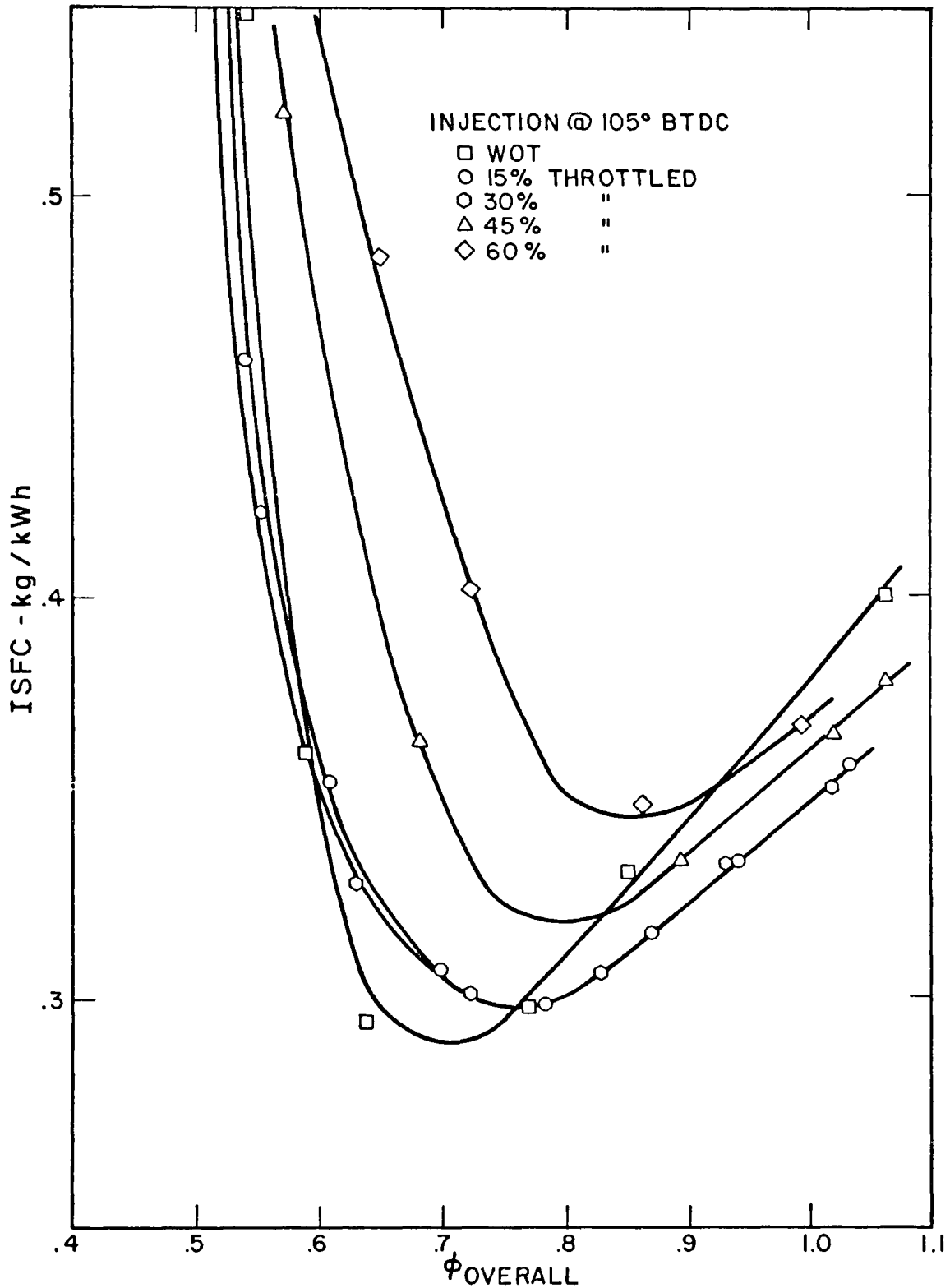


Figure 25. Calculated Specific Fuel Consumption (ISFC) versus Overall Equivalence Ratio - 105° BTDC Injection.

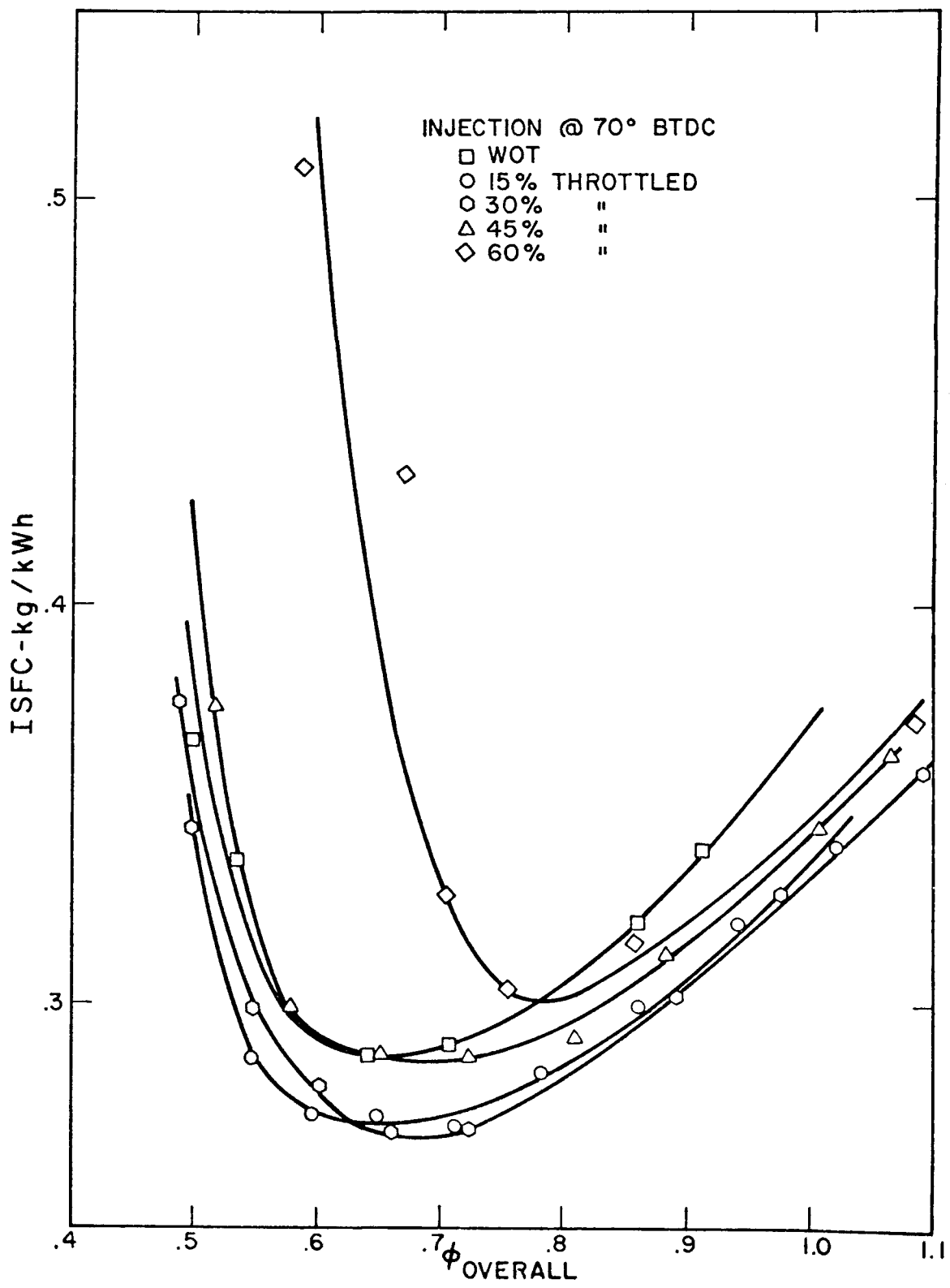


Figure 26. Calculated Specific Fuel Consumption (ISFC) Versus Overall Equivalence Ratio - 70° BTDC Injection.

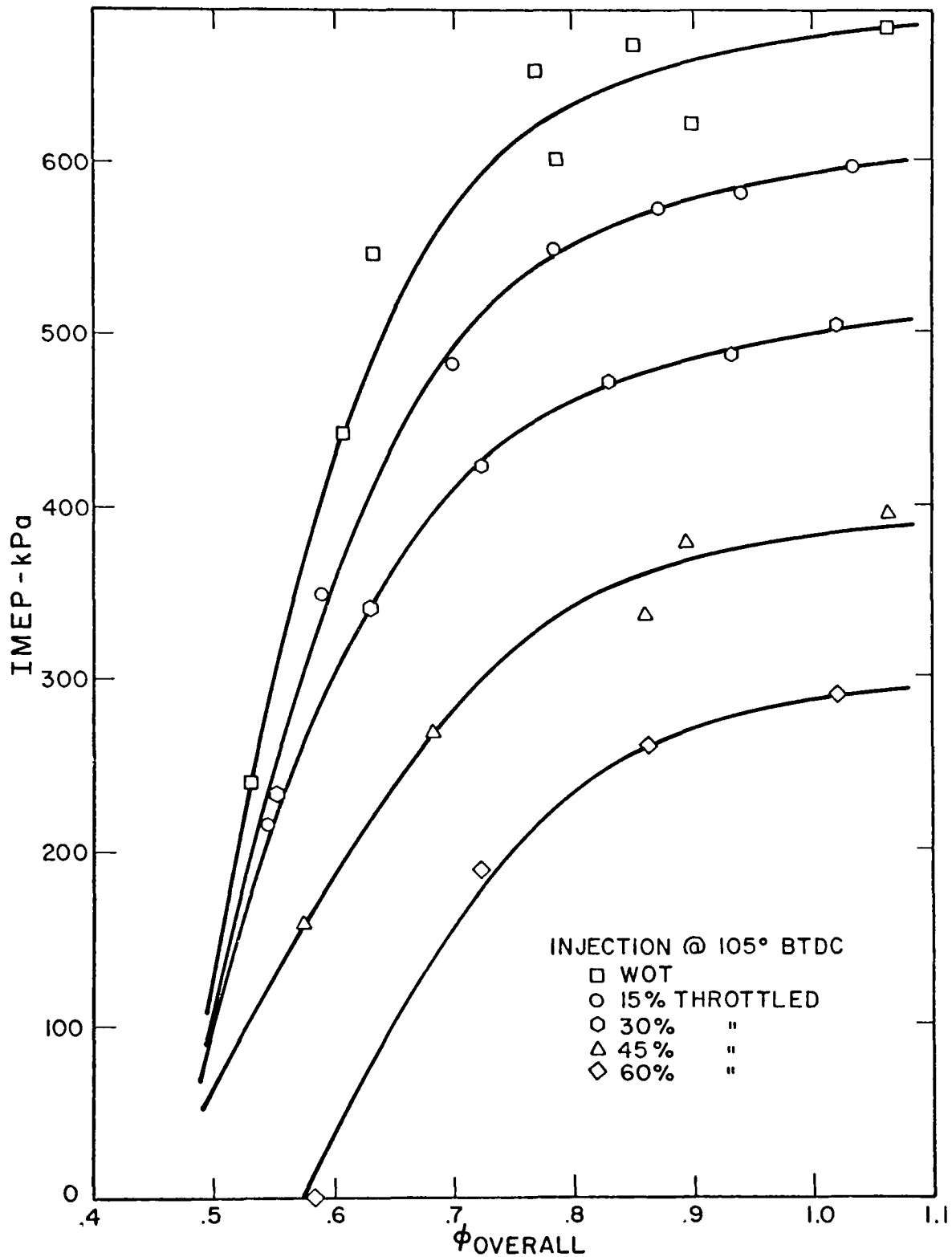


Figure 27. Calculated Mean Effective Pressure (IMEP) Versus Overall Equivalence Ratio 105° BTDC Injection.

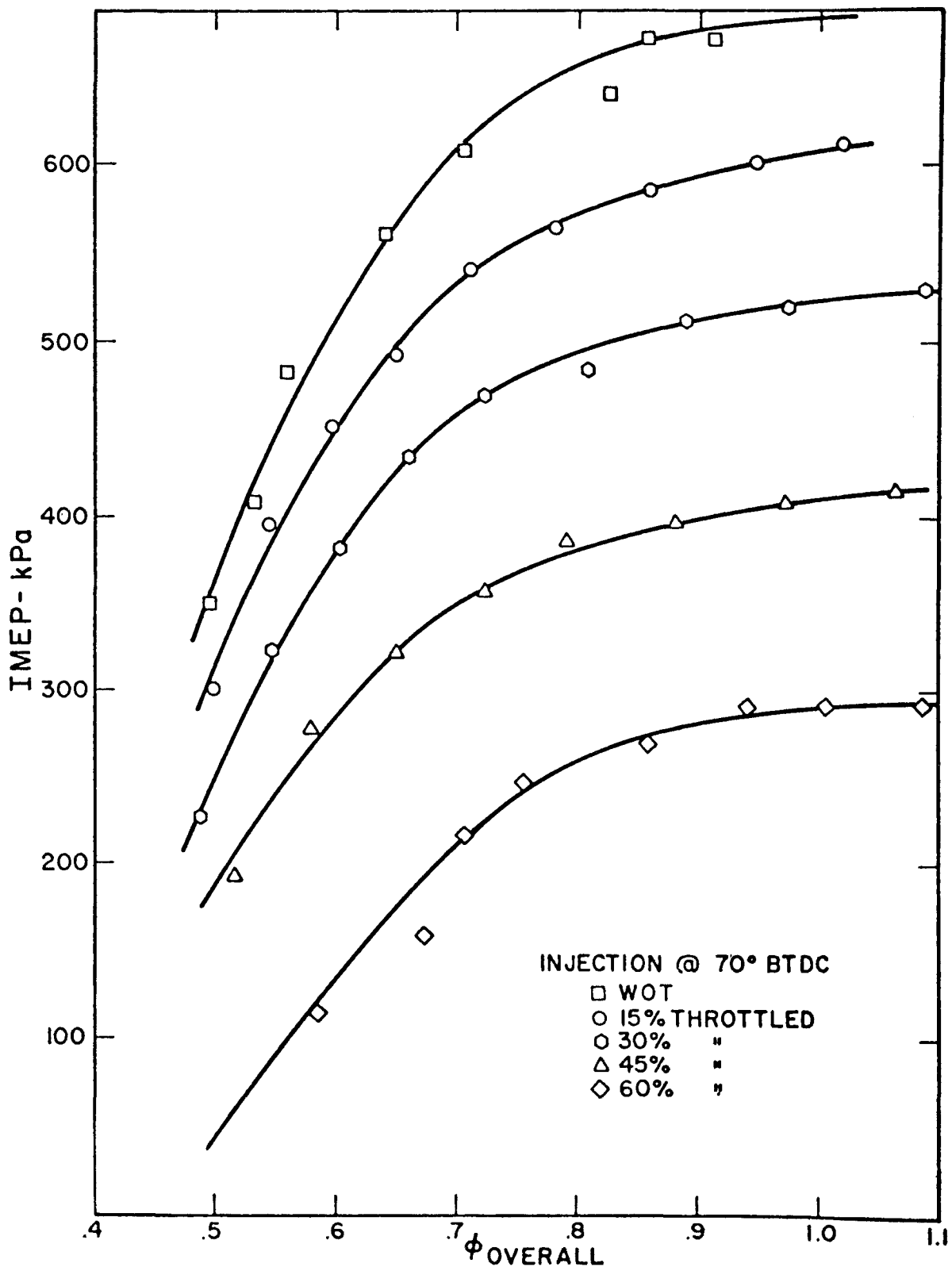


Figure 28. Calculated Mean Effective Pressure (IMEP) Versus Overall Equivalence Ratio - 70° BTDC Injection.

sharply so no data were recorded at this setting. Apparently, this injection timing did not allow sufficient time for adequate fuel vaporization and mixing with the air to occur before ignition.

Figures 29 through 36 are cross plots of calculated specific emissions and fuel consumption versus IMEP, at constant fuel-air equivalence ratios, for the two injection timings. The data were plotted in this fashion to display the load flexibility of the divided chamber engine under a variety of operating regimes. It was thought that such plots might identify a set of operating parameters by which emissions could be minimized while maximizing fuel economy and load flexibility. However, study of the plots did not indicate any such clear cut choice and in fact presented the same type of trade offs peculiar to the homogeneous charge engine.

Figures 29 and 30 present indicated specific nitric oxide (ISNO) versus IMEP. If we wished to minimize ISNO while maintaining the broadest possible load range, we might reasonably choose to run the divided chamber engine at a constant fuel-air equivalence ratio of  $\phi=1$  with injection starting at  $70^\circ$  BTDC. Examination of the corresponding plots for ISCO, ISHC and ISFC (Figures 32, 34 and 36) shows that this set of operating conditions would maximize specific emissions of CO and HC while yielding the worst possible fuel economy.

Figures 31 through 36 show that if we wished to minimize specific CO, HC and fuel consumption, we could do so by running the engine at an equivalence ratio between 0.7 and 0.8 with injection starting at  $70^\circ$  BTDC. However, the penalty of operating this way would be a narrowed operating load range and near maximization of specific NO emissions.

A casual comparison with available data showed that the divided chamber engine was capable of relatively low exhaust emissions levels of  $\text{NO}_x$ , CO and HC. Further, no

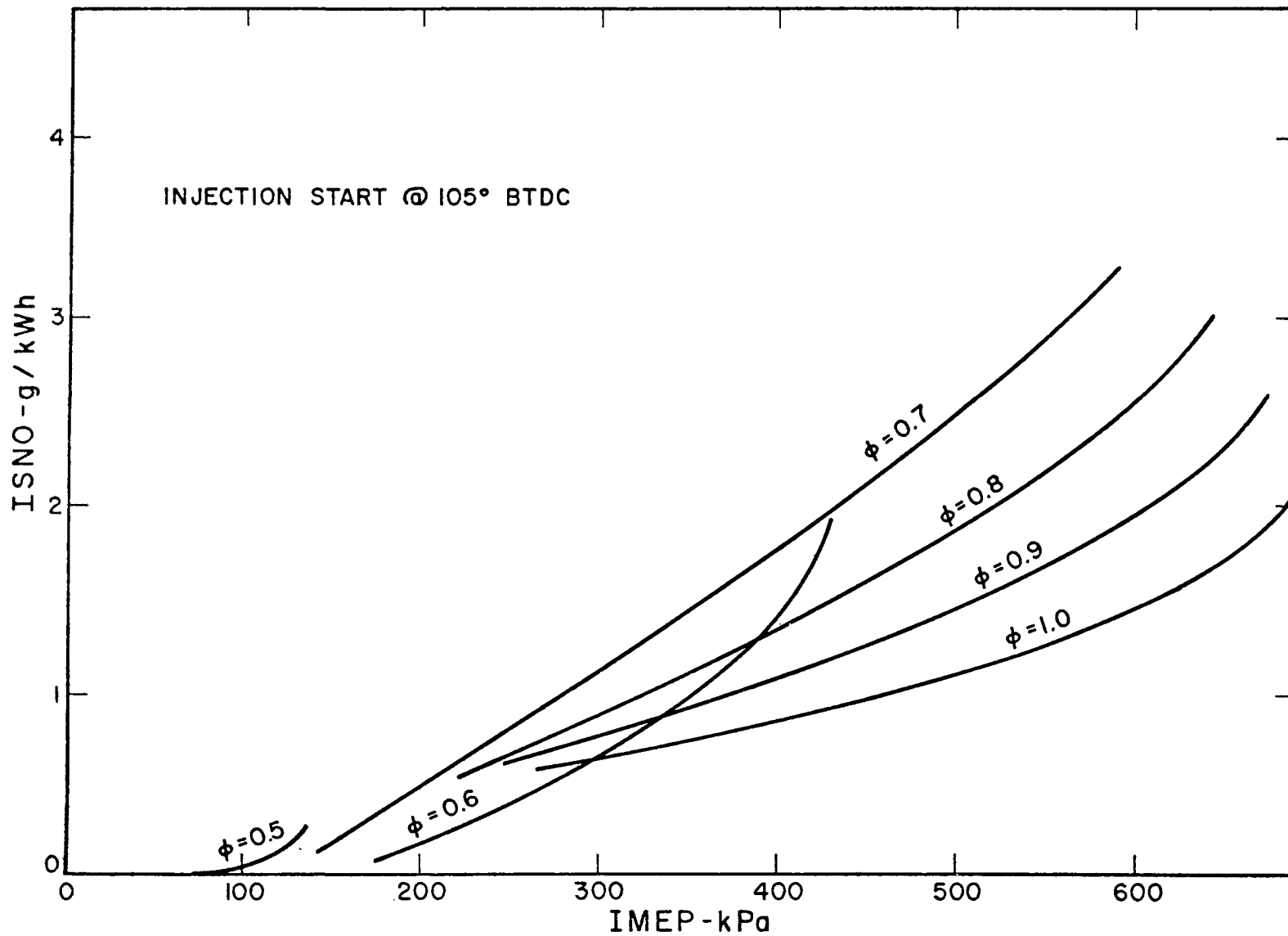


Figure 29. Calculated Specific NO Versus IMEP at Constant Equivalence Ratios - 105° BTDC Injection.

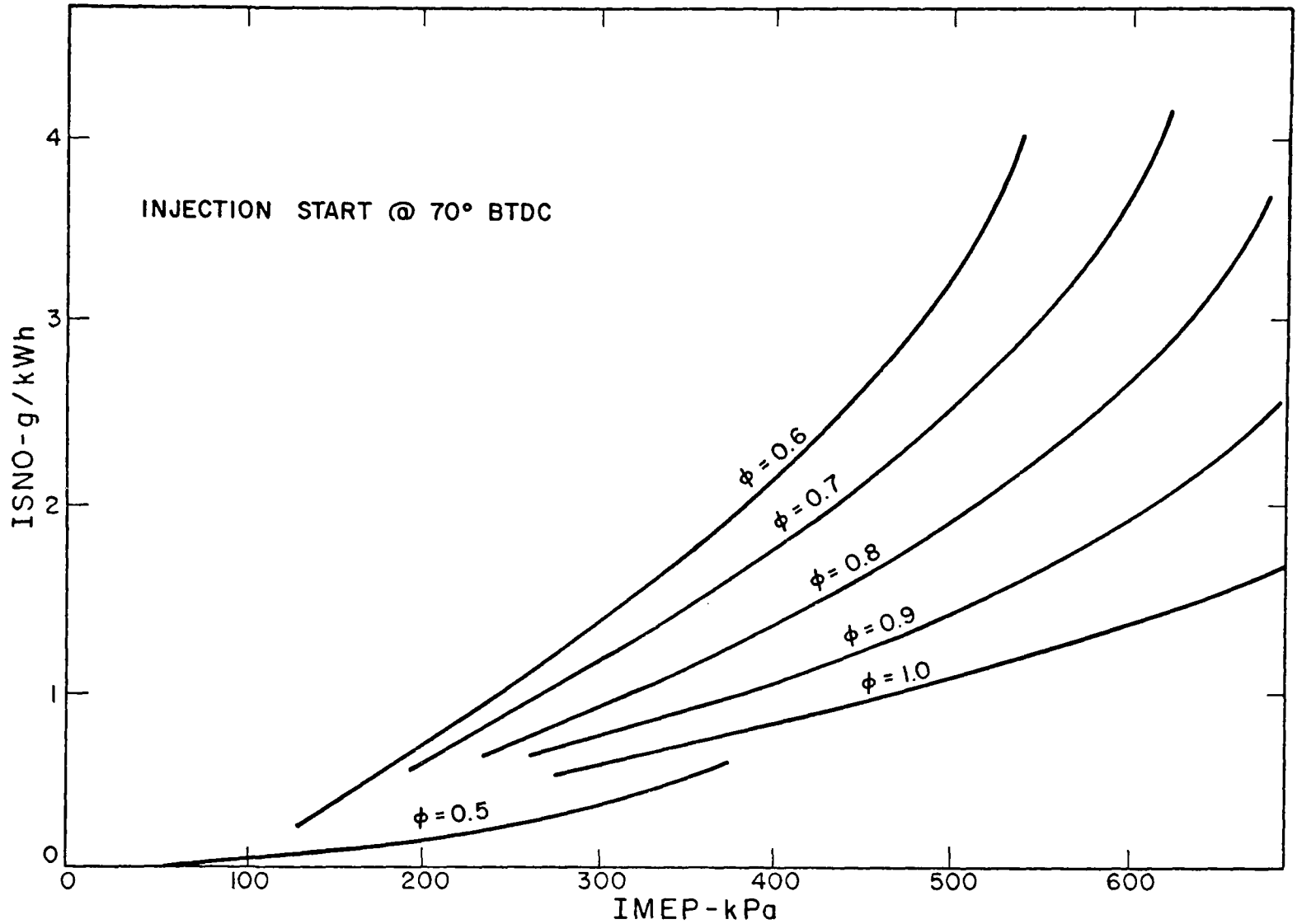


Figure 30. Calculated Specific NO versus IMEP at Constant Equivalence Ratios - 70° BTDC Injection.

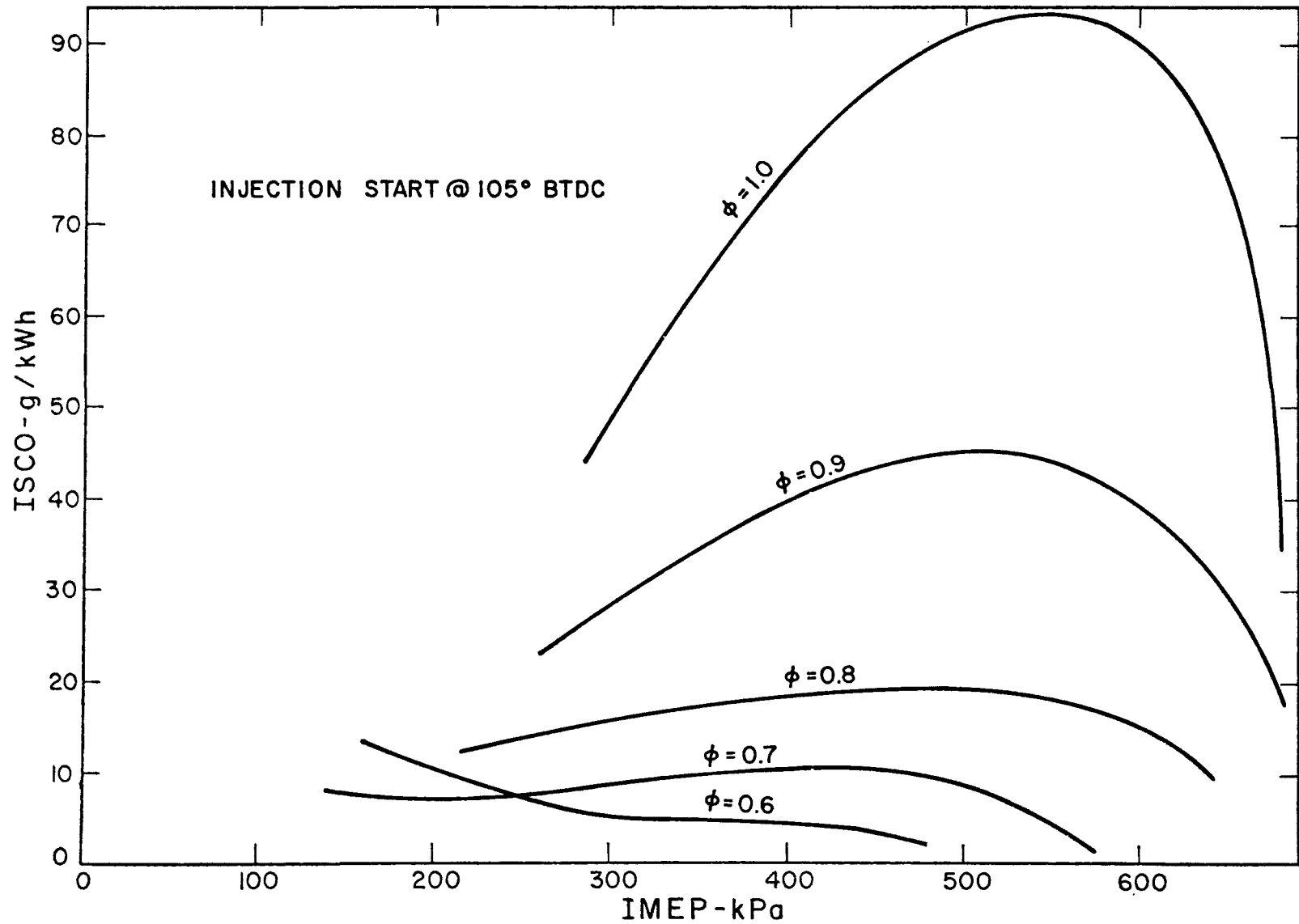


Figure 31. Calculated Specific CO Versus IMEP at Constant Equivalence Ratios - 105° BTDC Injection.

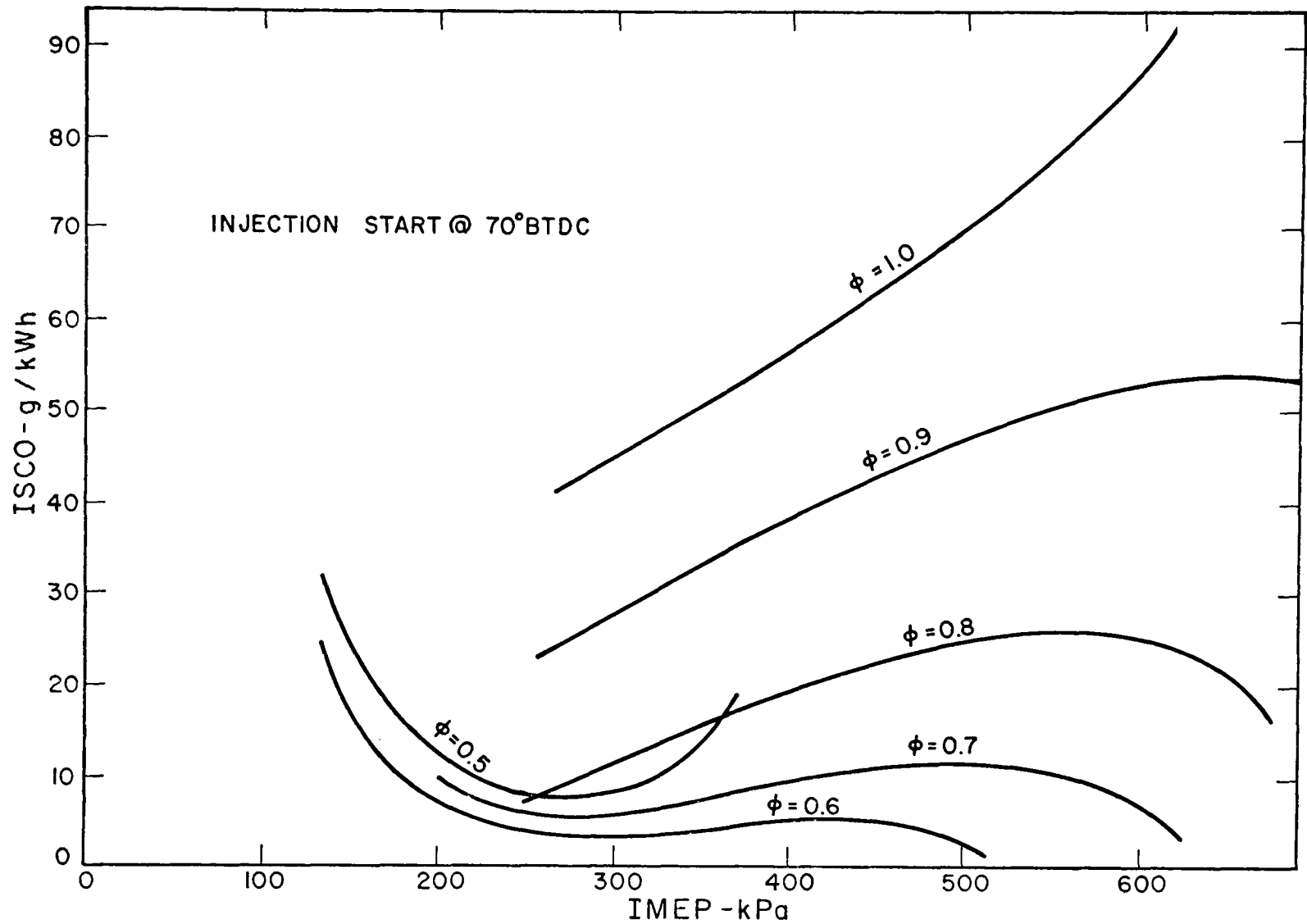


Figure 32. .Calculated Specific CO Versus IMEP at Constant Equivalence Ratios - 70° BTDC Injection.

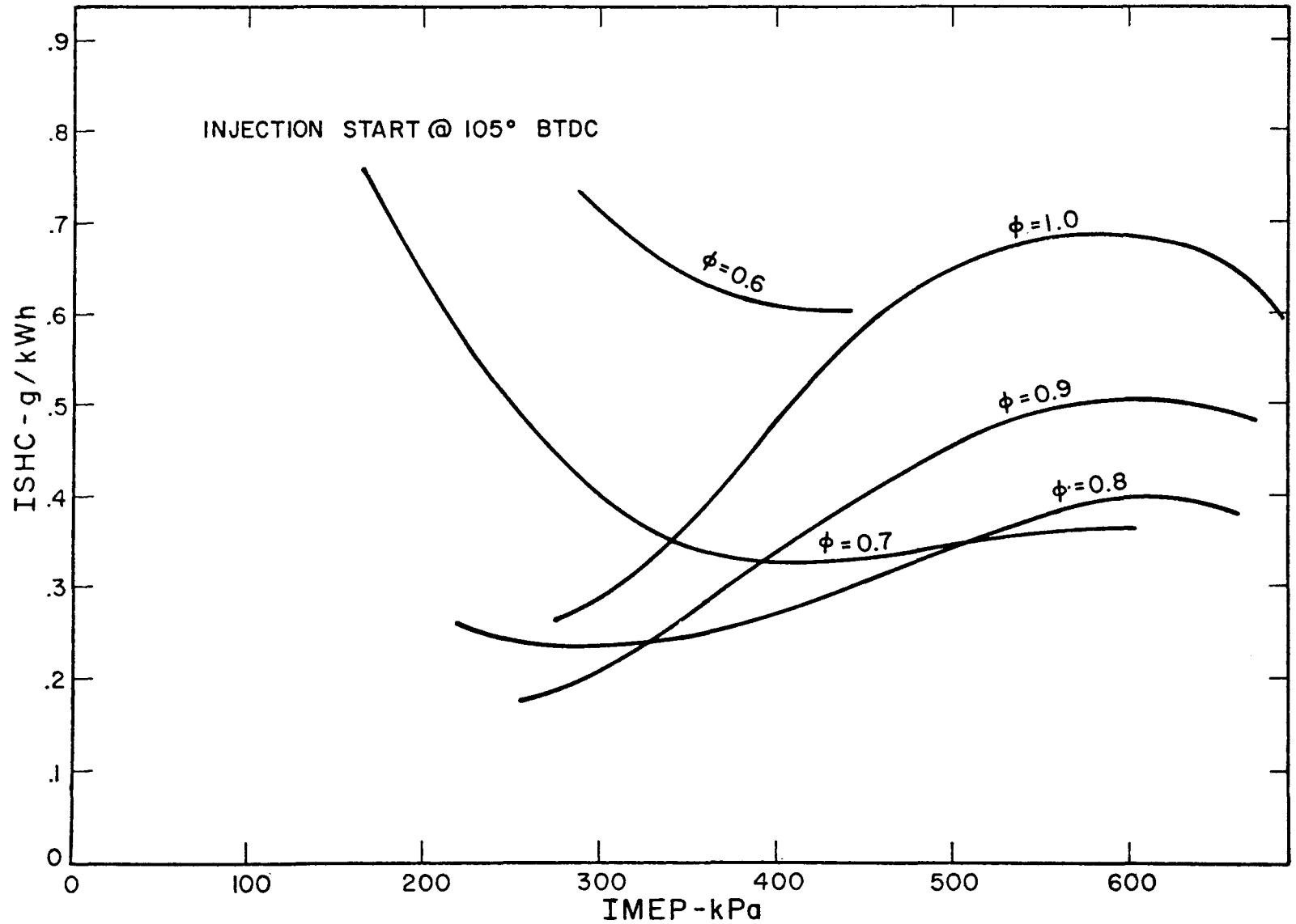


Figure 33. Calculated Specific HC Versus IMEP at Constant Equivalence Ratios - 105° BTDC Injection.

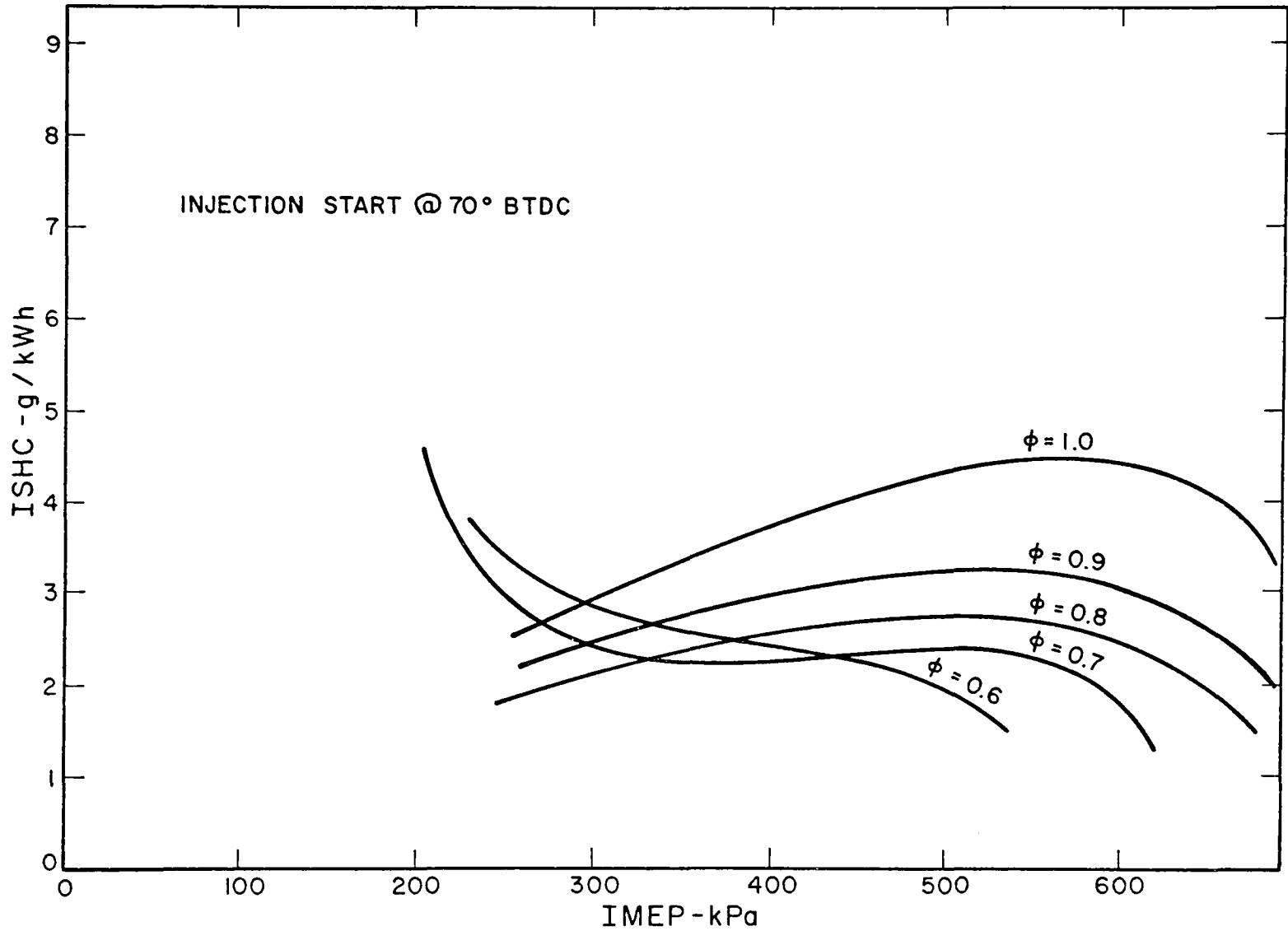


Figure 34. Calculated Specific HC Versus IMEP at Constant Equivalence Ratios - 70° BTDC Injection.

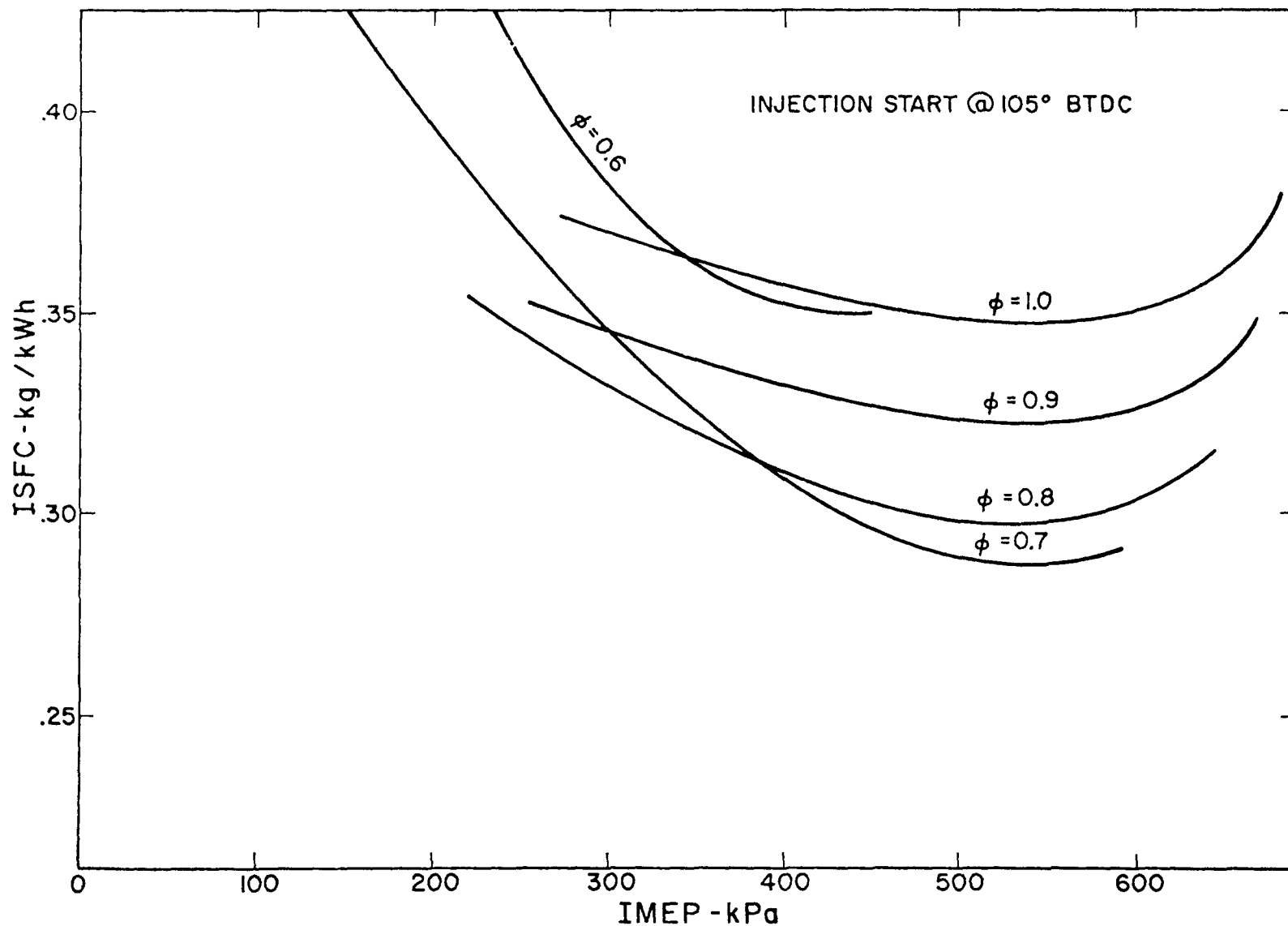


Figure 35. Calculated ISFC Versus IMEP at Constant Equivalence Ratios - 105° BTDC Injection.

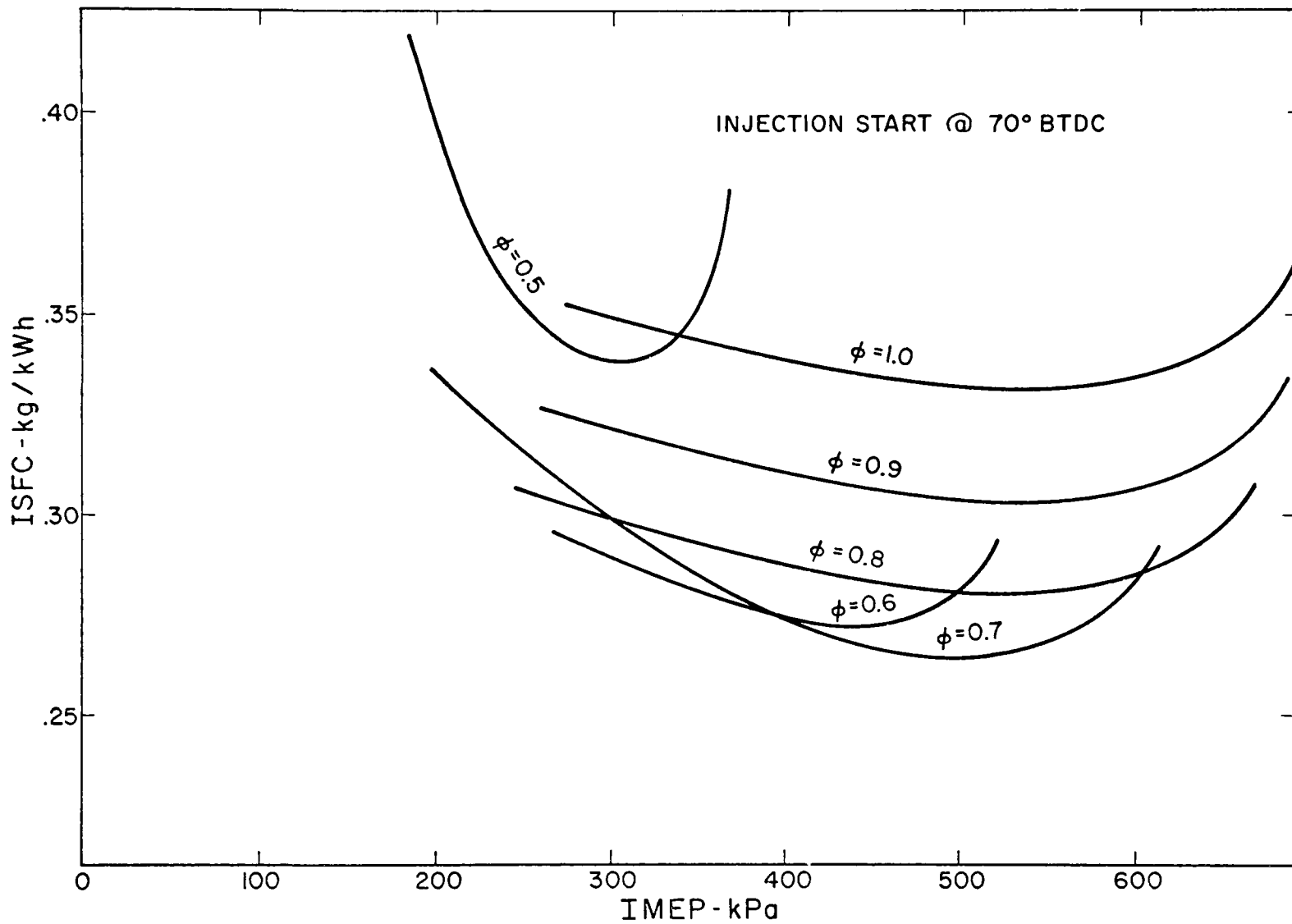


Figure 36. Calculated ISFC Versus IMEP at Constant Equivalence Ratios - 70° BTDC Injection.

recognizable operating regime would achieve a minimum level of NO, CO and HC simultaneously. However, this casual comparison suggested that regardless of the operating parameters used, the divided chamber engine as it was presently constituted was not capable of power output or fuel economy comparable to a conventional homogeneous charge engine.

One possible approach toward improving these two aspects of the divided chamber engines' performance seemed to be turbocharging. However, several factors encountered during the part load testing prompted us to delay exploration of the effects of simulated turbocharging in favor of some additional tests with the existing experimental set up.

Examination of a typical primary chamber combustion pressure trace, as shown in Figure 37, shows that combustion in the divided chamber engine occurs somewhat later in the cycle than in a conventional homogeneous charge engine. It became apparent during the part load testing that as the degree of throttling increased, spark had to be further and further retarded to secure ignition. The reason for this behavior was simply that combustible mixture was not entering the region of the connecting orifice and spark plug until later and later in the expansion process. It was felt that this late combustion was at least partially responsible for the low power and poor fuel economy.

In order to test this theory, a second spark plug was installed in the region of the prechamber furthest from the orifice. It was thought that by igniting the mixture in the region of this plug at some point before TDC, the resulting expansion would force combustible mixture into the region of the orifice earlier in the cycle. By using a long duration ( $\sim 2$  msec) ignition system to fire the spark plug at the orifice, we could fire both plugs simultaneously and ignite the mixture as it approached the orifice so that no unburned fuel would be blown into the quench region. Tests were run under

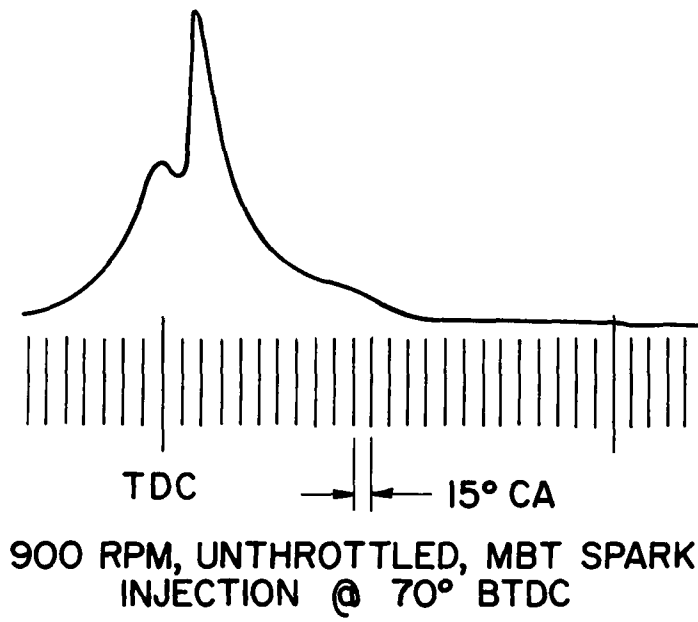


Figure 37. Typical Primary Chamber Combustion Pressure Trace.

unthrottled conditions using both single ignition at the orifice and dual ignition. The results of these tests are presented in Figure 38. It can be seen that specific fuel consumption at light load was improved some 20% by this dual ignition scheme, but the improvement decreases as load is increased. HC emissions are lower throughout the load range using the dual ignition, but  $\text{NO}_x$  and CO are increased at light to medium loads. No improvement in either emissions or fuel consumption was realized at peak load with this modified ignition scheme and in fact, the peak load output was unchanged from its previous level.

As a preliminary to experimenting with simulated turbocharging, it was decided to run some tests to evaluate the octane sensitivity of the divided chamber engine. Blends of iso octane and N-Heptane, having RON's in the range of currently available motor fuels, were run in the engine under unthrottled conditions. Pressure traces recorded while running on these fuels showed an increasing development of the pressure fluctuations associated with knock as the octane rating of the fuel was reduced. Audible knock was not observed but may have been masked by the high ambient noise level associated with the operation of the divided chamber engine.

Several inferences were drawn from the results of these additional tests. First, although the specific fuel consumption at light loads was improved by the dual ignition modification, it appeared that fuel consumption was still substantially greater than current conventional homogeneous charge engines operating in the same load range. Second, the apparent onset of knock under naturally aspirated running conditions seemed to rule out turbocharging as a means to improve the divided chamber engines' efficiency.

Taken together, these two points raised serious doubts as to the future potential of the divided chamber engine as

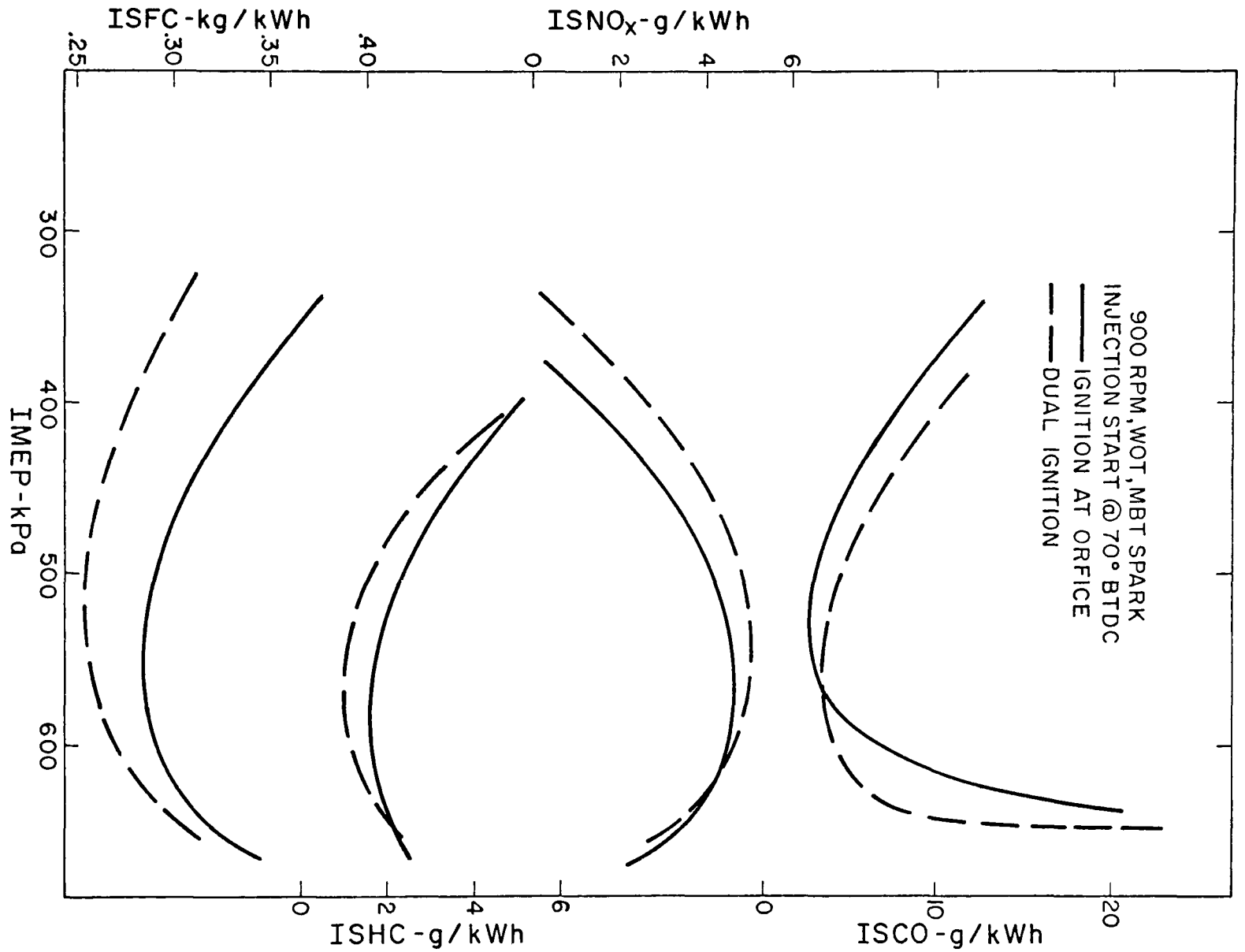


Figure 38. Calculated Specific NO<sub>x</sub>, CO, HC and Fuel Consumption Versus IMEP For Dual Ignition Tests.

an alternative vehicle powerplant. It was decided to postpone the proposed study of hydrocarbon formation in the divided chamber engine and instead, to gather together comparable emissions, power and fuel consumption data from conventional homogeneous charge, diesel and other hybrid engines for the purpose of making a comparison with the divided chamber engine.

Data from six other engines encompassing four different combustion systems were examined for purposes of comparison. To illustrate the conventional throttle controlled approach, the results of Wimmer and Lee<sup>4</sup> for their homogeneous charge, spark ignited CFR engine are used throughout the graphical comparison presented in Figures 39 through 42. The data on this engine were gathered in conjunction with data from a second CFR equipped with a prechamber and set up to run as a torch ignited homogeneous lean engine. The prechamber was designed to be installed in the spark plug opening and was equipped with an intake valve and spark plug. The volume of this prechamber was approximately 10% of the total clearance volume, and it received premixed fuel and air at an equivalence ratio of 5. Lean mixture was supplied to the cylinder during the intake stroke and subsequent dilution of the prechamber charge during the compression stroke produced a readily ignitable mixture. Upon ignition, a torch of flame issues from the prechamber inflaming the lean main chamber mixture. This engine was similar in many ways to the Honda CVCC, so where applicable, data from Date, et al<sup>5,6</sup> were also used to illustrate the state of the art for torch ignited engines.

Two hybrid stratified charge spark ignited engines representing two techniques of combustion control were also included in the comparison. The Ford PROCO, which uses early injection of fuel and controls combustion by flame speed and mixture quantity, was represented by data excerpted from the paper by Simko, et al<sup>7</sup>, while data for

the Texaco TCCS engine, which achieves combustion control through control of fuel injection rate, similar to an open chamber diesel, was taken from the paper by Mitchell, et al<sup>8</sup>.

Lastly, the modern open chamber diesel engine was felt to be relevant to the comparison, so data for the high output Labeco-TACOM single cylinder were taken from the extensive results published by Bolt, et al<sup>9</sup>.

The test conditions for the various engine data used in this comparison are not identical to the WOT conditions maintained for the divided chamber engine tests. However, it was felt that the data were taken under similar enough conditions that a valid comparison could be made.

The various data are presented in the form of plots of indicated specific emissions and fuel consumption versus indicated mean effective pressure. Indicated values were used because the majority of the data were taken from single cylinder engine tests.

Figure 39 displays  $ISNO_x$  versus IMEP for all of the engines included in the comparison. Note that the worst case seems to be the conventional homogeneous charge engine. It is believed that if data could have been found for a modern engine utilizing spark retard and EGR, this type of engine would have looked much better from an emissions standpoint. The divided chamber engine looks better than all of the others from the standpoint of  $NO_x$ . However, note that this is data for  $\phi=1$  and that  $ISNO_x$  for leaner equivalence ratios would be considerably greater. Note too that the maximum output data point for the divided chamber engine was recorded at a substantially lower IMEP than corresponding points for the other engines.

Figure 40 presents specific carbon monoxide emissions versus load. The divided chamber engine emits CO levels comparable to the homogeneous charge and torch ignited engines, and better than the two hybrid stratified charge engines, up to about 500 kPa IMEP. At this point, the

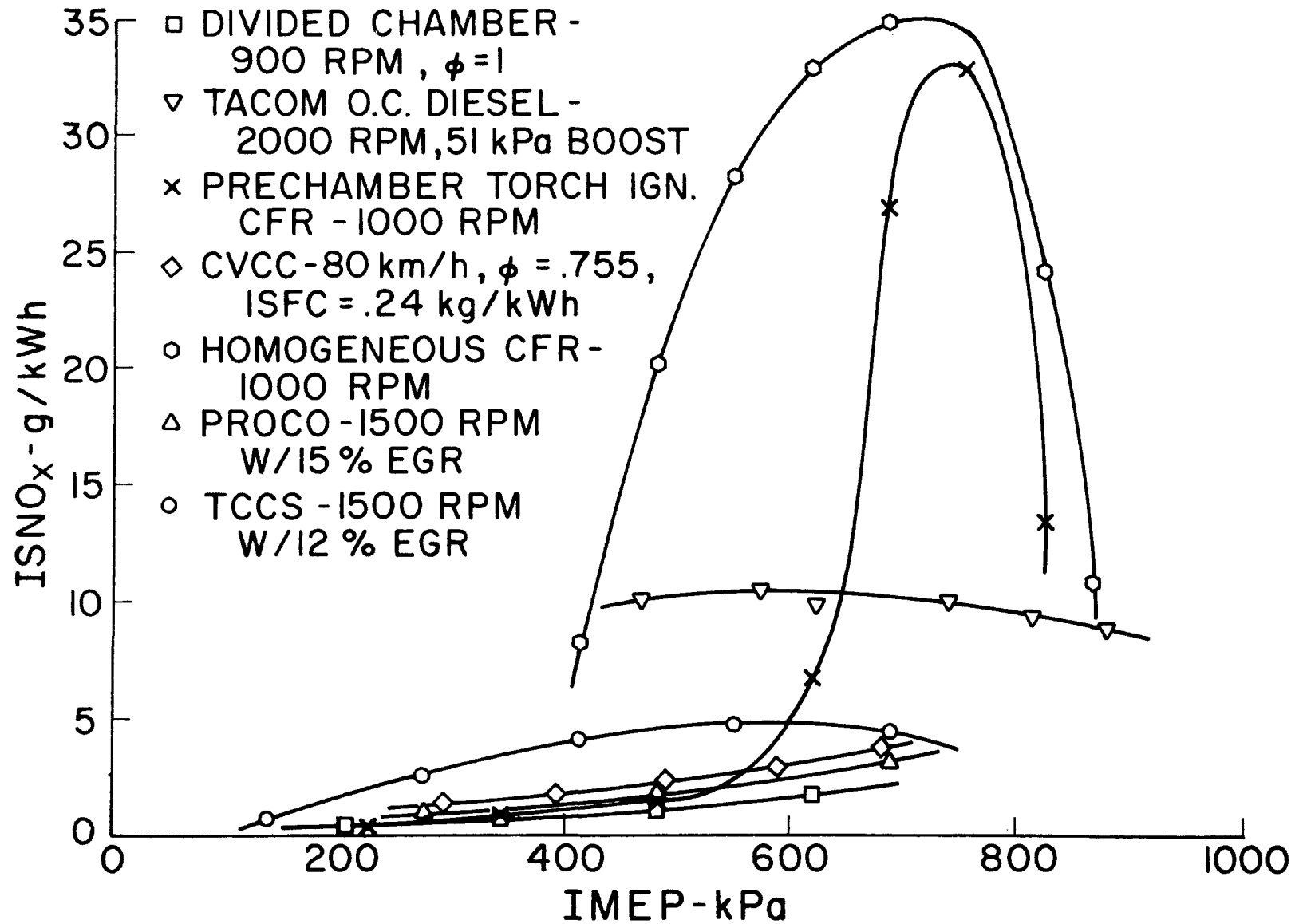


Figure 39. Specific  $\text{NO}_x$  Versus IMEP - Divided Chamber Engine Comparisons.

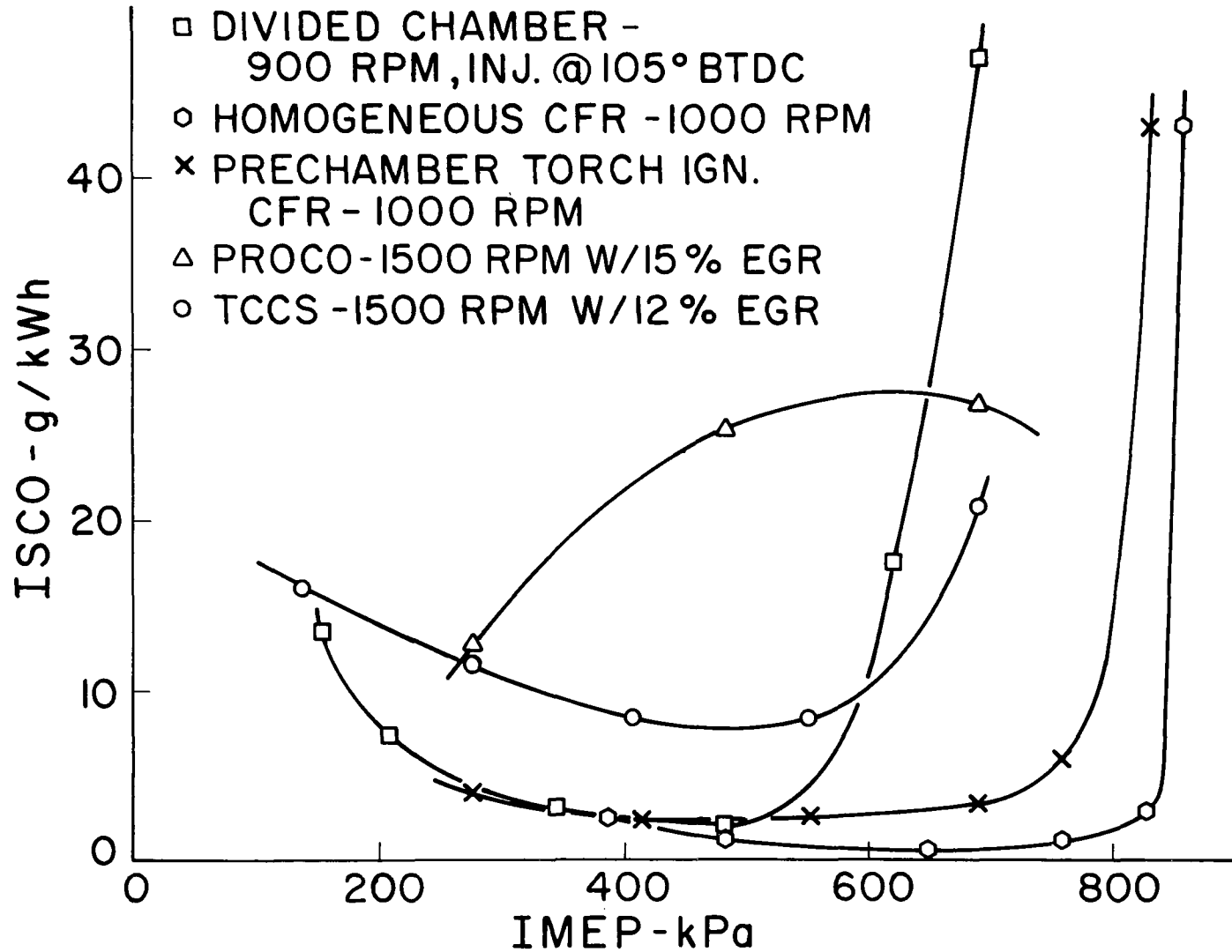


Figure 40. Specific CO Versus IMEP - Divided Chamber Engine Comparison.

divided chamber engine begins to approach its' output limit, demanding increasingly rich mixtures which result in a sharp rise in CO emissions.

Figure 41 compares specific hydrocarbon emissions for the various engines versus power output. Note the decrease in hydrocarbon emissions from the divided chamber engine which occurred when the injection timing was retarded from 105° to 70° BTDC. At the later timing, the HC emissions from the divided chamber engine are better than the other hybrids at light loads up to 400 kPa IMEP, but fall midway between the bracketing engines at higher loads.

Lastly, Figure 42 presents indicated specific fuel consumption versus IMEP. It is felt that this particular plot is the most important one with regard to the divided chamber engine. It shows that the specific fuel consumption of the divided chamber engine is 15 to 30 percent greater throughout its load range than the two hybrid stratified charge engines and the diesel. In addition, it shows clearly the limited peak output of the divided chamber engine when compared to the conventional homogeneous charge and diesel engines, as well as the other hybrids.

The results of the part load tests and the additional tests described previously, along with this comparison, were presented to the EPA grant officer at the grant review meeting. The merits of continuing the study of the divided combustion chamber concept, and specifically the mechanism of unburnt hydrocarbon formation peculiar to it, were discussed and it was decided that the original goals of the project would be more profitably accomplished by studying the origins and causes of hydrocarbon emissions from a combustion system of more recognized potential.

It was suggested at this time that we consider the possibility of studying the hydrocarbon formation process in the Texaco Controlled Combustion System (TCCS) stratified charge engine. Recent results from the TCCS engine

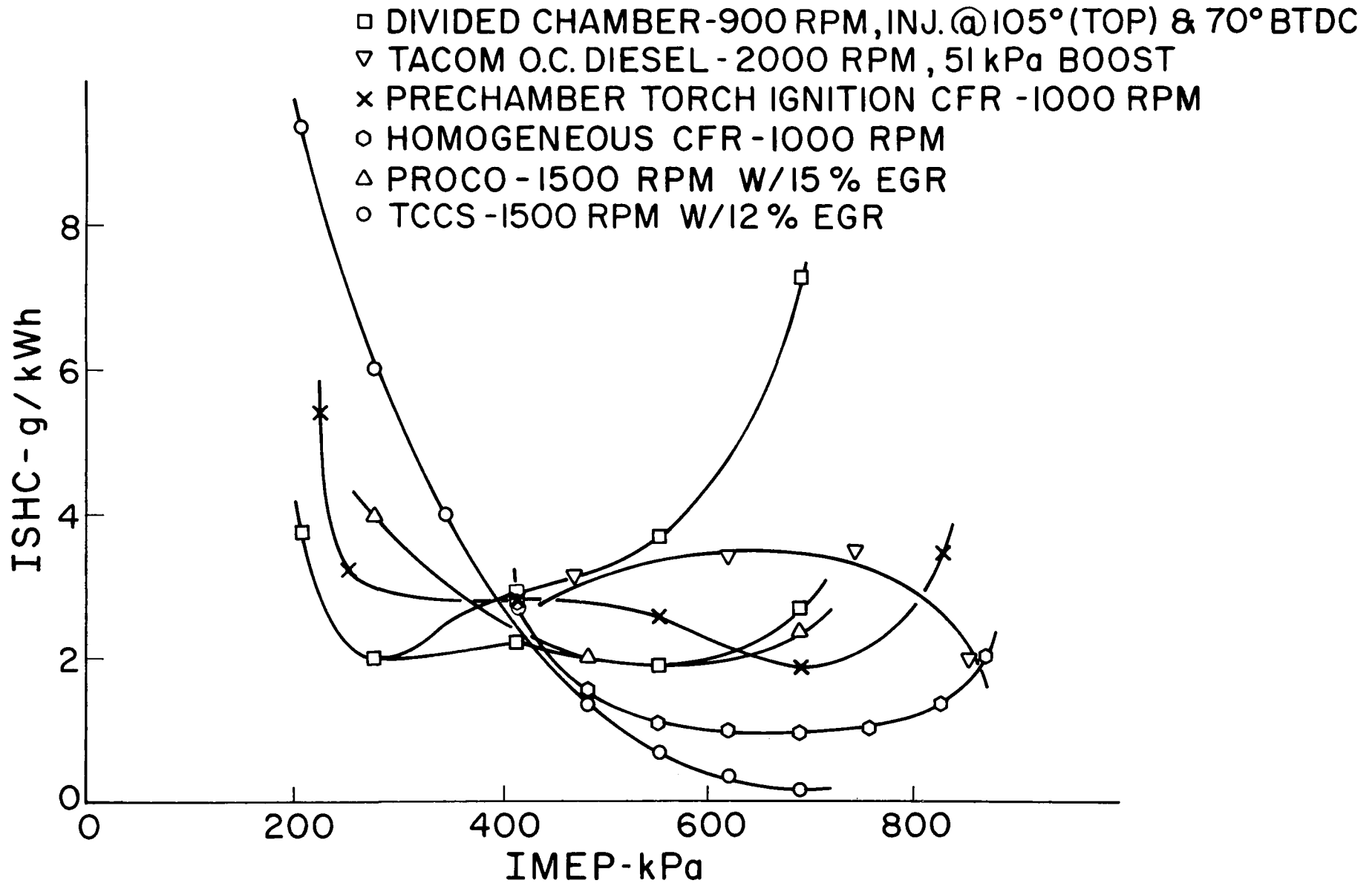


Figure 41. Specific HC Versus IMEP - Divided Chamber Engine Comparison.

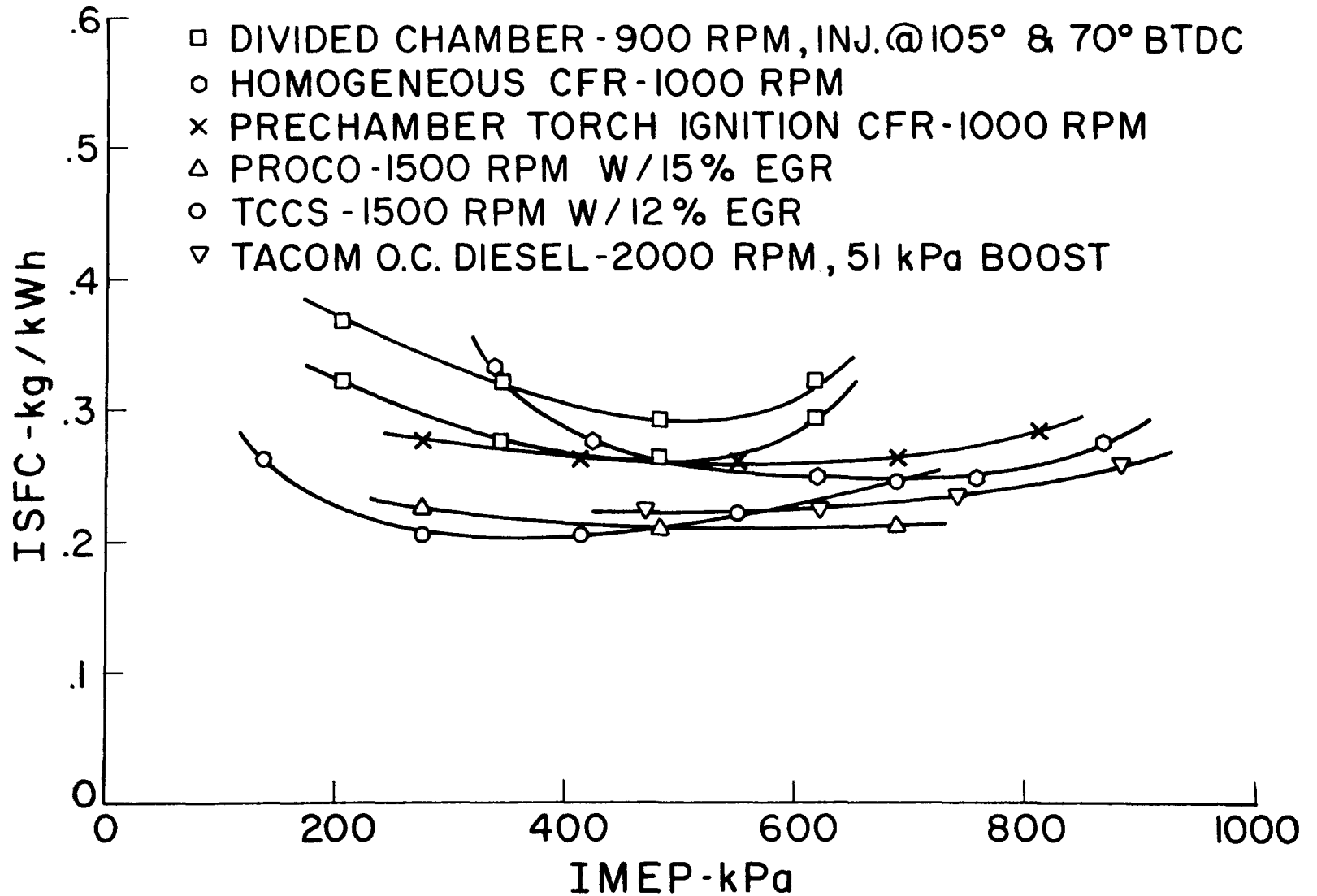


Figure 42. Specific Fuel Consumption Versus IMEP - Divided Chamber Engine Comparison.

development program funded by TACOM had demonstrated excellent fuel economy and low  $\text{NO}_x$  emissions levels in vehicle applications. However, these installations had utilized catalytic convertors to reduce HC emissions and it was felt that the hydrocarbon problem of the TCCS was severe enough to warrant a detailed study.

Before making a final decision regarding the TCCS, an extensive search of the literature pertinent to the heterogeneous combustion process occurring in the TCCS was conducted. Possible mechanisms of hydrocarbon formation were studied and a reasonable scheme of the mechanisms peculiar to the TCCS was proposed. In addition, literature dealing with in-cylinder gas sampling techniques was reviewed in an effort to determine the possible role of such techniques in studying and verifying the proposed mechanism of hydrocarbon formation in the TCCS.

The complete literature search appears in the appendix of this report. The following conclusions were drawn from the survey.

1. Literature dealing with hydrocarbon formation in heterogeneous combustion systems is sparse, and the mechanisms of formation involved are not yet well understood.
2. Based on available knowledge, we can postulate a reasonable hypothesis of the origins and causes of hydrocarbon formation in the Texaco combustion system.
3. A continuous flow, in-cylinder sampling technique would be the most straightforward way to investigate hydrocarbon formation in heterogeneous combustion.
4. Such a technique could be developed in conjunction with, and as a means to, the study of hydrocarbon formation in the Texaco combustion process.

The next step taken was to determine the feasibility of using an in-cylinder sampling technique in the TCCS engine. Two designs of the TCCS were subsequently examined for accessibility for such a device and it was found that the single cylinder M-151 TCP engine was the most suitable for this purpose. A request was made to TACOM for one of these engines and, after a prolonged series of negotiations, a single cylinder M-151 TCP engine was officially transferred from TACOM to the University of Wisconsin.

The next section of this report details the development of the engine test apparatus and the in-cylinder sampling device.

#### EXPERIMENTAL APPARATUS FOR TEXACO ENGINE STUDIES

The M-151 TCP engine obtained from TACOM for use in the proposed hydrocarbon study had some 2000 hours of previous test time on it. Upon disassembly, it was found that the engine was in need of a complete overhaul. The main and rod bearing journals of the crankshaft were badly scored and the bearing support surfaces of the connecting rods were nicked and generally in poor condition. In addition, the valve tappets of the working cylinder had apparently ceased to rotate at some point in the engines' prior life. Their faces were severely galled as were the matching cam lobes.

A new crankshaft and two new connecting rods were obtained along with a complete set of new bearings and the engine was reassembled. A new camshaft and tappets provided by Texaco were also installed.

An engine support cradle was fabricated for the engine and moved into one of the engine test cells along with a General Electric 30 kW dynamometer. The dynamometer has since been tied into the Ward-Leonard motor-generator system.

The engine was next installed in the cradle and, after alignment, was coupled to the dynamometer using a Falk model 8F tapered grid coupling.

A pair of 15 gallon (.057 m<sup>3</sup>) vertically mounted air receiver tanks were ordered from Kargard Industries, Inc., in Marinette, Wisconsin for use as intake and exhaust surge tanks. This volume is approximately 100 times the engines' displacement. The tanks were installed in the engine test cell on the port side. The exhaust tank has been coupled to the cylinder head exhaust port by means of a 2.5 in (6.35 cm) diameter flexible stainless steel conduit and a stainless mating flange. A bronze valve has been installed at the exhaust tank outlet so that the back pressure can be regulated and the outlet side of this valve has been connected to the building exhaust system with 2 in. (5 cm) diameter aluminum pipe. Chromel-alumel thermocouples have been installed at the cylinder head exhaust port and at the outlet of the surge tank for monitoring purposes. The intake surge tank was connected to the cylinder head intake port by means of an 18 in. (.46 m) section of 1.25 in (3.2 cm) diameter pipe. Eighteen inches was the length recommended by Texaco to give best overall performance.

It was decided to set the air system up so that the engine could be run with boost pressures up to 1 atmosphere and air temperatures to 200°F (93°C). The maximum air flow required was calculated and the heating requirement was worked out. Two chromalox model KSEF-24 heating elements, rated at 1950 W each, were subsequently ordered. In order to control the cycling of these heating elements, a West Instrument Model 802M temperature controller and a Crydom Model A2425 solid state zero crossing relay were purchased. The controller senses the intake air temperature at the intake port entrance by means of an iron-constantan thermocouple, switching the elements on and off as required by

means of the high capacity relay. A housing to enclose the two heating elements has been designed and is presently under construction. This assembly will connect directly to the inlet opening of the intake surge tank.

A set of three critical flow orifices were designed to match the anticipated air flow requirements of the engine. However, it was determined that to machine such orifices to the recommended ASME specifications would be both expensive and time consuming. It was discovered that synthetic sapphire jewel bearings having suitable orifice configurations could be purchased in the required sizes at a very attractive price. Since any nozzle would require calibration before it could be used, this approach did not seem to entail any additional work and enabled a cost savings as well. The jewel bearings have been ordered from the Swiss Jewel Company in Philadelphia, Pa. The related air line network and nozzle holders have been designed and are under construction.

The W.D. Ehrke Company, Inc., in Milwaukee was contacted for help in selecting an appropriate air regulator to control the pressure upstream of the critical flow nozzles. A Fischer type 95 HD differential air regulator has been ordered and delivery is expected shortly.

The cooling system of the engine was the next order of business. A Perfex Model B-310-121-A counterflow heat exchanger was obtained with the engine and plumbed into the system. Flow of cooling water through the exchanger is controlled by a Sterlco Model R-151 F reverse acting temperature control valve. The sensor from this valve is installed in the engine coolant expansion tank and the valve can be adjusted to vary the coolant temperature between 175° and 215° F (80°-100°C). A Doerr Electric Corporation 1/3 hp (1/4 KW) centrifugal pump is used to circulate the engine coolant through the heat exchanger.

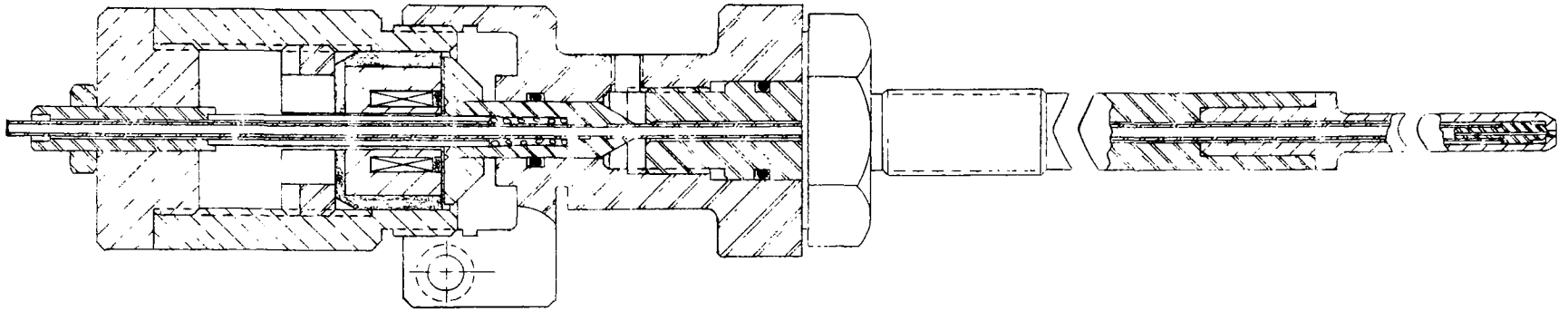


Figure 43. Sampling Valve Design for TCCS Hydrocarbon Study.

No steps have been taken to modify either the piston or the cylinder head for the accomodation of the sampling device. It was felt that a substantial data base should first be acquired for the unmodified engine so that the effect of future modifications could be more clearly understood.

The sampling valve design has progressed to the point shown in Figure 43. The valve will utilize the continuous flow concept described previously, with the majority of the flow being wasted and the sample being snatched from the flow at the desired sampling point. The valve will be actuated electro-magnetically in response to a trigger signal picked up by an optical sensor on the engines' camshaft. The positioning of the sensor is adjustable so that the timing of the triggering signal can be varied over the desired range of sampling points.

#### DISCUSSION OF CONCLUSIONS

The divided chamber engine has demonstrated emission levels of the oxides of nitrogen ( $\text{NO}_x$ ) considerably lower than conventional homogeneous charge spark ignition engines. However, other hybrid engines have displayed similar emissions levels while yielding substantially better fuel economy and power output than the divided chamber engine. It was concluded, therefore, that the study of hydrocarbon formation in an engine showing more promising fuel efficiency would be more productive.

This conclusion is based on the following findings:

1. The specific fuel consumption (kg/kWh) of the divided chamber engine is 20 to 25 percent greater throughout its useful load range than conventional homogeneous charge, diesel and hybrid stratified charge engines currently being considered for production use.
2. The maximum output (IMEP) of the divided chamber engine under naturally aspirated

operation is 15 to 30 percent lower than most of the conventional and hybrid engines undergoing serious study.

3. Octane sensitivity of the divided chamber design rules out turbocharging as a means of increasing the output and improving the fuel efficiency of the engine to an acceptable level.

### DISCUSSION OF RECOMMENDATIONS

The study of the origins of unburnt hydrocarbon emissions in the Texaco combustion system, which was initiated under the present, should be continued.

The study of combustion phenomena peculiar to hybrid combustion systems is an important and necessary step in the development of these engines to their fullest ecological and economical potential.

Hydrocarbon emissions have been and continue to be a serious problem in most hybrid combustion systems. Considerable attention has been given to the problems of  $\text{NO}_x$  and carbon monoxide formation in such systems, but little has been done about the hydrocarbon problem. The increasing emphasis on fuel economy demands that the hydrocarbon problem be attacked in the combustion chamber rather than eliminating it catalytically as has been the recent practice.

Many studies detailing the sources and causes of hydrocarbon emissions from homogeneous charge spark ignition engines are available in the literature. However, the same cannot be said for stratified charge engines. It is believed that the understanding of hydrocarbon formation in heterogeneous combustion to be gained through this study would provide a useful and much needed contribution to the body of knowledge of stratified charge combustion.

Lastly, discussions with members of the various organizations connected with the development of the Texaco

combustion system (Texaco, TACOM, M.I.T.) have indicated a high degree of interest in the results of such a study. The concentration of unburnt hydrocarbons in the untreated exhaust of the Texaco engine is recognized as one of its aspects which needs to be improved before serious consideration is given to widespread application. It is thought that the results of this hydrocarbon study might point the way to the necessary design changes.

## REFERENCES FOR SECTION VI

1. Rhee, K. T., G. L. Borman, O. A. Uyehara, and P. S. Myers. A Continuous-Flow Gas Sampling System for Engines. Combustion Science and Technology. 12: 105-109, 1976.
2. El-Messiri, I. A. The Divided Combustion Chamber Concept and Design for Control of S.I. Engine Exhaust Air Pollutant Emissions. University of Wisconsin. Madison, Wisconsin. Ph.D. Thesis. EPA Office of Air Programs. January 1973. 286 p.
3. Obert. E. F. Internal Combustion Engines, Third Edition. Scranton, Pennsylvania, International Text-book Company, February 1970, 736 p.
4. Wimmer, D. B., R. C. Lee. An Evaluation of the Performance and Emissions of a CFR Engine Equipped With a Prechamber. Research Center, Phillips Petroleum Co. 730474. Society of Automotive Engineers. May 1973, 15 p.
5. Date, T., S. Yagi, A. Ishizuya, and I. Fugii. Research and Development of the Honda CVCC Engine. Honda Research and Development Co., Ltd. 740605. Society of Automotive Engineers. August 1974. 18 p.
6. Date, T., S. Yagi, and K. Inoue. NO<sub>x</sub> Emissions and Fuel Economy of the Honda CVCC Engine. Honda Research and Development Co., Ltd. 741158. Society of Automotive Engineers. October 1974. 13 p.
7. Simko, A., M. A. Choma, and L. L. Repko. Exhaust Emission Control by the Ford Programmed Combustion Process-PROCO. Ford Motor Company. 720052. Society of Automotive Engineers. January 1972. 22 p.
8. Mitchell, E., M. Alperstein, J. M. Cobb, and C. M. Faist. A Stratified Charge Multifuel Military Engine - A Progress Report. Research and Technical Dept., Texaco Inc. 720051. Society of Automotive Engineers. January 1972. 9 p.
9. Bolt, J. A., M. F. El-Erian, J. Duerr, and A. Miklos. Diesel Engine Combustion and Emissions TACOM Research Engine. University of Michigan. 11796. USATACOM. April 1973. 302 p.

## SECTION VII

### PUBLICATIONS

1. Evers, L. W., P. S. Myers and O. A. Uyehara. A Search for a Low Nitric Oxide Engine. Presented before the 1973 Spring Meeting of the Midwest Section of the Combustion Institute.
2. Evers, L. W., P. S. Myers, O. A. Uyehara. A Search for a Low Nitric Oxide Engine. SAE 741172.
3. Evers, L. W. Nitrogen Control With the Delayed Mixing Stratified Charge Engine Concept. PhD Thesis. University of Wisconsin. 1976.
4. Evers, L. W., P. S. Myers and O. A. Uyehara. Nitrogen Oxide Control With Delayed-Mixing Stratified Charge Engine Concepts. EPA-460/3-76-022.
5. Evers, L. W., P. S. Myers and O. A. Uyehara. An Experimental Study of the Delayed Mixing Stratified Charge Engine Concept. SAE 770042.

## SECTION VIII

## GLOSSARY

<u>ATDC</u>	After top dead center
<u>BTDC</u>	Before top dead center
<u>CO</u>	Carbon monoxide
<u>CVCC</u>	Honda Controlled Vortex Combustion Chamber
<u>EI<sub>NO<sub>x</sub></sub></u>	Molar emissions index
<u>HC's</u>	Unburnt hydrocarbons
<u>IMEP</u>	Indicated mean effective pressure, psi
<u>ISCO</u>	Indicated specific carbon monoxide, g/kWh
<u>ISFC</u>	Indicated specific fuel consumption, kg/kWh
<u>ISHC</u>	Indicated specific unburnt hydrocarbon, g/kWh
<u>ISNO</u>	Indicated specific oxide, g/kWh
<u>ISNO<sub>x</sub></u>	Indicated specific oxides of nitrogen, g/kWh
<u>L-141</u>	Designation of standard "Jeep" engine
<u>MBT</u>	Minimum advance for best torque
<u><math>\dot{M}_{\text{FUEL}}</math></u>	Mass burning rate of fuel, g/sec
<u><math>\dot{M}_{\text{NO}}</math></u>	Molar rate of NO, moles/sec
<u><math>\dot{M}_{\text{NO}_x}</math></u>	Molar rate of NO <sub>x</sub> , moles/sec
<u>M-151-TCP</u>	Designation of single cylinder "Jeep" engine converted to Texaco Combustion Process
<u>n</u>	Molar density, moles/liter
<u>NO</u>	Nitric oxide
<u>NO<sub>x</sub></u>	Combined oxides of nitrogen
<u>ppm</u>	Parts per million
<u>PROCO</u>	Ford Programmed Combustion Process

<u>Q</u>	Volumetric flow rate, liters/sec
<u>TACOM</u>	U.S. Army Tank-Automotive Command
<u>TCCS</u>	Texaco Controlled Combustion System
<u>TCP</u>	Texaco Combustion Process
<u>TDC</u>	Top Dead Center
<u><math>\alpha</math></u>	Orifice to piston diameter ratio
<u><math>\beta</math></u>	Primary to clearance volume ratio
<u><math>\phi</math></u>	Fuel-air equivalence ratio

SECTION IX  
APPENDIX  
LITERATURE SEARCH FOR TCCS HYDROCARBON STUDY

In order to evaluate the nature of the hydrocarbon formation process in the Texaco Controlled Combustion System, a study of the literature pertinent to the heterogeneous combustion process peculiar to the TCCS has been conducted. The purpose of this study was to identify the probable mechanisms of hydrocarbon formation operating in the TCCS and to determine what technique for studying these phenomena would be most applicable.

The first part of this appendix reviews general heterogeneous combustion literature and discusses its relationship to the Texaco combustion process. Based on this review, the second part of the appendix explains the scheme of hydrocarbon formation thought to be operating in the TCCS and reviews literature dealing with the specific mechanisms believed to be involved. The final part deals with the experimental problem of conducting the proposed study and the possible role of available in-cylinder sampling techniques in verifying the hypothesis.

## BACKGROUND

The Texaco Controlled Combustion System (TCCS) is a hybrid, displaying characteristics in common with both Diesel and Otto cycles. As such, it seems logical to begin with a general description of the TCCS, pointing out these similarities, as well as its peculiarities, before proceeding to a detailed analysis of the combustion process.

Table 1 presents the salient features of Diesel and S.I. engine operation. The characteristics common to the TCCS (TCP) are denoted by an asterisk. One notes immediately that the TCCS appears to be much more closely related to the Diesel than the S.I. engine. Its use of direct injected, stratified charge combustion, with locally rich burning but overall lean operation and load control by variation of injected fuel quantity.

---

Table A Combined Features of the Compression Ignited  
and the Spark Ignited Engine, which are  
Present in the TCP Engine

<u>Compression Ignited</u>	<u>Spark Ignited*</u>
Fuel burned in excess air*	Fuel/air ratio limited near chemically correct
Smoke limited full power*	Air limited full power
Unthrottled air*	Throttled air
Fuel injector required*	Fuel injector & carburetor, optional
Rate of pressure rise, 100 psi/deg	Rate of pressure rise, 40 psi/deg*

\*Features of TCP engine

---

along with smoke limited output, clearly relate it to the Diesel concept. In addition, the TCCS employs moderate air swirl and a toroidal combustion chamber much like that used in numerous small displacement open chamber Diesels. However, the use of a positive ignition source in the TCCS eliminates the variable ignition delay period of the Diesel and its attendant fuel quality requirements. Use of spark ignition and compression ratio comparable to conventional homogeneous charge S.I. engines, as well as the more moderate rate of pressure rise characteristic of the TCCS, relate the concept to the Otto cycle as well. It should be pointed out that since only air is compressed in the TCCS and residence time for combustible mixture within the cylinder is quite short, the S.I. engine phenomenon of knock and its attendant fuel quality requirements are also eliminated.

With this description of the general features of the TCCS in mind, one can now begin to fill in the detail regarding the various combustion events.

## COMBUSTION

Figure 1 presents a plot of  $PV^\gamma$  versus crank angle for the Texaco process. The data were taken on an early model hemispherical combustion chamber Texaco engine<sup>[3]</sup> running at full load on a variety of fuels. The plot has been normalized using the value of  $PV^\gamma$  of the compressed air just prior to the start of injection. Injection starts at 20° BTDC and is followed by a period of apparent inactivity, or ignition delay if you will, of approximately 10° (~1.3 msec) before appreciable pressure rise begins. This delay has also been observed by Lazarewicz<sup>[10]</sup> on a more recent TCCS engine configuration using a toroidal bowl combustion chamber, implying that the delay period is peculiar to the process and not the specific engine. Between 10° BTDC and 10° ATDC, the product  $PV^\gamma$  rises linearly. Since volume is changing little during this period, and  $V/V_0 \sim 1$ , this rise is due primarily to pressure increase. This suggests that the rate of heat release is essentially constant and is probably proportional to the rate of fuel injection. Similar control of heat release rate is observed in diesels after the initial spike due to pre-mixed burning. An interesting feature regarding Figure 1 suggests itself at this point. The data for the three fuels were taken while holding the total energy input constant (i.e. mass injected x LHV = constant). This was accomplished solely by varying the injection duration which means that the rate of energy input was different for each fuel. The experimental

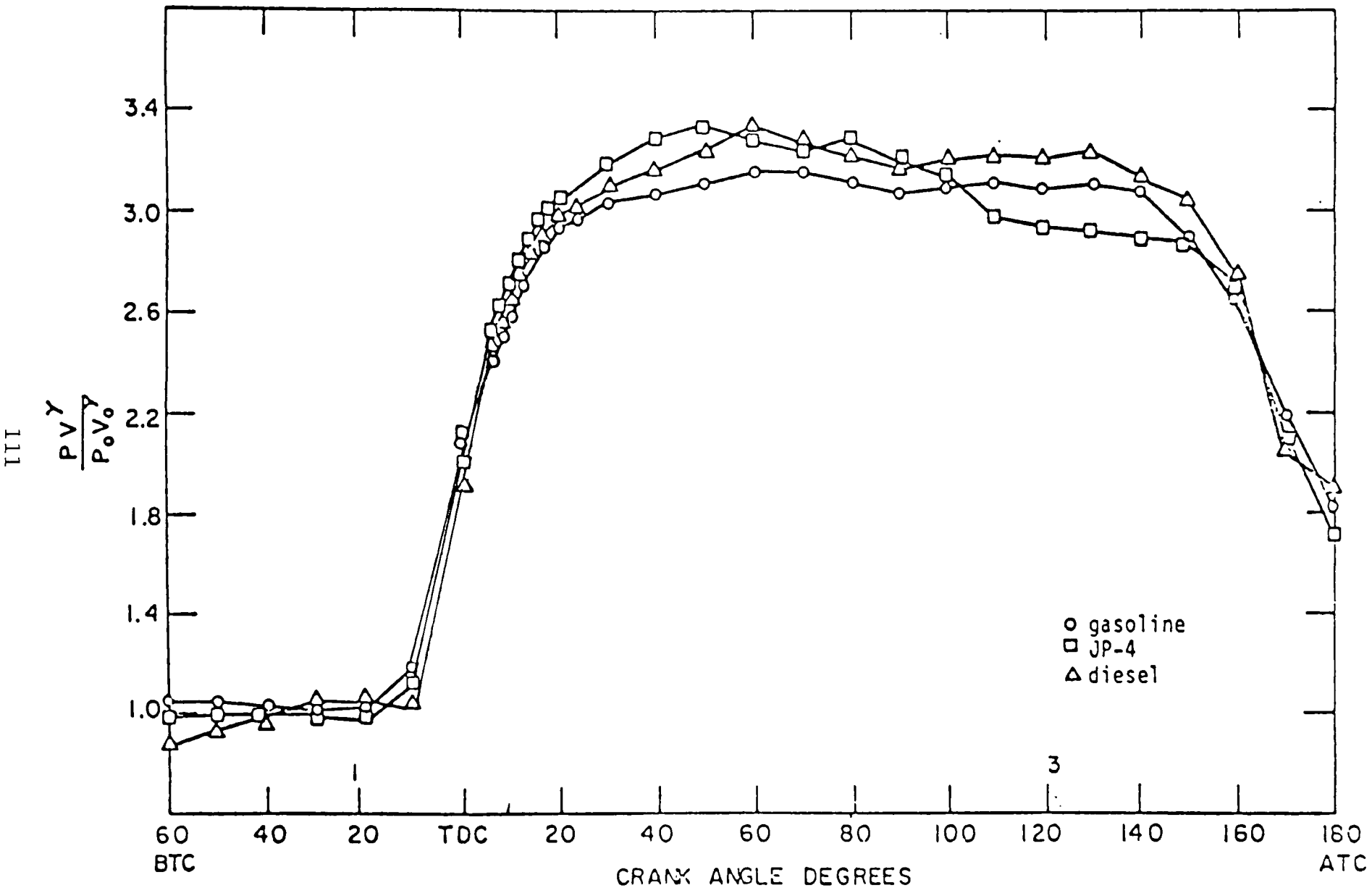
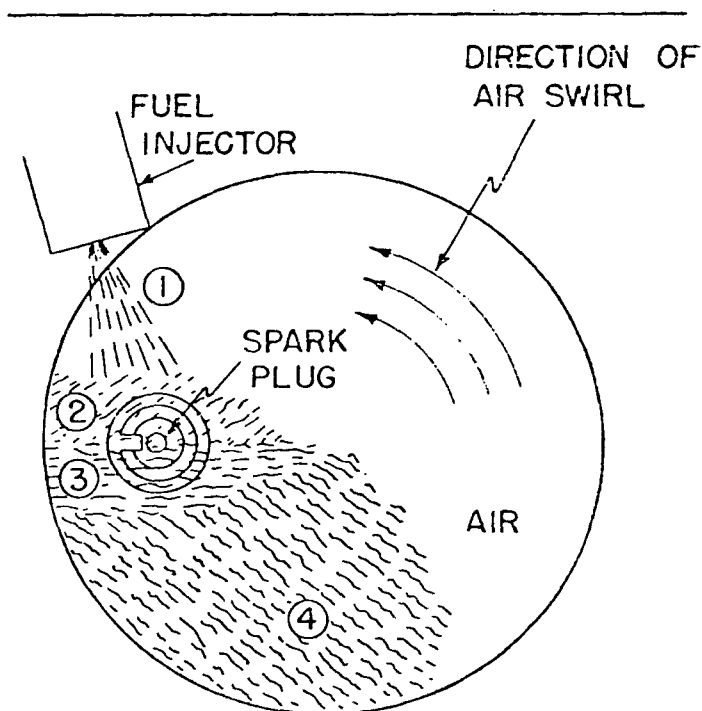


Figure 1  $PV^\gamma$  plot using experimental data on HCC engine - 1200 RPM, full load (ref. 9)

data seem to bear this out in that, during the injection period, the curves corresponding to the individual fuels have slope differences proportional to the differences in their rates of energy input. Barber, et al [2] theorize that the combustion process follows the description given pictorially in Figure 2. Fuel is vaporized and mixed with air to



- 1-FUEL SPRAY
- 2-COMBUSTIBLE AIR-FUEL MIXTURE
- 3-FLAME FRONT
- 4-COMBUSTION PRODUCTS

Fig. 2-Texaco combustion process - air-swirl method (ref. 2)

---

combustible proportions before reaching the spark plug. A quasi-stationary flame front is established at the spark plug by ignition of the first mixture flowing into the gap and persists for the duration of fuel injection due to the steady influx of fresh mixture. Combustion products are carried downstream, mixing with available air as they go and yielding additional heat release until all products have been oxidized to the overall

equivalence ratio. This explanation, although not accounting for the initial delay period, seems to be consistent with the remainder of the injection period. Nagao, et al<sup>[11]</sup> have demonstrated that a stationary flame front can be maintained in a combustion chamber utilizing moderate rates of swirl and a homogeneous mixture, so long as the ignition source is continuous. Heywood<sup>[12]</sup> suggests that the spark plug acts as a flame holder during the injection period with the fuel-air mixture burning in its turbulent wake. Martin<sup>[13]</sup> and Wong<sup>[14]</sup> have recorded high speed color photographic sequences of TCCS combustion simulated on a rapid compression machine. Their films show that the first visible burning occurs just downstream of the spark plug and that burning continues in this region throughout injection. The luminosity given off by the flame during this period is an intense white-yellow. According to Rife and Heywood<sup>[15]</sup> and Scott<sup>[16]</sup>, this coloration is associated with a turbulent diffusion flame, rich in carbon particulates, with a temperature as high as 4200°F. Both Martin and Wong noted a delay period (1.0-1.8 msec) between start of injection and first appearance of visible flame. Wong ascribed this to the first portion of combustible mixture being too cool (due to vaporization and air entrainment) to ignite. This explanation is unsatisfactory in that the first portion of fuel-air mixture should be the easiest to ignite since its temperature would be higher than all succeeding portions if no ignition occurred. Two other explanations seem more probable. It is conceivable that in its initial stages, the developing fuel jet from the nozzle misses the spark gap altogether. Another possibility is that premixed burning is occurring during the delay period. The energy release due to this burning would be partially offset by the heat transfer required for fuel

vaporization. This would explain the lack of appreciable pressure change during the delay period. Curiously, neither Martin nor Wong followed the recommendation of Scott<sup>[16]</sup> and Alcock<sup>[17]</sup> regarding the addition of copper oleate to the fuel. This measure would have assured that any pre-mixed burning would have sufficient luminosity to show up on the color film. Between 10° ATDC and 70° ATDC, the expansion appears to be characterized by the competing effects of further heat release due to entrainment and mixing of the remaining air with the swirling plume of rich combustion products and heat transfer, probably radiative as well as convective, to the combustion chamber surfaces. Heat release dominates until about 40° ATDC and is thereafter balanced by heat transfer. The movies of Scott<sup>[16]</sup> taken on a compression swirl chamber diesel have shown that the centrifugal force field resulting from the swirl causes the hot combustion products to move toward the center of the chamber while the cooler air migrates to the periphery. One might expect the same sort of segregation to occur in the TCCS (although clearly not on the same order of magnitude due to the differences in the swirl rate) creating an interface across which mixing and oxidation processes take place. Martin<sup>[13]</sup> observed localized areas of high vorticity, embedded in the swirling mixture, during the period of combustion following injection cutoff. Such random turbulence would probably promote mixing between the regions of products and air. Lyn and Valdmanis,<sup>[18]</sup> using a Schlieren photographic technique on a swirl chamber diesel, reported microturbulence in the form of small eddies, superimposed on the main swirl, which caused rapid diffusion of soot particles into the oxidizing region. Wong<sup>[14]</sup> observed a rather curious effect of swirl rate on the duration of visible combustion following the injection period in the TCCS.

With all other parameters held constant, the duration of visible flame (Scott<sup>[16]</sup> reports that the last visible portion of diesel combustion is a dull red color corresponding to a temperature of about 1850°F.) first increased and then decreased as the BDC swirl rate was increased from 500 to 1100 radians per second. The influence of swirl rate on mixing and combustion is apparently not straightforward. The remainder of the expansion after 70° ATDC is dominated by heat transfer effects until the blowdown process begins, somewhere around 150° ATDC, at which point the resulting expansion causes both the pressure and temperature of the combustion products to decrease rapidly.

Let us now retrace our steps and review, with the aid of the block diagram given in Figure 3, what is known about the heterogeneous combustion process occurring in the Texaco engine, pointing out as we go the various points at which hydrocarbon compounds may be formed. The discussion will follow the letters a, b, c, . . . , on the right side of the block diagram.

a) Air Intake

Davis, et al<sup>[3]</sup> describe the TCCS as a "coordination of fuel injection and positive ignition with swirling air." This last is brought about by use of an intake port and shrouded intake valve configuration (although the most recent version of the TCCS has abandoned the shrouded valve in favor of a swirl port) designed to cause unidirectional flow into the cylinder. Upon compression, the swirl set up by the constraint of the cylinder wall is intensified as the air is forced into the smaller diameter combustion chamber bowl. The design swirl rate at TDC is such that the smoke limited maximum power fuel injection duration is approximately 80 percent of the time necessary

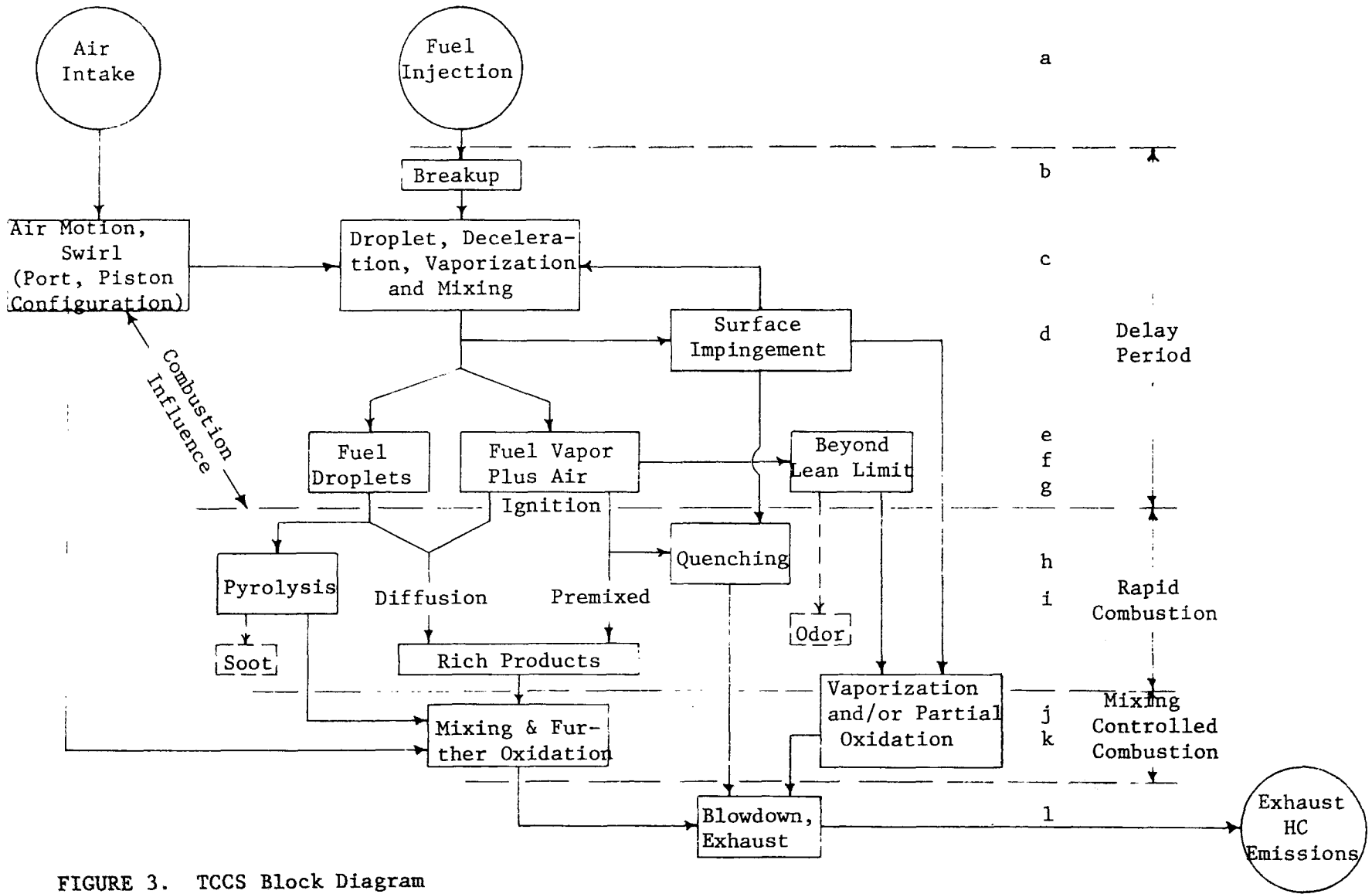


FIGURE 3. TCCS Block Diagram

for one complete revolution of the swirling air. Some squish occurs, but its effect on the general air motion is negligible according to Alcock and Scott.<sup>[17]</sup> The resulting air motion prior to fuel injection has been characterized by Watts and Scott<sup>[19]</sup> as somewhere between free and forced vortex and by Dent and Derham<sup>[20]</sup> as solid body rotation. Apparently, more study is needed in the area of air motion in the cylinders of engines, both prior to and during combustion, before the motion can be adequately described.

### Fuel Injection

Fuel is injected through a single hole nozzle utilizing a flat seating arrangement and a short length to diameter ratio. Several adequate models are available for predicting fuel injection flow rates as a function of injection system design and operating parameters and fuel properties.

#### b) Breakup

According to El Wakil, et al,<sup>[21]</sup> breakup of the fuel jet in diesel engines occurs within a few orifice diameters of its leaving the nozzle. The spray chamber observations of Burt and Troth,<sup>[22]</sup> and the rapid compression machine study of Rife and Heywood<sup>[15]</sup> indicate that this will also be the case for injection and combustion chamber pressures typical of the TCCS. The spray analysis of Jain, et al,<sup>[23]</sup> based on a continuum model of the fuel jet, predicts that the combination of injection parameters used in the TCCS is sufficient to insure "complete and immediate" disruption of the fuel jet for a wide variety of fuels ranging from methanol to a wide boiling range distillate.

#### c) Droplet Deceleration, Vaporization and Mixing

The interaction of the atomized fuel spray with the swirling air,

in the time period between its leaving the injection nozzle and reaching the plane of the ignition source, is probably the most critical part of the TCCS. Other than the model of Jain, et al,<sup>[23]</sup> no analysis of the fuel spray-air interaction peculiar to the TCCS has been found in the literature. By equating the change in momentum of fuel droplets to the corresponding aerodynamic drag force, Jain calculated that the droplets would decelerate to the velocity of the entrained air within a very short distance (~1.5 mm) of leaving the nozzle. Using an equation for the evaporation time of a single stagnant drop in an infinite atmosphere, modified to include the effects of forced convection, Jain next calculated that all the fuel would be vaporized before it reaches the ignition source. Although it is stated at the outset that the analysis is strictly for performance modeling, it is not at all clear that the authors recognize the inaccuracies introduced by neglecting the interaction of proximate droplets and most particularly by the assumption of a monodisperse (10  $\mu\text{m}$  droplets) spray. Sass<sup>[24]</sup> reports that typical droplets from diesel injection nozzles vary in diameter from 2  $\mu\text{m}$  to 50  $\mu\text{m}$ . More recently, Hiroyasu and Kadota<sup>[25]</sup> have put forth an experimentally determined drop size distribution based on an empirical expression for the Sauter's mean diameter (roughly, the ratio of the integral of droplet volume distribution to the integral of droplet surface area distribution). However, no verification of this expression has as yet been found in the literature. Clearly, if different droplet sizes exist in the TCCS spray, then we also need to know something of their velocity distribution. Borman and Johnson,<sup>[26]</sup> in their single droplet study, have shown that initial droplet diameter affects both the droplet's path of motion and its vaporization history and conclude that accurate simulation of the

spray must include consideration of the reduction in vaporization rate caused by the presence of fuel vapor from nearby droplets. Jain treats the mixing of the fuel jet with the swirling air by adopting the analytical scheme of Rife and Heywood.<sup>[15]</sup> This scheme was based on turbulent entrainment parameters developed from observation and modeling of air entrainment into smokestack plumes and gave good agreement with spray tip penetration and spray centerline trajectory observations made by the authors in their rapid compression machine studies. Khan and Wang<sup>[27]</sup> believe that the rate of preparation of combustible mixture is controlled by two scales of mixing. They define these as macromixing, the gross entrainment of air into the fuel jet, and micromixing, the small scale mixing of fuel and air occurring within the fuel jet. They indicate that macromixing is increased by jet impingement on combustion chamber surfaces and that micromixing is dependent on the rates of droplet evaporation and turbulent diffusion of fuel vapor within the jet. Micromixing is also thought to control the distribution of equivalence ratio and temperature within the jet. This latter has been reported by El Wakil, et al<sup>[21]</sup> to increase by several hundred degrees between the central spray core and the outer fringe of the spray. Clearly, numerous concepts of fuel spray-air interaction and mixture formation are available. However, none is universally accepted and further basic studies are needed to provide the foundation for an accurate, flexible model.

#### d) Surface Impingement

Although the TCCS fuel spray analysis of Jain, et al<sup>[23]</sup> predicts that all the fuel will be vaporized before reaching the spark plug, Wong,<sup>[14]</sup> in his rapid compression machine studies of the TCCS, has observed liquid fuel impingement on the combustion chamber bowl surface. Some of this

fuel was deflected toward the center of the bowl where it quickly vaporized and mixed with the swirling air. According to Henein,<sup>[28]</sup> the fuel remaining on the bowl surface will vaporize slowly, due to the relatively low temperature of the surface, and may contribute to hydrocarbon emissions by taking part in wall quenching and partial oxidation reactions during the remainder of combustion. These possibilities will be discussed further in the appropriate section as indicated on the block diagram.

e) Fuel Droplets

It seems probable that liquid fuel droplets still exist at the start of combustion in the TCCS, particularly in the core of the fuel jet where the temperature is lowest and vaporization rates slowest. Alperstein<sup>[29]</sup> indicates that injection tailings may be a source of unburned hydrocarbons in the TCCS. These large droplets are introduced into the combustion chamber at the end of the injection period when the pressure differential across the nozzle is insufficient to cause breakup and penetration of the fuel. Numerous experimental and analytical studies of droplet combustion have appeared in the literature over the years. However, Williams,<sup>[30]</sup> in his review of recent developments, concluded that further study is required before an adequate description of combustion of a moving droplet in a high pressure, high temperature environment can be formulated.

f) Fuel Vapor Plus Air

In addition to liquid fuel droplets, we also expect that a substantial portion of the injected fuel will have vaporized completely prior to the onset of combustion. The Schlieren pictures of Lyn and Valdmanis<sup>[18]</sup> suggest that mixing and evaporation are controlled by air entrainment at the fuel jet boundary where turbulent eddies are seen to form and roll

away from the jet to be carried along by the swirling air. These eddies contain small packets of fuel vapor and the premixed portion of the charge is thought to form in this way. The remainder of the vaporized fuel spray will burn as a turbulent diffusion flame with the burning rate controlled by the rates of turbulent diffusion of fuel vapor within the jet and entrainment of oxidant into the burning zone.

g) Beyond Lean Limit

We might expect a portion of the premixed charge formed at the fringe of the fuel jet to become so thoroughly mixed with air prior to ignition that it passes beyond the lean flammability limit of the fuel. Henien<sup>[28]</sup> indicates that such regions of premixed charge are an important source of unburned hydrocarbon emissions in open chamber diesels, particularly at light loads. In addition, Barnes<sup>[31]</sup> correlated odor intensity with lean flammability limit, and thus with the proportion of fuel existing in premixed regions with fuel-air ratios beyond the lean limit, by replacing the intake air with mixtures of oxygen and a variety of inert diluents such that the lean flammability limit, using the same fuel, would be different. Odor compounds are generally identified as unburned, decomposed and partially oxidized fuel fractions and as such also enter the hydrocarbon emissions picture.

h) Pyrolysis

Droplets existing at ignition will burn as droplets with the rate of heat release governed by the rates of diffusion of fuel vapor and oxidant into the burning zone surrounding the drop. If the temperature of the droplet becomes high enough, due to convective and radiative heat transfer, thermal cracking (endothermic breakdown of the fuel molecules to species of lower molecular weight) may occur yielding new non fuel

hydrocarbons into the reaction scheme. Pyrolysis reactions are also observed in the region between the droplet surface and the burning zone. These reactions lead to the formation of small carbon particles (50-2500 Å) composed of carbon and 1 to 3% hydrogen. The hydrogen probably appears in such small quantities since it is more readily oxidized than the carbon in the fuel. Although the reaction kinetics of soot formation are for all practical purposes unknown, it is recognized that the previously mentioned carbon particles figure heavily in the overall scheme. Soot is also thought to form in the rich core of the turbulent diffusion flame. Khan, et al<sup>[32]</sup> have suggested that the overall rate of soot formation can be adequately predicted by an Arrhenius equation of the form

$$\frac{dS}{dt} \propto \phi^n \exp(-E/RT)$$

where  $\phi^n$  accounts for the influence of fuel-air equivalence ratio and  $n$  is estimated by comparison of predictions with experimental data. However, this approach is an interim one and more fundamental study is needed before the actual mechanism comes to light.

#### i) Quenching

We expect some contribution to the overall hydrocarbon emissions from quenching phenomena occurring during the combustion process. Specifically, we would expect a flame propagating into a region of premixed charge adjacent to the combustion chamber surface to be quenched in much the same manner as quenching occurs in conventional premixed charge S.I. engines. This situation might occur at the surface of the bowl where fuel spray impinged. The diesel movies of Scott<sup>[16]</sup> show that near TDC the large velocity gradient near the cup surface tends to shear the liquid fuel off, vaporizing and mixing it with air. If the resulting mixture

ratio is within the flammability limits, flame will burn through this premixed layer to within a small distance of the surface and then be quenched due to heat transfer effects and radical destruction in the cool unburned mixture. This so-called quench distance will be determined by the instantaneous pressure, by the local mixture temperature and by fuel-air ratio.

In addition, we expect that stratification of the fuel-air mixture will be extreme in certain regions, particularly at light loads, and that a flame will cease to propagate through such a gradient when the energy released in the flame is no longer sufficient to sustain the reaction. This occurrence is often called air quenching.

Lastly, if combustion duration extends late into the expansion process, the reactions which complete oxidation to the overall equivalence ratio may be quenched by the cooling effect of the expansion.

j) Mixing and Further Oxidation

At the end of the injection period, the combustion chamber is filled with a rich burning plume surrounded by the remaining unused air. As the expansion process continues, the rate of heat release available from the rich products, and the duration of combustion, will be controlled by the rate of entrainment and mixing of this remaining air with the plume. Jain, et al<sup>[9]</sup> have modeled this portion of combustion by using the turbulent eddy entrainment parameters derived by Blizzard and Keck<sup>[33]</sup> for their turbulent burning model. Agreement between Jain's model predictions for  $PV^\gamma$  versus crank angle and the available experimental data is reasonably good. However, the turbulent burning model of Blizzard and Keck was developed for a flame propagating through a homogeneous, pre-mixed charge in a non swirling environment. The possibility that Jain's

model's agreement with experimental results is partially fortuitous should probably be taken under consideration.

k) Vaporization and/or Partial Oxidation

As stated previously, Wong<sup>[14]</sup> has observed fuel impingement on the surface of the combustion chamber cup. The portion of the liquid fuel which remained on the cup surface and did not vaporize early in the combustion cycle and take part in premixed burning, as described in (i), will find it increasingly difficult to encounter sufficient oxygen for complete combustion. Henein<sup>[28]</sup> suggests that this late vaporizing fuel will decompose, forming unburned hydrocarbons, partial oxidation products and carbon particulate. This occurrence is clearly demonstrated in Scott's<sup>[16]</sup> movies when the swirling combustion products spill out of the cup and begin to diffuse into the clearance volume between the edge of the cup and the cylinder wall. Adjacent to the points of spray impingement, large smoke clouds appear indicating insufficient oxygen. Alperstein<sup>[29]</sup> reports that unburned hydrocarbon reduction in the cylinder of the TCCS can be enhanced by promotion of small scale turbulence between the piston and cylinder head and by increased swirl rate.

Premixed charge whose fuel-air ratio was beyond the lean flammability limit prior to ignition may, if sufficiently isolated, pass through the combustion process relatively intact or it may be partially oxidized by the high temperatures attained during the combustion period. Either way, it will enter the overall hydrocarbon emissions picture.

l) Blowdown and Exhaust Process

Extensive research with homogeneous, premixed charge, spark ignited engines has shown that hydrocarbon compounds are selectively exhausted from the cylinder, depending on their physical origin. Daniel and

Wentworth<sup>[34]</sup> were the first to document the variation in exhaust HC concentration with crank angle by sampling at the exhaust port. Tabaczynski, et al<sup>[35]</sup> carried this one step further by measuring instantaneous mass flow rate of HC during the exhaust process. Both papers explained the variation in HC in terms of the physical origin of the gases leaving the chamber. They also demonstrated that a large proportion of the unburnt hydrocarbons formed during premixed combustion are not subsequently entrained into the flow leaving the cylinder, but remain in the cylinder as residuals, primarily because of their physical locations (i.e. combustion chamber surfaces far removed from the exhaust valve and also the piston face). We expect that hydrocarbon compounds formed in the TCCS by mechanisms, and in locations, similar to those occurring in conventional spark ignition engines will behave in the manner predicted by these studies.

This concludes the review of the heterogeneous combustion process occurring in the TCCS. Due to the lack of literature dealing specifically with the TCCS, much of the material presented was drawn from studies of open chamber, direct injection diesels utilizing combustion chamber configurations and air swirl rates similar to those used in the TCCS. The points at which hydrocarbons appearing in the exhaust are thought to originate have been identified and a brief description of the particular mechanism(s) involved has been presented.

The next section will construct the hypothesis of hydrocarbon formation in the TCCS and review the literature dealing with the specific mechanisms involved in the scheme.

## HYDROCARBON FORMATION IN THE TCCS

We are now in a position to begin formulating the mechanisms responsible for hydrocarbon emissions from the TCCS. Figure 4 is a plot of specific hydrocarbon emissions (grams C/ihp-hr) versus fuel-air equivalence ratio taken from the experimental data of Lazarewicz.<sup>[10]</sup> The inset plot for a direct injected, open chamber diesel was extracted from Yumlu and Carey,<sup>[36]</sup> and the plot for the homogeneous charge S.I. engine is from Jackson, et al.<sup>[37]</sup> The order of magnitude or more difference in the rates of hydrocarbon emission between the TCCS and the diesel can be attributed to the higher average temperatures attained during combustion in the diesel as a result of its higher compression ratio (~16:1 vs 10:1 for the TCCS). This difference in emission levels probably accounts for the lack of reference to hydrocarbon emissions in the majority of the diesel literature; they are just not a serious problem in diesels. However, present vehicle applications of the TCCS are able to meet current HC emission standards only with the addition of an oxidation catalyst. With more stringent standards on the horizon, an understanding of the in-cylinder HC formation mechanisms occurring in the TCCS will be fundamental to improving its emissions characteristics.

One feature of Figure 4 worth noting is that the minimum specific hydrocarbon emission for each type of engine occurs at approximately the same fuel-air equivalence ratio. The shape of the homogeneous S.I. curve is reasonably well understood at this point. Flame quenching theory predicts that for premixed burning, the minimum quench layer thickness (and thus minimum HC emissions) should occur at fuel-air ratios slightly richer than stoichiometric where the flame speed is greatest. However, as

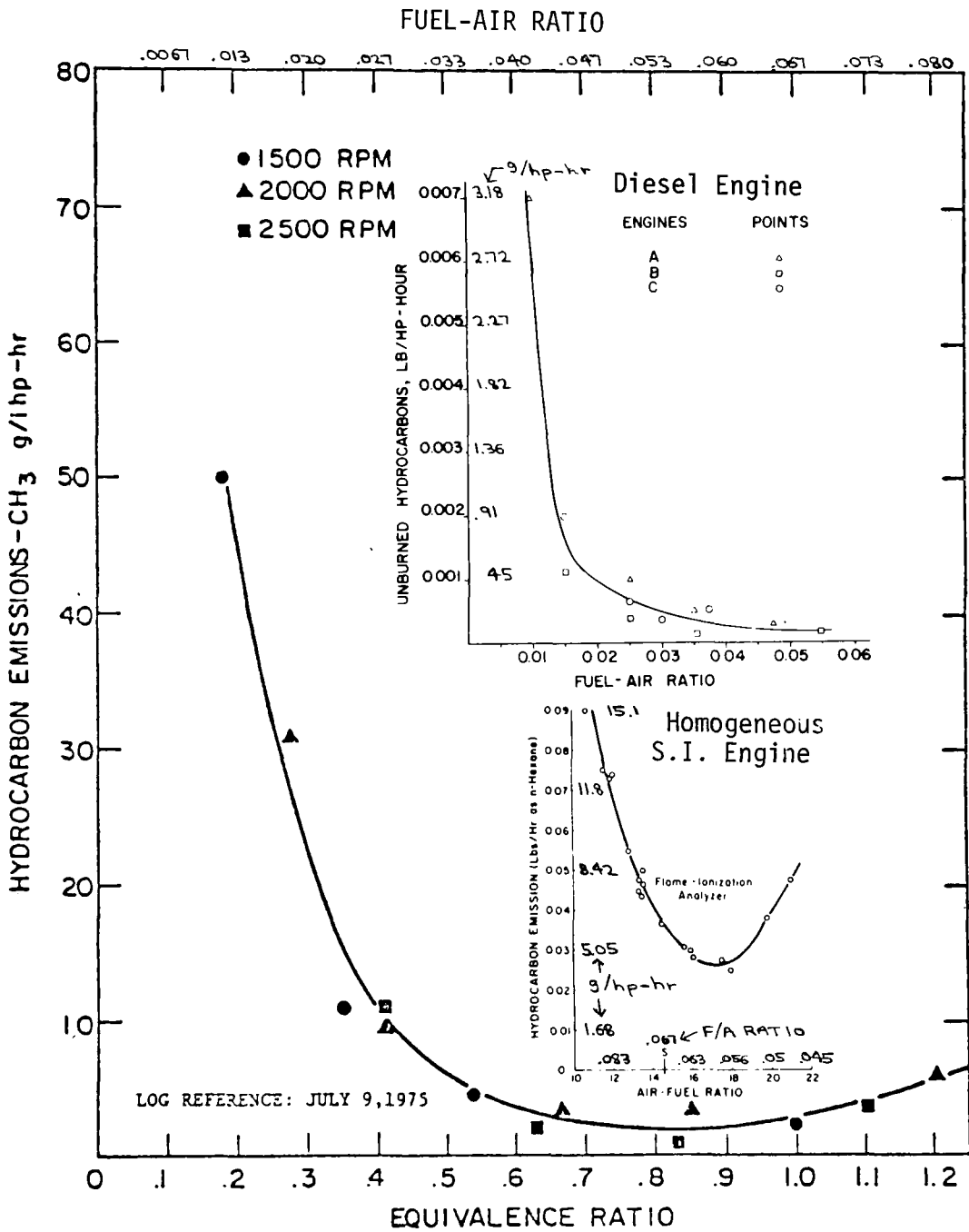


FIGURE 4 HYDROCARBON CONCENTRATION VS EQUIVALENCE RATIO (ref. 10)

Huls, et al<sup>[38]</sup> point out, quench theory does not account for any post combustion oxidation which may occur during the remainder of the expansion and exhaust processes in an engine. Exhaust temperature remains quite high as the fuel-air ratio is leaned beyond stoichiometric. Figure 5 is a plot of average exhaust temperature versus fuel-air equivalence ratio for the TCCS. The dashed line represents typical exhaust temperatures for a homogeneous charge S.I. engine. The high exhaust temperature, in conjunction with the excess air available on the lean side of stoichiometric, causes the minimum hydrocarbon emission to occur slightly lean of stoichiometric. Leaning the mixture further causes the quench layer thickness to increase, although the concentration of fuel in it is lower, and the lower exhaust temperatures slow oxidation reactions by a factor greater than the increase in oxygen concentration can balance. The net result is an increase in hydrocarbon emissions. At mixture ratios richer than the ratio corresponding to the minimum quench thickness, both the quench thickness and the fuel concentration in the quench layer increase. Also, fuel penetrates into crevices such as the region between the piston crown and top compression ring and the cylinder wall. Burning is quenched before entering these regions and the fuel remains intact. Exhaust temperatures remain quite high, but there is insufficient oxygen available to promote oxidation reactions. The result is that hydrocarbons rise sharply on the rich side of stoichiometric. Referring again to Figure 5, we can see that when operating at similar equivalence ratios, exhaust temperatures in the TCCS approach those in the homogeneous charge S.I. engine (as we expect since their compression ratios are similar). We can assume then that exhaust destruction of hydrocarbons in the TCCS under these operating conditions is probably as important as it is in the

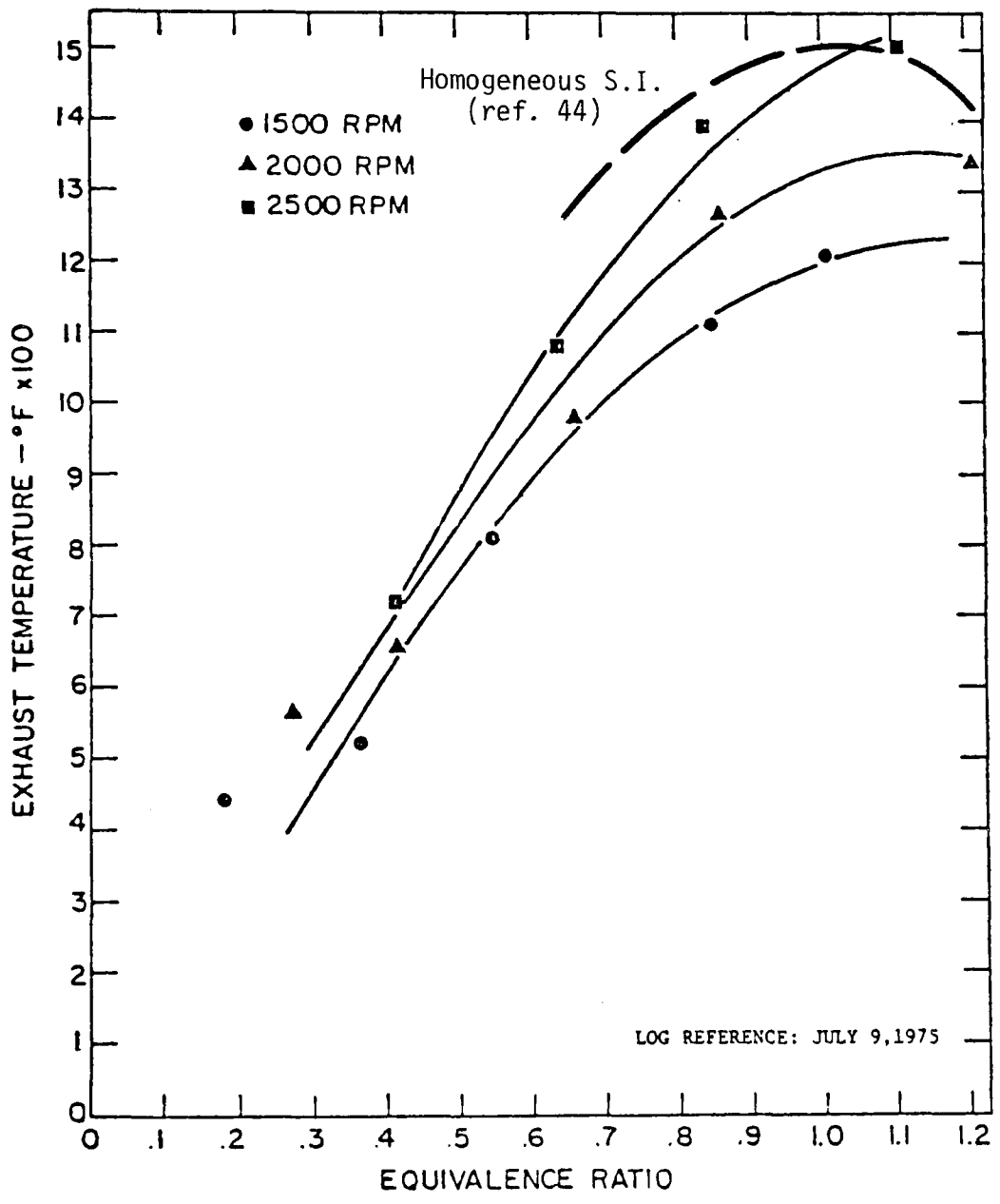


FIGURE 5 EXHAUST TEMPERATURE VS EQUIVALENCE RATIO (ref. 10)

homogeneous charge engine. However, as we reduce the load in the TCCS, its exhaust temperature drops rapidly. It is not yet clear whether the rapid increase in hydrocarbon emissions from the TCCS which occurs as load is reduced, as shown in Figure 4, is due primarily to reduced destruction in the exhaust, or to increased formation during combustion, or some combination of these effects.

### Spray Tailings

One problem occurring in engines which utilize direct, high pressure, fuel injection systems is the injection of large fuel droplets at the end of the fuel injection period because of the reduced pressure differential across the nozzle. The kinetic energy imparted to such drops is so low that they do not atomize or penetrate far from the nozzle. Rife and Heywood<sup>[15]</sup> observed spray tailings at all fueling levels in their rapid compression machine study of diesel combustion. Alperstein<sup>[29]</sup> has indicated that fuel spray tailings are a probable source of hydrocarbon emissions in the TCCS although he indicates that post injections, another possible source of HC, have been successfully designed out of the TCCS injection system. The length to diameter ratio ( $l/d$ ) of the TCCS injection nozzle is quite small so we expect minimal dribble of fuel after the end of injection. Consequently, we state at the outset that injection of large fuel droplets at the end of the injection period may be a source of exhaust hydrocarbons at all loads. Whether these droplets burn completely or not will be a function of local temperature and oxygen availability. In addition, their burning will be diffusion controlled and thus time dependent.

## Light Loads

Air Quenching of combustion reactions may be an important mechanism of hydrocarbon formation in the TCCS at idle and light loads. Light load combustion in both the TCCS and the diesel requires extreme stratification of the fuel-air mixture because of the small quantities of fuel injected. Overall fuel-air ratios at idle approach .01:1. Since the delay period between the start of injection and appreciable pressure rise in the TCCS has been observed by Wong<sup>[14]</sup> to be relatively invariant with load, we can assume that as load is reduced, a greater proportion of the injected fuel will have been vaporized, mixed with the swirling air and swept past the spark plug before combustion starts. That this charge is premixed seems a reasonable assumption since most investigators agree that the initial "spike" of heat release in diesels results from premixed burning and since the time available for fuel vaporization and mixing in the TCCS is comparable to the ignition delay period in diesels. Upon ignition, the flame will propagate through this mixture until the energy released by the flame no longer exceeds the heat transferred to the surrounding mixture. This so-called air quenching of the flame leaves a portion of the injected fuel in an unreacted state. How much fuel is left will depend on how far the flame propagates through the mixture gradient. This will be a function of the heat transferred to this mixture from prior combustion, insofar as the mixture temperature affects the lean flammability limit. Average gas temperatures resulting from combustion at idle and light load are relatively low. This is reflected in the low exhaust temperatures shown in Figure 5. The low combustion temperature, in conjunction with the diffuse concentration of the remaining fuel molecules, causes the post flame oxidation reactions to proceed slowly.

The result is that some of this fuel winds up in the exhaust in an unburned or partially oxidized state. We don't expect much destruction of such products in the exhaust because of its low temperature. Figure 6, compiled from the data of Hurn,<sup>[39]</sup> shows that at idle hydrocarbon compounds found in diesel exhaust have molecular weights similar to that of the original fuel. Figure 7, taken from Johnson, et al,<sup>[40]</sup> shows that for direct injected, open chamber diesels, both the specific rate of hydrocarbon emission and the fraction of unburnt fuel are highest at the lowest fueling level. Figure 8, also from Hurn, shows that the highest concentrations of unburnt hydrocarbons and aldehydes (partially oxidized hydrocarbon compounds identified as contributors to diesel exhaust odor) occur at idle in diesel exhaust. Barnes<sup>[31]</sup> suggests that compounds associated with odor result from partial oxidation reactions occurring in the regions where the fuel-air mixture was beyond the lean flammability limit prior to the start of combustion. Mitchell, et al<sup>[6]</sup> confirm that diesel-like odor is noticeable in the TCCS exhaust at idle and light loads.

Fuel Impingement on the bowl surface may or may not occur in the TCCS at light loads. Henein<sup>[28]</sup> states that it does not occur in diesels, but offers no experimental proof or logical reasoning to support his view. Khan and Wang<sup>[27]</sup> suggest that it is unimportant at light load but won't go as far as claiming it does not occur. Wong<sup>[14]</sup> observed impingement in his rapid compression machine study of the TCCS, but it is not clear from his thesis that it occurred at all fueling levels. The spray penetration theory of Borman and Johnson<sup>[26]</sup> says that succeeding droplets penetrate further because of momentum transferred from preceding drops to the entrained air. This implies that ultimate spray tip penetration is a function of the total momentum transferred from the droplets to the

NA	TC	rpm
*	*	1600
□	■	2000
○	●	2400
◇	◆	2800

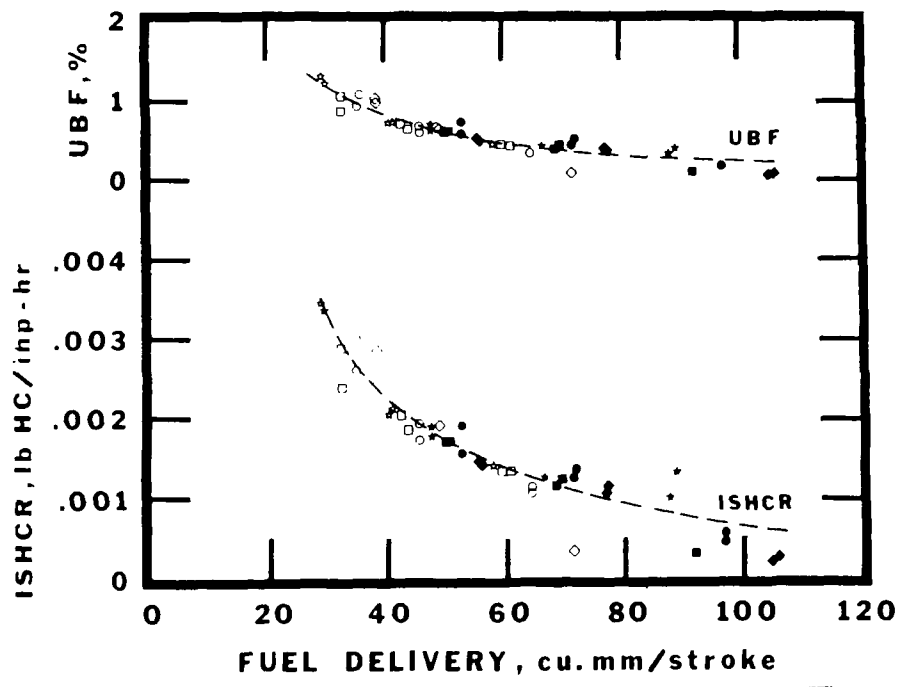


Fig. 7 - Effect of fuel delivery on specific hydrocarbon rate and per cent unburned fuel (1600, 2000, 2400, and 2800 rpm; naturally aspirated and turbocharged conditions) (ref. 38)

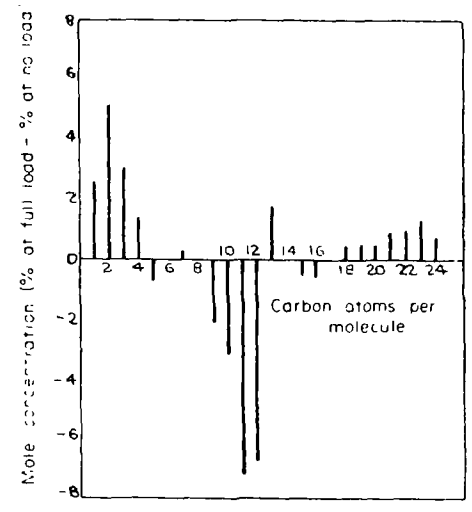


Fig. 6 Effect of load on distribution of unburned hydrocarbon emissions in a DI engine (ref. 39)

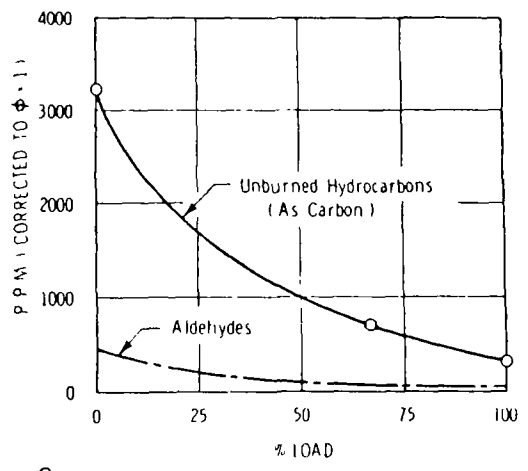


Fig. 8 Effect of load on unburned hydrocarbons and aldehyde emissions in a DI engine (ref. 39)

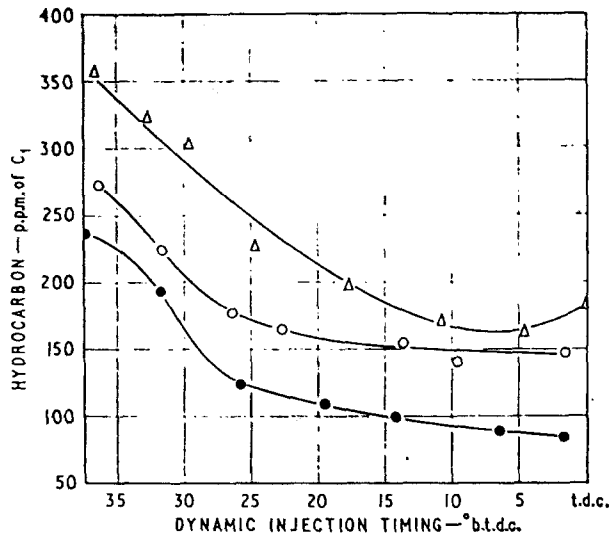
air. Therefore, decreasing injection duration should reduce the penetration of the spray. It is conceivable then that at idle and light loads penetration of the fuel spray is insufficient to reach the bowl surface. However, should the spray reach the bowl surface we would then have additional possibilities for hydrocarbon emissions. The velocity gradient near the bowl surface is large and, according to Scott,<sup>[16]</sup> tends to shear off liquid fuel, vaporizing it and mixing it with air. If this mixture is subsequently ignited, we would expect the flame to propagate in close to the bowl surface and be quenched in the same way that burning is quenched in homogeneous charge engines. This quenching would leave a layer of unburned mixture which might or might not leave the cylinder during the exhaust process. At light loads, ignition of this mixture might not occur and vaporization of the fuel would continue well into the expansion. Both of these possibilities could contribute substantially to overall hydrocarbon emissions. Spray tailings occurring at idle and light load probably represent a substantial part of the injected fuel. If these drops descend into the bowl before being ignited, they will be spread across the bowl surface by the swirling air and will undergo the same processes as impinged fuel. If they ignite, they will burn at a diffusion controlled rate. At the low combustion temperatures attained at light load, they may not burn to completion in the time available.

#### Moderate Loads

As load is increased, several competing factors come into play. Less time is available for combustion of the last portion of the fuel spray and proportionately less oxygen is available to complete this combustion. However, these two conditions are more than offset by the increased rates of the oxidation reactions, promoted by the higher temperatures resulting

from combustion of larger quantities of fuel. The higher temperatures extend the lean flammability limit, so we expect a smaller quantity of unburned fuel resulting from air quenching. In addition, the higher post flame reaction rates will oxidize much of this unburned fuel further reducing the influence of air quenching on overall hydrocarbon emissions. Fuel impingement is more assured at moderate loads and Figure 9, taken from Khan and Wang,<sup>[27]</sup> demonstrates clearly its effect on hydrocarbon emissions. It shows that at a constant fueling rate, advance of injection timing (i.e. earlier in the compression stroke) results in increased hydrocarbon emissions. Khan and Wang attribute this rise to increased fuel impingement and resultant wall quenching. This seems reasonable since earlier injection occurs against lower combustion chamber air density and spray penetration should increase. With this in mind, it seems appropriate to discuss more fully the phenomenon of wall quenching and its effect on hydrocarbon emissions.

Wall Quenching of flames in spark ignited engines was first observed by Daniel.<sup>[41]</sup> He measured quench distances (thickness of the layer of unburned fuel-air mixture between the flame front and chamber surface at the time of flame extinction) ranging from .002" to .015", depending on cylinder pressure, local gas temperature and stoichiometry, and obtained good agreement with state-of-the-art quench distance predictions. Daniel concluded by postulating that a large proportion of hydrocarbons appearing in homogeneous S.I. engine exhaust originate in the quench layers formed by flame quenching. This theory received support from the combustion bomb study of Shinn and Olson.<sup>[42]</sup> To avoid the cyclic variability associated with engine combustion, they constructed a combustion bomb and control apparatus which allowed simulation of the engine combustion cycle,



Injection shape	Injection period	Rate
△ Steep front	17° c.a.	3.35
○ Pilon front	22° c.a.	2.73
● Steep front	22° c.a.	2.73

Engine speed, 2000 rev/min;  $\phi_0 = 0.72$ .  
 Nozzle: 4 hole  $\times$  0.28 mm diameter.

Fig. 9 Effect of timing and rate of injection on hydrocarbon emissions (Engine B) (ref. 27)

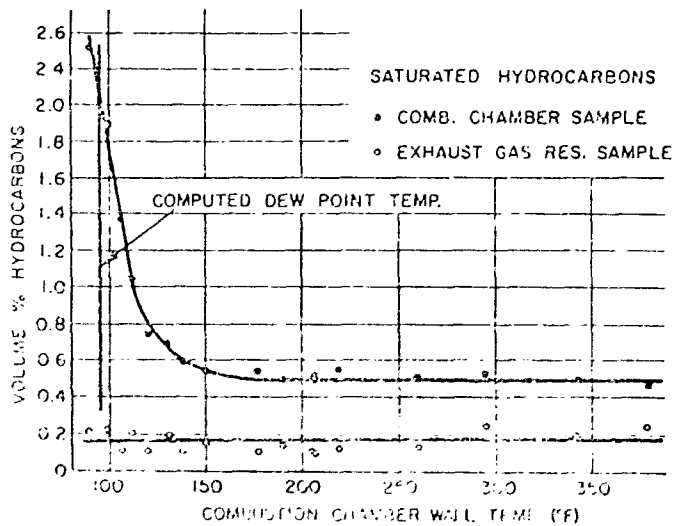
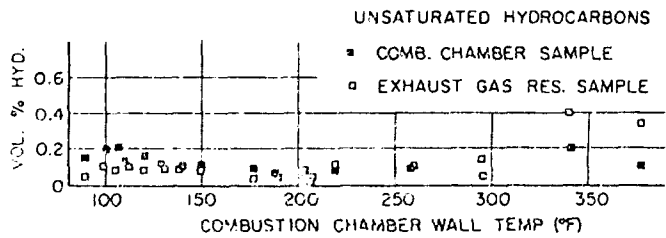


Fig. 10 Hydrocarbon content in product from combustion chamber showing effect of wall temperature on sample from combustion chamber and from exhaust gas reservoir (ref. 42)

but with independent control of many variables. Figure 10 shows their measurements of hydrocarbons resulting from isooctane combustion. It can be seen that the proportion of hydrocarbons in the combustion chamber sample, which was taken by means of a sampling valve mounted flush with the surface of the combustion chamber, is roughly 2.5 times greater than the proportion contained in the bulk exhaust gases. The predominance of saturated (fuel-like) compounds in the chamber sample suggests that the fuel-air mixture near the wall was left unburned by the quenching process. In addition, it was noted that condensation of fuel becomes important when the combustion chamber surface temperature approaches the dew point temperature of the fuel-air mixture. Shinn and Olson accounted for the difference in hydrocarbon concentration between the bulk exhaust gas and the chamber sample by theorizing that quench layers far removed from the exhaust valve are unlikely to leave during the exhaust process and that viscous drag will retard entrainment of quench regions near the valve into the bulk flow. Daniel and Wentworth<sup>[34]</sup> sampled combustion gases near the head surface in an operating engine by means of a small, inwardly opening poppet valve. The general layout of the sampling valve is shown in Figure 11 and the measured sample hydrocarbon concentration versus sampling rate (controlled by adjusting valve lift in this study) is shown in Figure 12. The results show that as sampling rate is reduced, the concentration of unburned hydrocarbons in the sample increases. The reason for this is that small sample flow rates contain greater proportions of gas withdrawn from the region close to the surface. They identified the reason for this gradient in hydrocarbon concentration as wall quenching. Further, they showed that the concentration of hydrocarbons in well mixed residual gases remaining in the combustion chamber at the

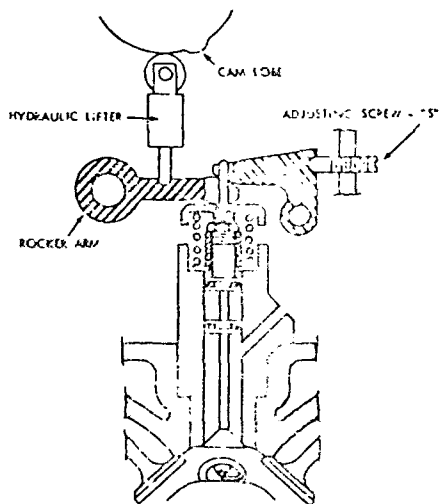


Fig. 11 Quench zone sampling valve actuating mechanism (ref. 34)

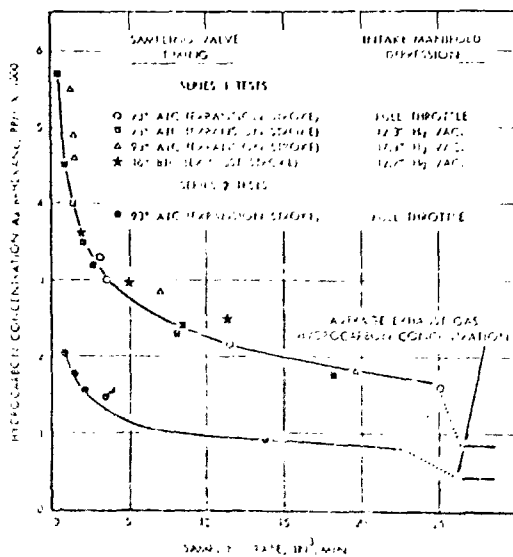


Fig. 12 Hydrocarbon concentration of gases sampled with quench zone sampling valve (ref. 34)

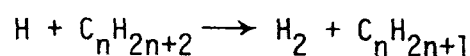
end of the exhaust process is some eleven times greater than the measured average exhaust hydrocarbon concentration. This confirms Shinn and Olson's theory that much of the hydrocarbon-rich quench regions remain in the combustion chamber as residuals.

Numerous additional literature dealing with the effects of wall quenching phenomena on hydrocarbon emissions could be referenced. However, the portion presented is sufficient to show that wall quenching resulting from vaporization and burning of fuel which impinged on combustion chamber bowl surface is probably an important hydrocarbon formation mechanism at moderate to heavy loads. Fuel in the bowl which does not vaporize and burn early in the combustion process will continue to vaporize during expansion. However, the higher gas temperatures and excess oxygen available will promote oxidation of at least part of this fuel vapor. Whether or not fuel vapor remaining in the bowl at the start of the exhaust process will leave is open to some question. It would appear from Daniel and Wentworth's observations that the vapor would probably not be entrained into the exhaust flow.

Spray tailings should ignite quickly at moderate loads. Heating of these droplets from surrounding combustion may cause some pyrolysis of the fuel, but the droplet should burn to completion in the excess air. Lastly, exhaust temperatures rise rapidly as load is increased, as shown in Figure 5, and we expect that destruction of hydrocarbons in the exhaust will become more important. The net result is a rapid decrease in hydrocarbon emissions as load is increased from light to moderate levels, as can be seen in Figures 4, 7 and 8.

## Heavy Loads

As load is further increased, the fuel-air ratio approaches stoichiometric and the hydrocarbon emissions from the TCCS begin to increase. The longer period of injection results in increased fuel impingement in the bowl. If this fuel vaporizes early in the combustion process, it will probably mix with air and burn. The resulting flame will be quenched near the bowl surface and a thin layer of unburnt hydrocarbons will be formed. If, however, this fuel vaporizes slowly, as Henein<sup>[28]</sup> suggests, the fuel vapor will probably decompose forming unburnt hydrocarbons, partially oxidized compounds and possibly some carbon particulate. Hurn<sup>[39]</sup> suggests that in diesels operating near full load, time factors begin to limit oxidation processes. Since more fuel is injected, we expect a larger proportion of the mixture at the core of the jet to be richer than the rich flammability limit. Mass transport, mixing and heat transfer from the surrounding combustion ultimately determine how much of this initially over rich mixture subsequently burns; these processes are all time dependent. If droplets other than spray tailings exist, they will be found in the core and upon ignition they will burn at a diffusion controlled rate. We have previously noted that radiant and convective heat transfer from nearby combustion can raise temperatures sufficiently to cause thermal cracking of the fuel in both its liquid and vapor phases, particularly in regions where there is insufficient oxygen to complete combustion. Such cracking produces hydrocarbon compounds of lower molecular weight than the original fuel. Fristrom and Westenberg<sup>[43]</sup> suggest that combustion of a typical fuel molecule in a rich flame proceeds according to the following scheme.



They indicate that radical concentrations resulting from this reaction can be high enough to make recombination reactions important. If such recombination occurs, it will result in production of hydrocarbon species of higher molecular weight than the original fuel. These two phenomena (thermal cracking and recombination reactions) may explain Figure 6 which shows that at full load, the hydrocarbon composition of diesel exhaust consists mainly of species having either lower or higher molecular weight than the original fuel molecules. Barnes<sup>[31]</sup> also noted that diesels operating at heavy load on a pure fuel emit a broad spectrum of hydrocarbon compounds having greater and lesser carbon atoms than the fuel. Combustion of spray tailings at heavy loads is a probable source of hydrocarbon emissions also. The temperature of surrounding gases is high and oxygen is not so readily available as it is at moderate loads. The droplets may pyrolyse, forming lower molecular weight compounds or carbon particles which then take part in soot formation. Soot may also form in the rich core of the fuel jet at heavy loads. Exhaust temperatures at heavy loads approach those of the conventional homogeneous S.I. engine, so we expect comparable hydrocarbon destruction in the exhaust. However, as the mixture ratio nears stoichiometric, oxygen will be scarce in the exhaust and destruction may decrease somewhat.

### Summary

Literature pertaining to the mechanisms of hydrocarbon formation thought to be important in homogeneous charge S.I. engines and diesels has been reviewed. Those mechanisms which appear to be operating in the TCCS have been identified and their varying influence on overall hydrocarbon emissions has been discussed. In conclusion, we can summarize the mechanisms operating in the TCCS as follows.

1. At all loads, large droplets of fuel introduced at the end of injection may burn to completion or decompose depending on local conditions of temperature and oxygen concentration and the time available for their diffusion controlled combustion.
2. At idle and light loads, air quenching of the burning plume leaves much of the injected fuel unburned. Post flame oxidation rates are too slow to eliminate this fuel because of the low average temperature resulting from combustion. Impingement of fuel spray on the bowl surface may occur. If it does, this fuel may vaporize quickly, mix with the swirling air and burn, leading to wall quenching of the flame near the bowl surface. If this fuel vaporizes slowly and does not burn, it may enter the exhaust system intact. Exhaust temperatures are low at light loads and little destruction of hydrocarbons is expected.
3. At moderate loads, higher average combustion temperatures extend the lean flammability limit and increase post flame oxidation rates, thus reducing the effect of air quenching on overall hydrocarbon emissions. Fuel impingement on bowl surfaces occurs. Gradual vaporization of this fuel promotes wall quenching reactions early in the combustion process and may add raw fuel vapor to the bulk gases late in the expansion. Exhaust temperatures rise rapidly with load and oxidation of hydrocarbons in the exhaust becomes important.
4. At heavy loads, longer injection periods result in more fuel being deposited on the bowl surface. If this fuel vaporizes early, it probably mixes with air and burns with quenching

reactions resulting. If it vaporizes slowly, its chances of finding adequate oxygen are reduced and the high temperatures resulting from combustion will decompose it, forming unburned and partially oxidized hydrocarbons and carbon particles. Lack of sufficient oxidant in the core of the jet and time limited diffusion, mixing and heat transfer processes will lead to incomplete combustion. Also high temperatures caused by heat transfer from surrounding combustion will cause pyrolysis of the liquid and vapor fuel in this region. Exhaust temperatures will be high and destruction in the exhaust will be important until the mixture ratio exceeds stoichiometric.

#### EXPERIMENTAL PROBLEM

Ideally, we would like to be able to formulate a kinetic model for hydrocarbon formation in heterogeneous combustion. Such a model could then be incorporated into an engine simulation program for use as a design tool. However, such kinetic models appear to be a long way off even for homogeneous charge S.I. engines. Heywood<sup>[12]</sup> reports that over 200 organic compounds have been identified in the exhaust from such engines by means of gas chromatography. Many of these are trace species, but even ignoring them, the number of compounds to be accounted for is formidable. We don't know many of the reactions involved and for those we do, much of the reaction rate data is questionable.

The current approach to understanding the mechanisms of hydrocarbon formation has been to study the effect on hydrocarbon concentration

of variation of engine design and operating parameters. Daniel and Wentworth<sup>[34]</sup> studied the variation, with engine operating parameters, of hydrocarbon concentration both in the quench layer and the exhaust by means of sampling valves. More recent works have investigated the effects of piston design, cylinder wall temperature and blowby on hydrocarbon emissions. Daniel<sup>[44]</sup> has developed a model for hydrocarbon emissions from homogeneous charge S.I. engines based on empirical functions for quench layer thickness, unburned fuel due to crevices, post flame oxidation and exhaust destruction. It treats all hydrocarbons as a single species and involves a trial and error fit of various parameters in order to obtain an acceptable level of agreement with experimental observations. However inelegant this technique may appear, it is the only one currently available for predicting hydrocarbon emissions from homogeneous charge engines.

Pollutant formation in heterogeneous combustion such as that occurring in the TCCS is considerably more obscure. Spatial and temporal variations in burning stoichiometry cause rapid fluctuations in reaction rates and species concentrations. In order to gain a more complete understanding of the reactions taking place, we would like to be able to do two things: (1) to follow a small parcel of fuel from the time it leaves the fuel injector until the time it passes out the exhaust port, noting in detail its participation in combustion reactions; (2) to be able to sit at a point in the combustion chamber and observe the reactions taking place in the vicinity of that point. Recent studies of  $\text{NO}_x$  formation in diesels have adopted the latter approach because of its relative simplicity. Nightingale's<sup>[45]</sup> study is typical of the work being done. He utilized an inwardly opening sampling valve which could be inserted to

various depths at a number of positions in a variety of combustion chamber configurations. His results include measurements of hydrocarbon concentration as well as  $\text{NO}_x$ , CO and  $\text{CO}_2$  and he notes variations of two orders of magnitude in HC concentration between sampling points in line with and far removed from the fuel spray. However, hydrocarbons are only of peripheral concern to the study and little comment is devoted to the subject. It is not clear whether he recognized the possibility of a quench layer forming over the sampling valve tip in the interim between sampling points and how such a quench layer might affect the sample composition. Ben-nethum, et al<sup>[46]</sup> have indicated that as much as 30% of the mass in a given sample could come from the boundary layer formed at the valve tip. Rhee,<sup>[47]</sup> in reviewing available sampling techniques, recognized this drawback of intermittent sampling devices and developed a design permitting continuous flow of combustion products with the capability of snatching part of this flow for sampling purposes at desired points in the cycle.

It would appear that such a continuous flow sampling device, with the additional requirement that it be capable of insertion into the specific regions mentioned previously, could be used to determine spatial and temporal variations in hydrocarbon concentration in the TCCS. Such information would assist in establishing the existence and quantifying the influence of the various hydrocarbon formation mechanisms ascribed to the TCCS.

## REFERENCES

1. E.M. Barber, J. B. Malin and J. J. Mikita, "The Elimination of Combustion Knock." J. Franklin Institute, Vol. 241, No. 4 (1946), pp. 275-298.
2. E. M. Barber, B. Reynolds and W. T. Tierney, "Elimination of Combustion Knock -- Texaco Combustion Process." SAE Quarterly Transactions, Vol. 5, No. 1 (1951), pp. 26-42.
3. C. W. Davis, E. M. Barber and E. Mitchell, "Fuel Injection and Positive Ignition -- A Basis for Improved Efficiency and Economy." SAE Transactions, Vol. 69 (1961), pp. 120-134.
4. W. A. Summerson and E. Mitchell, "Small Military Engine-Stratified Charge Combustion Yields Multifuel Capability." Automotive Industries, Vol. 142, No. 11 (1967), pp. 71-76.
5. E. Mitchell, J. M. Cobb and R. A. Frost, "Design and Evaluation of a Stratified Charge Multifuel Military Engine." SAE Transactions, Vol. 77 (1968), pp. 118-131.
6. E. Mitchell, M. Alperstein, J. M. Cobb and C. H. Faist, "A Stratified Charge Multifuel Military Engine -- A Progress Report." Paper 720051 Presented at the SAE Automotive Engineering Congress, Detroit, January 1972.
7. M. Alperstein, G. H. Schafer and F. J. Villforth, III, "Texaco's Stratified Charge Engine -- Multifuel, Efficient, Clean, and Practical." Paper 740563 Presented at the SAE Southern California Section Meeting, May 1974.
8. R. E. Canup, "The Texaco Ignition System -- A New Concept for Automotive Engines." Paper 750347 Presented at the SAE Automotive Engineering Congress, Detroit, February 1975.
9. B. C. Jain, J. C. Keck and J. M. Rife, "A Performance Model for the Texaco Controlled Combustion, Stratified Charge Engine." Paper 760116 Presented at the SAE Automotive Engineering Congress, Detroit, February 1976.
10. M. L. Lazarewicz, "Performance of Texaco Stratified Charge Engine on Gasoline." M.S. Thesis, M.I.T., August 1975.
11. F. Nagao, T. Kobayakawa and F. Adachi, "Stationary Flame Front in a Swirl Combustion Chamber." Bulletin of JSME, Vol. 1, No. 2 (1958), pp. 150-155.
12. J. B. Heywood, "Pollutant Formation and Control in Spark Ignition Engines." 15th Symposium (International) on Combustion, Tokyo, Japan, August 1974.

13. M. Martin, "Photographic Study of Stratified Combustion Using a Rapid Compression Machine." M.S. Thesis, M.I.T., January 1975.
14. V. W. Wong, "A Photographic and Performance Study of Stratified Combustion Using a Rapid Compression Machine." M.S. Thesis, M.I.T., June 1976.
15. J. Rife and J. B. Heywood, "Photographic and Performance Studies of Diesel Combustion with a Rapid Compression Machine." Paper 740948 Presented at the SAE Automobile Engineering Meeting, Toronto, Canada, October 1974.
16. W. M. Scott, "Looking in on Diesel Combustion." SAE Paper SP-345. December 1968.
17. J. F. Alcock and W. M. Scott, "Some More Light on Diesel Combustion." Proceedings, Automobile Division, Inst. of Mech. Engineers, 1962-3, No. 5.
18. W. T. Lyn and E. Valdmanis, "The Application of High Speed Schlieren Photography to Diesel Combustion Research." The Journal of Photographic Science, Vol. 10 (1962), pp. 74-82.
19. R. Watts and W. M. Scott, "Air Motion and Fuel Distribution in High Speed Direct Injection Diesel Engines." Inst. of Mech. Engineers, Symposium on Diesel Engine Combustion, April 1970, Paper No. 17.
20. J. C. Dent and J. A. Derham, "Air Motion in a Four-Stroke Direct Injection Diesel Engine." Proc. Inst. of Mech. Engineers, Vol. 188, No. 21 (1974).
21. M. M. El Wakil, P. S. Myers and O. A. Uyehara, "Fuel Vaporization and Ignition Lag in Diesel Combustion." SAE Transactions, Vol. 64 (1956), pp. 712-729.
22. R. Burt and K. A. Troth, "Penetration and Vaporization of Diesel Fuel Sprays." Inst. of Mech. Engineers, Symposium on Diesel Engine Combustion, April 1970, Paper No. 15.
23. B. C. Jain, J. C. Keck and J. M. Rife, "A Model for Fuel-Air Mixing in the Texaco Controlled Combustion, Stratified Charge Engine." M.I.T. Fluid Mechanics Laboratory Report No. 76-1, January 1976.
24. F. Sass, "Kompressorlose Dieselmotoren." Berlin, Julius Springer, 1929.
25. H. Hiroyasu and T. Kadota, "Droplet Size Distribution in Diesel Engines." SAE Paper No. 740150.
26. G. L. Borman and J. H. Johnson, "Unsteady Vaporization Histories and Trajectories of Fuel Droplets Injected into Swirling Air." Paper 598C Presented at the SAE National Power Plant Meeting, Philadelphia, Pa., November 1962.

27. I. M. Khan and C. H. T. Wang, "Factors Affecting Emissions of Smoke and Gaseous Pollutants from D.I. Diesel Engines." Inst. of Mech. Engineers, Symposium on Air Pollution Control in Transient Engines, November 1971, Paper No. C151.
28. N. A. Henein, "Combustion and Emission Formation in Fuel Sprays Injected in Swirling Air." Paper 710220 Presented at the SAE Automotive Engineering Congress, Detroit, January 1971.
29. Private Communication with M. Alperstein, Texaco, Inc.
30. A. Williams, "Combustion of Droplets of Liquid Fuels: A Review." Combustion and Flame, Vol. 21 (1973), pp. 1-31.
31. G. J. Barnes, "Relation of Lean Combustion Limits in Diesel Engines to Exhaust Odor Intensity." SAE Paper No. 680445.
32. I. M. Khan, G. Greeves and D. M. Probert, "Prediction of Soot and Nitric Oxide Concentrations in Diesel Engines." Inst. of Mech. Engineers, Symposium on Air Pollution Control in Transport Engines, November 1971, Paper No. C142.
33. N. C. Blizzard and J. C. Keck, "Experimental and Theoretical Investigation of Turbulent Burning Model for Internal Combustion Engines." SAE Paper No. 740191.
34. W. A. Daniel and J. T. Wentworth, "Exhaust Gas Hydrocarbons -- Genesis and Exodus." Paper No. 486B Presented at the SAE National Automobile Week, Detroit, March 1962.
35. R. J. Tabaczynski, J. B. Heywood and J. C. Keck, "Time-Resolved Measurements of Hydrocarbon Mass Flowrate in the Exhaust of a Spark Ignition Engine." Paper No. 720112 Presented at the SAE Automotive Engineering Congress, Detroit, January 1972.
36. V. S. Yumlu and A. W. Carey, Jr., "Exhaust Emission Characteristics of Four-Stroke, Direct Injection, Compression Ignition Engines." Paper 680420 Presented at the SAE Mid-Year Meeting, Detroit, May 1968.
37. M. W. Jackson, W. M. Wiese and J. T. Wentworth, "The Influence of Air-Fuel Ratio, Spark Timing and Combustion Chamber Deposits on Exhaust Hydrocarbon Emissions." Paper 486A Presented at SAE National Automobile Week, Detroit, March 1962.
38. T. A. Huls, P. S. Myers and O. A. Uyehara, "Spark Ignition Engine Operation and Design for Minimum Exhaust Emission." Paper 660405 Presented at the SAE Mid-Year Meeting, Detroit, June 1966.
39. R. W. Hurn, "Air Pollution and the Compression-Ignition Engine." 12th Symposium (International) on Combustion (1969), pp. 677-687.

40. J. H. Johnson, E. J. Sienkki and O. F. Zeck, "A Flame Ionization Technique for Measuring Total Hydrocarbons in Diesel Exhaust." Paper 680419 Presented at the SAE Mid-Year Meeting, Detroit, May 1968.
41. W. A. Daniel, "Flame Quenching at the Walls of an Internal Combustion Engine." 6th Symposium (International) on Combustion (1956), pp. 886-894.
42. J. N. Shinn and D. R. Olson, "Some Factors Affecting Unburned Hydrocarbons in Engine Combustion Products." SAE Technical Progress Series, Vol. 6, "Vehicle Emissions" (1964), pp. 137-145.
43. R. M. Fristrom and A. A. Westenberg, Flame Structure, McGraw-Hill (1965).
44. W. A. Daniel, "Why Engine Variables Affect Exhaust Hydrocarbon Emission." Paper 700108 Presented at the SAE Automotive Engineering Congress, Detroit, January 1970.
45. D. R. Nightingale, "A Fundamental Investigation into the Problem of NO Formation in Diesel Engines." Paper 750848 Presented at the SAE Off-Highway Vehicle Meeting, Milwaukee, September 1975.
46. J. E. Bennethum, J. N. Mattavi and R. R. Toepel, "Diesel Combustion Chamber Sampling -- Hardware, Procedures and Data Interpretation." Paper 750849 Presented at the SAE Off-Highway Vehicle Meeting, Milwaukee, September 1975.
47. K. T. Rhee, G. L. Borman, O. A. Uyehara and P. S. Myers, "A Continuous-Flow Gas Sampling System for Engines." Combustion Science and Technology, Vol. 12 (1976), pp. 105-109.

**TECHNICAL REPORT DATA**  
(Please read instructions on the reverse before completing)

1. REPORT NO. EPA-460/3-77-006		2.	3. RECIPIENT'S ACCESSION NO.	
4. TITLE AND SUBTITLE Emission Formation in Heterogeneous Combustion			5. REPORT DATE February, 1977	
			6. PERFORMING ORGANIZATION CODE	
7. AUTHOR(S) G.L. Borman, P.S. Myers, O.A. Uyehara, L. Evers, M. Ingham, D. Jaasma			8. PERFORMING ORGANIZATION REPORT NO.	
9. PERFORMING ORGANIZATION NAME AND ADDRESS Department of Mechanical Engineering University of Wisconsin Madison, Wisconsin 53706			10. PROGRAM ELEMENT NO.	
			11. CONTRACT/GRANT NO. R-803858-01-1	
12. SPONSORING AGENCY NAME AND ADDRESS Environmental Protection Agency Emission Control Technology Division 2565 Plymouth Rd. Ann Arbor, Michigan 48105			13. TYPE OF REPORT AND PERIOD COVERED 11/10/76 - 2/9/77	
			14. SPONSORING AGENCY CODE	
15. SUPPLEMENTARY NOTES				
16. ABSTRACT Three research projects are reported under the grant. The first is an investigation of a stratified-charge engine concept in which spark ignited combustion in an engine with a homogeneous rich charge is completed and then air is injected during the expansion stroke giving a leaner overall fuel-air ratio. The study showed substantial reduction of nitric oxides without increasing other emissions. Combustion efficiency was not increased and, because substantial work was needed to supply the compressed air, the engine efficiency was decreased. The second project is an investigation of nitrogen oxides produced by burning of liquid normal heptane from a fuel wetted porous cylinder in a cross flow of air. Variation of free stream air velocity and cylinder diameter showed the moles of nitric oxide per mole of fuel burned to be a weak function of Reynolds number. Soot produced by the flame and collected downstream has been identified as giving off significant amounts of nitric oxide indicating a carbon, nitric oxide interaction in the flame envelope. The third project consisted of a study of the part load operation of the Newhall divided chamber engine previously developed at U.W., Madison, an emissions and fuel economy evaluation of this engine relative to other engines and initiation of a study of the formation of hydrocarbons in a Texaco engine by utilization of an in-cylinder sampling technique. Reasons for abandonment of the divided chamber engine were its higher hydrocarbons and lower fuel economy relative to other engines and its sensitivity to knock.				
17. KEY WORDS AND DOCUMENT ANALYSIS				
a. DESCRIPTORS		b. IDENTIFIERS/OPEN ENDED TERMS		c. COSATI Field/Group
exhaust emissions, combustion products, internal combustion engines, nitrogen oxides, valves, burning rate		stratified-charge engines		0702, 1311, 2102, 2107, 2111
18. DISTRIBUTION STATEMENT Unlimited		19. SECURITY CLASS (This Report) Unclassified		21. NO. OF PAGES
		20. SECURITY CLASS (This page) Unclassified		22. PRICE